ASSESSING THE ROLE OF NETWORK TOPOLOGY, DEMAND VARIATIONS AND RECOVERY STRATEGIES IN ROAD NETWORK RESILIENCE

Philippe Y.R. Sohouenou

December 2021

Thesis submitted in partial fulfilment of the degree of
Doctor of Philosophy

to the

Department of Civil Engineering
University of Nottingham, UK

ASSESSING THE ROLE OF NETWORK TOPOLOGY, DEMAND VARIATIONS AND RECOVERY STRATEGIES IN ROAD NETWORK RESILIENCE

In the beginner's mind there are many possibilities,
but in the expert's mind there are few.

— Shunryu Suzuki, Zen Mind, Beginner's Mind

Abstract

Road networks are critical to society as they support people's daily mobility, the freight industry, and emergency services. However, a range of predictable and unpredictable events can affect road networks, disrupting traffic flows, connectivity, and, more generally, the functioning of society. With the increased interconnectivity and interdependency of the economic sectors, the need to manage this threat is more critical than ever. To this end, stakeholders need to understand the potential impacts of a multitude of predictable and unpredictable events. The present thesis aims at developing a framework to evaluate and understand the resilience (ability to sustain, resist and recover from perturbations) of road networks under a multitude of potentially unpredictable disruptions, and at assessing the role of different network design (e.g. network topology) and operation (e.g. travel-demand distribution) characteristics in road network resilience.

To this end, this thesis adopts a hazard-independent approach that considers all possible scenarios disrupting multiple links (more specifically up to a certain number of links). Novel indicators—including a robustness, unsatisfied-demand and resilience indicator measuring the demand-weighted-average increase in travel time in the disrupted network, the proportion of stranded travellers, and the speed of network-performance recovery, respectively—are developed and tested as part of this thesis. A link-criticality-assessment method based on multiple-link failures is also developed to identify the links that should be given priority for pre-event reinforcement and post-event restoration. To assess the effects of network size, topology, and demand distribution on network resilience, the thesis considers a variety of case studies, including artificial networks generated by a random road network model (developed as part of this thesis) and real network models derived from real-world maps. To assess the influence of demand variations, capacity constraints and congestion on network resilience, this thesis performs a resilience analysis of a network under several demand conditions. Finally, to assess the effects of recovery strategies on network resilience and characterize the optimal recovery strategy, this thesis performs a resilience analysis of a network considering all possible link-repair sequences.

This research should ultimately contribute to the incorporation of resilience considerations into transport planning and management standards, which currently give priority to transport efficiency—the efficient movement of vehicles through a transport network under normal conditions—rather than the movement of vehicles under disrupted conditions.

Funding

The research presented in this thesis was carried out as part of the H2020-MSCA-ETN-2016. This project has received funding from the European Union's H2020 Programme for research, technological development and demonstration under grant agreement number 721493.

Acknowledgements

In many ways, a PhD is more a journey than a degree or thesis. Well... my journey has been challenging, rewarding and amazing. Hence, I sincerely thank the people that allowed, helped or simply accompanied me in this journey.

Firstly, I would like to thank the European Commission for the Marie Sklodowska-Curie programme that provides thousands of students and researchers an amazing opportunity to work for three years as researchers, get PhDs, collaborate with companies and universities across Europe, and develop technical and interpersonal skills. In many ways this programme allowed me to rediscover and appreciate more Europe through the travel experiences and bonding with my co-fellows coming from all over the world.

I sincerely thank my supervisor Luis Neves for giving me this opportunity and for his guidance, support and honesty throughout this journey. I am grateful to have had such a smart, flexible and patient supervisor, who helped me mature professionally and personally. I also thank Davide Lo Presti for his guidance as my second supervisor during the first half of this PhD and his work as coordinator of the SMARTI programme.

Speaking about SMARTI, I would like to thank the whole team. This includes my co-fellows (of course!) that I thank for their support and friendship but also the supervision and administrative team, which worked hard to support us and organise the SMARTI training weeks.

Many thanks to the EU's Joint Research Centre for accepting to host me in its Seville centre for a five-month period that was extended to seven! I particularly thank Panayotis Christidis, who in some way was an unofficial supervisor for me during part of the PhD. I don't think that he and Aris realise how much their collaboration and guidance helped me grow as a professional. I thank Elena for her guidance as well as Aris, Stephane and Ana (the fabulous A51 office) along with the C6 Unit that welcomed me and helped me feel at home in a foreign city. I do not forget all my friends in Seville from the JRC basketball team to my Spanish school (MAUS) who made this secondment amazing.

I sincerely thank my colleagues and friends in Nottingham for their support. This includes the Resilience Engineering Research Group composed of Rasa—my master's supervisor who in a way planted a seed in my mind that made me consider doing a PhD—,the other supervisors (Darren, John and Kate), as well as, the postdocs (the twins, Shawn,...) and the PhDs (Omar, Gareth, Jack, Antonio, Ratthaphong, Matteo,...). I also thank my other research group, NTEC, especially the PhDs who shared an office with me (Diana, Nilo, Monketh, Mario, Rufus, Laura, Van...) as well as Ivan, Jose and Federico. In a nutshell, I got inspired just by being around some of you.

A special thanks to Andrew Dawson, my internal assessor during the first two years of this PhD, for his wise words and humour. Thanks to Tony Parry and Harry Evdorides,

my thesis examiners, who helped me improve further the present manuscript.

I would like to thank my friends and family's friends for being themselves and being there for me. Luc, it's been fun to kind of relive our Master's experience in Nottingham as PhD students (who would have imagined that when we both left Nottingham in 2016?). I have to thank my sweetheart Laetitia for her support and patience in this journey (although I could use a bit more of that :D). Finally, there are no words to adequately thank my family for their unconditional support and love during this journey (but really during my whole life). You are forever with me.

I also have a thought for my uncle, Paul Celestin Sohouenou, who recently left us and will not have the opportunity to look at the final version of this thesis as promised.

Publications

A portion of the work presented in this thesis appears in the following publications:

Journal papers

Sohouenou, P. Y. R., Christidis, P., Christodoulou, A., Neves, L. A. C., & Lo Presti, D. (2020). Using a random road graph model to understand road networks robustness to link failures. *International Journal of Critical Infrastructure Protection.* doi.org/10.1016/j.ijcip.2020.100353

Sohouenou, P. Y. R., Neves, L. A. C., Christodoulou, A., Christidis, P., & Lo Presti, D. (2021). Using a hazard-independent approach to understand road-network robustness to multiple disruption scenarios. *Transportation Research Part D: Transport and Environment.* doi.org/10.1016/j.trd.2020.102672

Sohouenou, P. Y. R. & Neves, L. A. C. (2021). Assessing the effects of link-repair sequences on road network resilience. *International Journal of Critical Infrastructure Protection.* https://doi.org/10.1016/j.ijcip.2021.100448

Conference paper

Sohouenou, P. Y. R., Neves, L. A. C., & Lo Presti, D. (2019). Resilience indicators for road networks: the role of robustness and rapidity. *2019 International Conference on Smart Cities (ICSC).* Retrieved from https://nottingham-repository.worktribe.com/output/2546559.

Book chapter

Sohouenou, P. Y. R., Christodoulou, A. & Neves, L. A. C. (2021). The criticality of high betweenness links in road networks. In Remenyte-Prescott, R. & Kopustinskas, V. (Ed.) *Modelling the Resilience of Infrastructure Networks.* European Safety, Reliability & Data Association (ESReDA)

Contents

Chapter 1

Introduction

1.1 Background and research motivations

1.1.1 The need for research on road network resilience

Extreme weather events and human-made hazards could damage critical infrastructures (such as electricity, water and transport networks) resulting in casualties, service disruptions and significant economic losses. The resilience (i.e. ability to sustain, resist and recover from perturbations) of these infrastructures is thus essential for society.

The interest around the concept of resilience rose over the last twenty years (Manca et al., 2017; Martinson, 2017; Woods, 2015) as society had to face several shocks including the 1995 earthquake in Kobe (Japan), the 2005 bombing of the London (UK) public transport system, or the more recent (2018) collapse of the Morandi bridge in Genoa (Italy). The resilience of critical infrastructures is hence now at the heart of several policies and research programmes including the EU Adaptation strategy (Manca et al., 2017) and the 100 Resilient Cities Programme (Spaans and Waterhout, 2017). In particular, researchers, industry professionals and policy-makers acknowledge the need for metrics to pro-actively manage the resilience of critical infrastructures (Martinson, 2017; Omer et al., 2013; UK Department for Transport, 2014) as metrics provide an effective tool to assess the current resilience of infrastructures, compare strategies for resilience enhancement and measure progress.

The present doctoral thesis addresses this need in the context of road networks because road infrastructures are essential to our increasingly connected society as they support people's daily mobility, the freight industry, and also emergency services. Road disruptions directly affect users through greater congestion, loss of time, and higher fuel consumption, but also lead to indirect impacts, including constrained access to jobs and services as well as poorer air quality (Hallegatte et al., 2019). The impacts on businesses include sales losses, delays in supply and delivery as well as diminished competitiveness in international markets (Hallegatte et al., 2019). Pelling et al. (2002) estimated that the 1995 earthquake in Kobe (Japan) increased the regional transportation costs and cost of goods by over 50% and 10%, respectively. The UK Department for Transport (2014) estimated that the July 2007 flood in London (UK) led to almost 10,000 people being stranded while the repair costs were estimated at £40 to 60 million.

1.1.2 The future incorporation of "resilience thinking" into transport modelling, planning and management

Transport models, representing the complex real-world transport and land use systems, provide a powerful tool to predict transport systems performance under different conditions and assess the impact of transport infrastructure options. Transport models are thus essential to plan, design, and manage transport networks and land use.

Transport modelling and planning standards (Highways England, 2015; Ortúzar and Willusem, 2011) currently give priority to transport efficiency—the efficient movement of vehicles through a transport network under normal conditions—rather than the movement of vehicles under disrupted conditions (Ganin et al., 2017). However, as explained above, transport networks are critical infrastructures subject to service disruptions that can severely impact society. Hence, society could benefit from the incorporation of the "resilience thinking" approach into transport planning, operation and maintenance standards.

The present thesis seeks to contribute to this effort as it aims to develop a framework that adapts the resilience modelling approach into aspects of transport planning. Classical transport planning and modelling methods are used to develop, test and validate novel road network resilience assessment methods, but also to develop a better understanding of road network resilience.

1.2 Research gaps

The literature review (Chapter 2) allowed the identification of several research gaps. The present sub-section provides an overview of the research gaps addressed in this thesis.

1.2.1 The limitations of current approaches to road network resilience

As the main function of road networks is to provide mobility, that is, to connect trip origins and destinations in a timely manner, the resilience of road networks should characterise their ability to deliver this function under a multitude of potentially unpredictable conditions. Indeed, the resilience concept accepts the possibility that a wide range of disruptive events may occur but are not necessarily predictable, and focus on anticipating and enhancing the performance of the disrupted system rather than preventing or mitigating the loss of assets (ARUP, 2014; Park et al., 2013).

However, assessments of the potential impact of disruptive events on road networks generally focus on a limited set of scenarios illustrating the proposed methodology (Nogal et al., 2016; Omer et al., 2013; Zhang and Wang, 2016) or the worst-case scenario using a game theory approach (Alderson et al., 2017; Bhavathrathan and Patil, 2015a, 2015b, 2018). These studies do not uncover the potential impact of all possible disruption scenarios as suggested by the resilience paradigm. This is unfortunate as such findings could be useful to practitioners and public authorities. For example, considering that a wide range of events (e.g. road accidents, flooding, etc.) can unpredictably disrupt any parts of the network, the identification of multiple worst-case scenarios rather than the single worst-case scenario would be more useful in practice.

A range of recent studies (reviewed in Chapter 2) consider multiple disruption scenarios in the road transport context. However, these studies present one (or several) of the following shortcomings:

- Focus on risk analysis (e.g. Wisetjindawat et al., 2017; Zhou et al., 2017), which relies on records of past disruptions that may overlook unpredictable events.
- Use full dismantling processes to model disruptive events in road networks (Buhl et al., 2006; Casali and Heinimann, 2020), which lack applicability to a range of road perturbations such as car accidents, sabotage actions and landslides that disrupt only a limited number of roads. Dismantling process analyses are useful to determine the critical number of failed components after which networks can no longer function. However, this information is relevant only when analysing major disasters (e.g. earthquakes or large floods) that can potentially damage many roads. Besides, the unavailability of a small fraction of a transport network can lead to major consequences, for instance, the collapse of the I-35W Bridge (Minneapolis, USA) resulted in economic losses of US$71,000 - $US220,000 a day (Xie and Levinson, 2011). Hence, a better understanding of the potential impacts of events disrupting a limited number of links and intersections remains important.
- Consider only single-link failures (Omer et al., 2013; Sullivan et al., 2010; Taylor et al., 2006). However, the consequences of multiple-link failures are not simply the combination of those resulting from single-link failures (Wang et al., 2016). The consideration of single-link failures only may lead to inefficient prevention and restoration measures in the advent of events disrupting several road segments or several events concurrently affecting different parts of the network.

Besides, some of these studies (Buhl et al., 2006; Casali and Heinimann, 2020) rely on network topological models that while accounting for the arrangement of the roads and intersections, disregard traffic flows and capacity constraints. The resulting robustness analyses are hence unable to capture dynamic effects of disruptions such as increased congestion on alternative routes (Mattsson and Jenelius, 2015).

Ganin et al. (2017) performed twenty realisations of disruption scenarios affecting a random and finite number of links on traffic flow models of 40 US cities to compare efficiency and resilience. However, the impacts of the different disruption scenarios were not studied in detail and the number of scenarios considered relatively limited.

Therefore, although research has contributed to the understanding of road network resilience, characterisation of the potential impacts of a full range of predictable and unpredictable disruption scenarios is still lacking.

1.2.2 The role of recovery strategies in road network resilience

Resilient systems are associated with several properties (presented in the literature review of Chapter 2). Among these properties, there are robustness—the ability to absorb perturbations—and rapidity (or recoverability)—the ability to recover quickly. In the context of road networks, most works (Bhavathrathan and Patil, 2018; Ganin et al., 2017; Gauthier et al., 2018; Omer et al., 2013) focus on robustness while rapidity has attracted less

attention. Still, considering the socio-economic consequences of road disruptions, recovery processes can have an important influence on the welfare of society as they can help alleviate disruption consequences in the early stage recovery. The studies that consider recovery processes propose different approaches. Nogal et al. (2016) and Nogal and Honfi (2019) focus on the gradual adaptation of road users following both the perturbation and restoration phases. Tuzun Aksu and Ozdamar (2014) develop a scheduling mathematical model optimising the link-repair sequence to quickly recover the network connectivity to facilitate evacuations. Zhang et al. (2017) develop a scheduling mathematical model optimising the link-repair sequence to quickly improve the network performance under stochastic damage levels and repair durations. Finally, Hu et al. (2016), compare different repair strategies under random (damaging random sets of links), localised (damaging adjacent links), and malicious (seeking to maximise the damage to the system performance) dismantling processes. However, the studies of Hu et al. (2016), Tuzun Aksu and Ozdamar (2014) and Zhang et al. (2017) rely on topological network models and performance metrics that do not consider link capacity constraints. Furthermore, these studies do not assess the performance of the recovery strategy across a full range of predictable and unpredictable disruption scenarios as mentioned above.

1.2.3 The effects of road-network characteristics on network resilience

In addition to the limited understanding of road network resilience to a multitude of potentially unpredictable disruption scenarios, there is a limited understanding of the effects of the characteristics of road networks on network resilience. Most studies (e.g. Gauthier et al., 2018; Wang et al., 2016; Zhang et al., 2015) focus on a limited set of case studies such that their findings may be valid for the specific networks studied only. Further investigations are thus required to evaluate the effectiveness of these approaches and the generality of their findings.

Some authors (Buhl et al., 2006; Ganin et al., 2017; Zhang et al., 2015) considered multiple networks to understand the effects of certain network characteristics on road network resilience. Zhang et al. (2015) assessed the role of network topology in transport resilience, considering 17 network structures with some relation to the layout of transport systems. This study demonstrates that redundant networks had greater resilience level. However, Zhang et al. (2015) considered very regular and abstract network structures that do not hold many features of real road networks such as the heterogeneity of road intersections. Buhl et al. (2006) analysed the topological patterns of 40 self-organised street networks (e.g. Rome). As part of this study, the authors assessed the relationship between the network robustness (measured by the impact of dismantling processes on the network structure) and the network size and topology. This study was however limited to self-organised street networks, and as stated above relied on dismantling process that lack applicability to a range of real road perturbations. The study of Ganin et al. (2017) focused on the relationship between efficiency and resilience.

Therefore, the understanding of the effects of the network size and topology on road network resilience can be increased further by considering a large set of real road networks and a multitude of potential disruptions affecting a limited number of links. Besides, it would be interesting to asses the effects of other network characteristics (such as the

distribution of the travel demand) on network resilience.

1.3 Research aim, objectives and approach

1.3.1 Research aim and objectives

The purpose of the present thesis is to contribute to the reduction of the impacts of disruptions on road network operations. To this end, this thesis aims at developing a theoretical framework to evaluate and understand the resilience of road networks. This work will support decision-makers (especially transport planners) in anticipating, assessing, and ultimately reducing the impact of disruptive events on road networks.

The framework should address the research gaps identified above—lack of characterisation of the potential impacts of a full range of predictable and unpredictable disruption scenarios, lack of characterisation of the rapidity component (i.e. recovery strategies) in road network resilience, and limited understanding of the effects of road networks' characteristics (topology, travel demand distribution, congestion, etc.) on road network resilience. Hence, this thesis more specifically aims to develop a framework suitable to evaluate the resilience of road networks under a multitude of potentiality unpredictable disruptions, and assess the role of different network design (e.g. network topology) and operation (e.g. recovery strategies) characteristics in road network resilience.

To this end, this thesis has three objectives:

- develop accurate metrics and methods for quantifying the resilience of road networks to a multitude of predictable and unpredictable disruption scenarios;
- assess the effects of different network characteristics (including size, topology, demand distribution and demand intensity) on network resilience;
- assess the effects of recovery strategies on network resilience.

1.3.2 Main approach and assumptions

Hazard-independent approach

To reach its first objective, the present thesis adopts a hazard-independent approach that considers all possible scenarios disrupting multiple links (more specifically up to a certain number of links). This approach is based on the assumption that road disruptions are rarely predictable and can occur in any parts of the network.

In reality, some events are more predictable (e.g. maintenance works) than others (e.g. terrorist attacks) and some parts of a road network can be more frequently affected than others. Such considerations could help decision-makers optimise the allocation of resilience investments to the more probable hazards and more exposed parts of the network. However, the predictability of a hazard depends on several parameters, including the nature of the hazard and the state of knowledge around this hazard, which is often related to historical data available. Hence, disruptions can happen for reasons that seem extraordinary prior to catastrophe, but in retrospect involve familiar and generalizable patterns (Park et al., 2013). In the transport context, unknown hazards could refer to cascading events

leading to road damage, warnings signs being ignored, or poor decision-making from maintenance operators, etc. Hence, the hazard-independent approach ensures that unknown and unpredictable hazards are considered in the resilience analysis. This approach is in line with the resilience paradigm, which contrary to the risk paradigm accepts the possibility that a range of disruptive events may occur but are not necessarily predictable, and focus on anticipating and protecting the performance of the disrupted system rather than preventing or mitigating the loss of assets due to specific events (ARUP, 2014).

Besides, this approach focuses on combinations of link failures concurrently disrupting up to a certain number of links for computational reasons. The maximum number of concurrently disrupted links is chosen depending on the case study. Hence, this approach does not explicitly address large scale events (e.g snow) that can affect most of the network. However, it is expected that above a certain number of affected roads the network performance would drop to zero. This assumption is validated in the case studies of Chapter 3 where the maximum numbers of failed links are sufficient to reach a near-zero performance and in Chapter 4 where full dismantling processes are modelled. Hence, the choice of the maximum number of concurrently disrupted links can help determine the impact of large scale events.

Fixed travel-demand assumption

Hazards can impact both the supply and the demand side of the transport system. The supply side (i.e. the network) is affected by the obstruction or damage induced on the infrastructures, which in turn impacts traffic conditions. The demand side representing the flow of users can also be impacted as trips may be cancelled or delayed due to usual routes and destinations being affected. As this research seeks to evaluate how the availability of alternate routes and capacity helps remediate the consequences of network disruptions, travel demand was considered fixed to effectively compare the network performance under different disruption scenarios (all other things being equal). Hence, in this thesis, the "travel demand" generally refers to the undisrupted network travel pattern. Nonetheless, Chapter 5 considers different demand distribution and intensity possibilities, which provide some insights into the potential effect of the travel demand alteration caused by disruptions on the resilience assessment.

Case studies

To test the metrics and methods developed (objective 1), the thesis considers a variety of case studies. The case studies include a four-node highway network model, the well-known Sioux Falls network model (LeBlanc et al., 1975), a set of abstract network models generated by a random road graph model (developed as part of this thesis), and a set of real road network models.

To assess the effects of network size, topology, and demand distribution on network resilience (objective 2), the present thesis compares the robustness to multiple disruption scenarios of hundreds of abstract and real network models. The abstract networks result from a novel model developed to randomly generate graphs presenting the topological and operational characteristics of real-road networks. This random network model is used because contrary to real maps its characteristics are controllable and allow for a sound

sensitivity analysis of network resilience, which in turn can provide practical insights for network planning and management. The results derived from the analysis of the abstract networks are ultimately validated on a set of models based on real network samples, whose data was extracted from *OpenStreetMap* (www.openstreetmap.org).

To assess the effects of travel demand distribution and intensity on network resilience (objective 2), the thesis compares the robustness to multiple disruption scenarios of the Sioux Falls network model under different travel demand conditions (e.g., concentrated vs distributed demand, and low vs medium vs high demand level). To assess the effects of recovery strategies on resilience (objective 3), the thesis compares several recovery strategies in the Sioux Falls network model. The Sioux Falls network model is studied for three reasons. The first reason is computational effectiveness. This network model is composed of 24 nodes and 76 directed links, leading to reasonable traffic-simulation run times (under 5 seconds). This short run time allowed the performance of over five hundred thousand disruption simulations using parallel processing on a desktop. The second reason is reproducibility. The Sioux Falls network dataset is readily available, for example on the Transportation Networks for Research repository (Transportation Networks for Research Core Team, 2019), and has been extensively used in the transport literature (Bhavathrathan and Patil, 2015b; Mitradjieva and Lindberg, 2013; Wang et al., 2016). Finally, the Sioux Falls case study includes the data necessary to perform traffic simulations (i.e. the travel demand data), which provides a more realistic assessment of the impacts of disruptions on the network. This was not the case for the abstract and real networks mentioned above. Therefore, the increased understanding of road network resilience developed in this thesis also comes from the comparisons of all of these case studies.

1.3.3 Thesis workflow

Figure 1.1 presents the workflow of the present thesis, including its purpose, aim, objectives, and chapters.

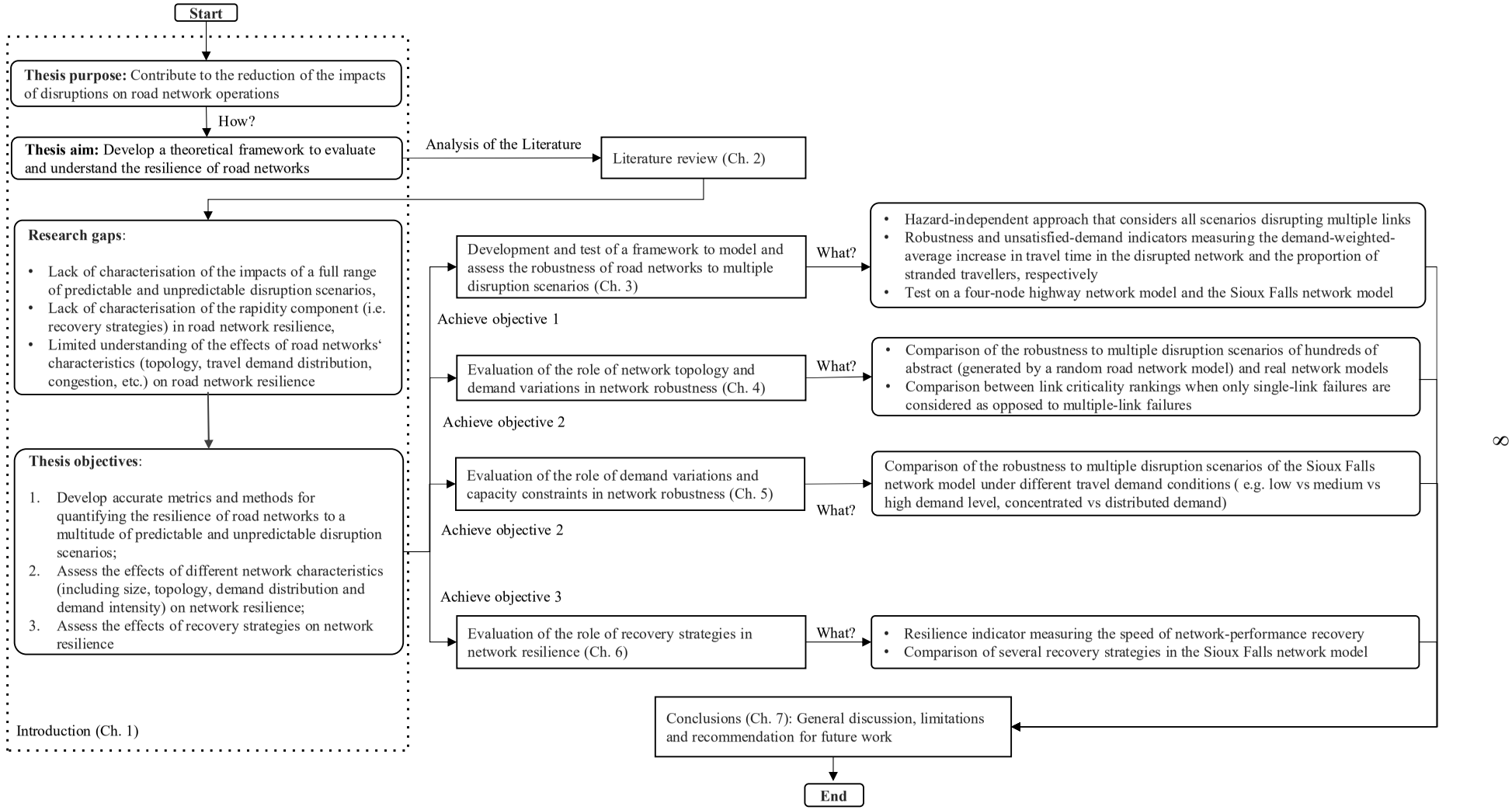

Figure 1.1: Work flow of the thesis

1.4 Outline of the thesis

This doctoral thesis is organised as follows:

Chapter 1 corresponds to the present introduction, which provides a background to this doctoral thesis as well as the research aim, objectives, approach and main assumptions.

Chapter 2 provides an analysis of the literature related to the doctoral thesis. Firstly, background information on road network management is provided. Then, the common properties of road networks and their graph representations are identified through a literature survey. This survey also considers random road graph models. Afterwards, Chapter 2 focuses on disruptive events, traffic incident management and risk analysis. This topic leads to the concept of resilience, which is the focus of the remainder of the chapter. The definitions and concepts associated with resilience are analysed, then several topics related to road-network-resilience assessments are discussed including transport, disruption, and resilience-quantification models.

Chapter 3 builds on the analysis of the literature to develop a robustness assessment framework for road networks. This framework provides two main tools: a hazard-independent approach that considers all possible scenarios disrupting multiple links (more specifically up to a certain number of links) and a set of meaningful robustness indicators suitable to discriminate between the impacts of a wide range of disruptive events. The framework is tested on two case studies: a four-node highway network model and the Sioux Falls network model. The case studies are also used to demonstrate the ability of the proposed robustness indicator to discriminate between a wider range of disruption scenarios than the indicators currently used in the literature.

Chapter 4 also focuses on road network robustness but seeks to evaluate the effects of several network attributes including size, topology and demand distribution on robustness. To this end, this chapter explores the correlation between these network attributes and network robustness to single-, multiple-, random- and targeted-link failures. For this purpose, the GREREC model was developed to randomly generate a variety of abstract networks presenting the topological and operational characteristics of real-road networks, on which a robustness analysis is performed. This analysis quantifies the difference between the link criticality rankings when only single-link failures are considered as opposed to multiple-link failures and the difference between the impact of targeted and random damage. The effects of the network attributes on the network robustness and on the two differences mentioned above are assessed and discussed. Finally, this analysis is also performed on a set of real road networks to validate the results obtained with the artificial networks.

Chapter 5 adopts and improves the hazard-independent model (developed in Chapter 3) to quantify and understand the difference between the impacts of random-, localised-, and targeted-link failures. This Chapter also explores the predictability of the link combinations whose failure would lead to the highest impacts on the system performance, and

the difference between of the link criticality rankings when only single-link failures are considered as opposed to multiple-link failures. Finally, the effects of demand intensity and distribution variability (and therefore congestion) on the network robustness and link criticality metrics are assessed by repeating the robustness analysis under different travel demand conditions in the Sioux Falls network model.

Chapter 6 focuses on quantifying the impacts of recovery processes and, more specifically, link-repair strategies on resilience. This chapter analyses the performance of several link-repair strategies in the Sioux Falls network across a full range of disruption scenarios using the disruption model developed and improved in Chapters 3 and 5, respectively. The strategies considered include: (i) the optimal (minimising the disruption consequences over the recovery process), (ii) average (representing a recovery process where the disrupted links are repaired in random order), (iii) flow-based (where the links with the highest traffic flow in the undisrupted network are repaired first), and (iv) criticality-based (where the links whose individual failure result in the highest impacts on the system performance are repaired first) recovery. The results of this comparison are then used to evaluate the correlation between robustness and resilience, and characterise the optimal repair strategy.

Chapter 7 concludes the thesis by providing a general discussion of the research contributions, implications and limitations, as well as recommendations for future research investigations.

Chapter 2

Literature review

2.1 Introduction

The present literature review aims to provide a background to the different topics approached in this thesis. Section 2.2 focuses on road network administration and road classification to provide a general background to this thesis. Section 2.3 identities the main characteristics of road networks and their graph representations to provide a basis for chapter 4, where a model is developed to randomly generate graphs presenting the main characteristics of road networks. The existing random road network generators are reviewed in Section 2.4. Subsequently, Section 2.5 focuses on disruptive events, traffic incident management and risk analysis. This topic leads to the concept of resilience, which is the focus of section 2.6. Finally, Section 2.7 discusses several topics related to road network resilience assessment including transport, disruption, and resilience-quantification models.

2.2 Road network management

This section introduces two elements of road transport management related to road network resilience: road network administration and road classification.

2.2.1 Road network administration

The present thesis should be of direct interest to road administrations around the world as well as their advisors (e.g., transport consultants, researchers, etc.). The structure of road network administrations varies widely from country to country. In the UK Highways England (formerly called Highways Agency) is responsible for managing motorways and trunk roads in England, whereas other roads fall within the responsibility of local authorities (e.g. Nottinghamshire County Council in the Nottingham area). In contrast, all roads in Northern Island are operated by a single entity: Transport NI.

These authorities have the lead responsibility for developing, implementing and monitoring better incident management procedures as well as managing the response to disruptive events. For example, both Highways England and the county councils manage highway drainage and roadside ditches under the Highways Act 1980 (DEFRA, 2011). Considering that the effective management of the response to disruptive events is as important as the

physical resilience of the infrastructures to extreme events (UK Department for Transport, 2014), road agencies and their procedures play a key role in network resilience.

2.2.2 Road classification

A key aspect of road network management is road classification. Road classification is important for resilience assessments as the latter can focus on certain groups of roads depending on the scope of the assessment and the objectives of the stakeholders.

Road and traffic agencies historically categorise roads based on vehicular traffic (Austroads, 2017). Two main types of "designed" roads are considered: traffic routes serving primarily mobility and local streets serving primarily property access. The movement function being theoretically the inverse of the access function a road with higher traffic movement function has restricted access and vice versa.

This conventional classification was questioned by Marshall (2005) because the theoretical inverse relationship between mobility and access can not fully represent a wide range of multifunctional street types. The author argues that urban streets could be independently classified with regards to travelling speeds, transit orientation (i.e. strategic contiguity or routes connected up contiguously) and urban space criteria.

Nonetheless, the two-dimensional relationship between mobility and access has been incorporated into many road design and management schemes. The UK Department for Transport (2012) adapts this principle to consider five road categories:

- Motorways
- A roads: major roads providing large-scale transport links within or between areas;
- B roads: connecting different areas and feeding traffic between A roads and smaller roads in the network;
- Classified unnumbered roads (also called minor roads): smaller roads connecting unclassified roads with A and B roads, and often linking a housing estate or a village to the network.
- Unclassifed roads: local roads intended for local traffic. The vast majority (60%) of roads in the UK fall within this category.

Besides this road classification, the UK Department for Transport considers a Strategic Road Network (SRN) and a Primary Route Network (PRN) for management purposes. The Strategic Road Network comprises the motorways and major trunk roads in England that are managed by Highways England. The SRN represents approximately 7080 km (4,400 miles) of road (UK Department for Transport, 2012). The Primary Route Network designates "roads between places of traffic importance across the UK, with the aim of providing easily identifiable routes to access the whole of the country" (UK Department for Transport, 2012). Hence, the SRN forms a part of the PRN. Outside of national parks, few places in England are more than 16 km (10 miles) from a primary route (UK Department for Transport, 2012).

2.3 Road network properties

The abstract representation of a transport system as a network of nodes (or vertices) and links (or edges), whether it involves roads, railways or airspace, defines a network topology. Depending on the scope of the study, nodes can represent real-life intersections, major intersections or cities. The same principle applies to the links. Hence, the network nodes and links are given attributes that reflect the field of application and scope of the study. In the case of road networks, the most intuitive and popular approach is to model both intersections and dead-ends as nodes and the road segments between them as links. This section surveys the literature to characterise road networks and their graph representations (based on the popular modelling approach). For the sake of illustration, Figure 2.1 shows examples of urban road maps and their graph representations.

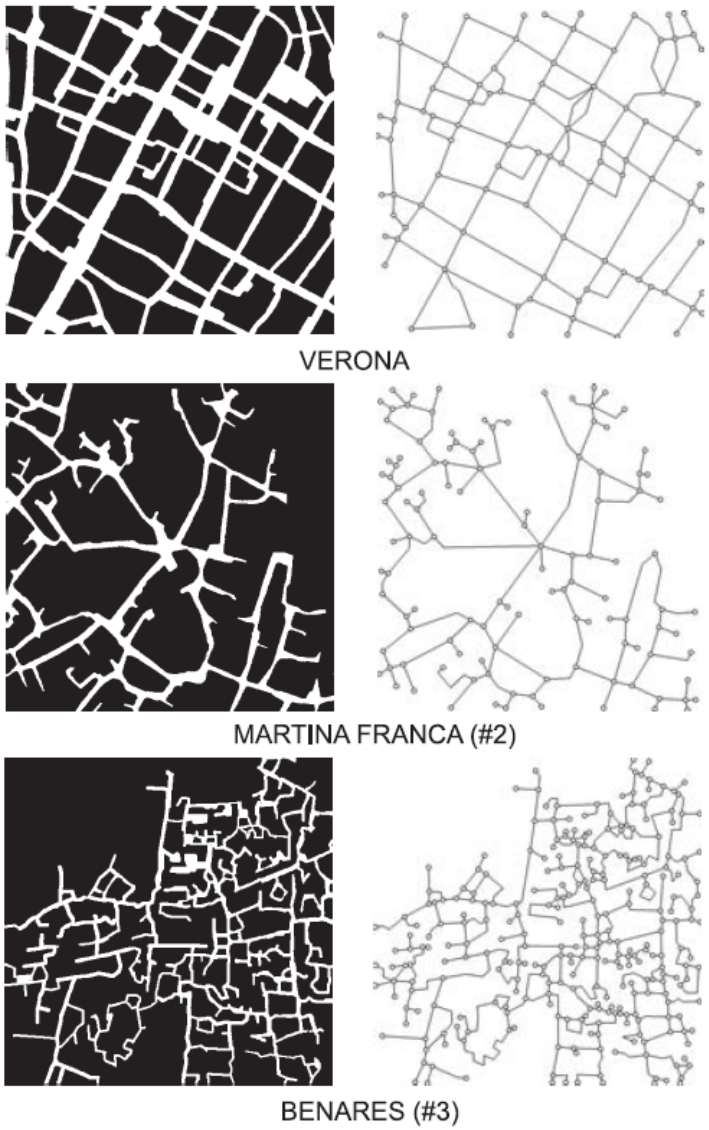

Figure 2.1: Examples of urban road maps (left) and their graph representations (right), extracted from Buhl et al. (2006).

2.3.1 Road networks approximate planarity and patterns

An important characteristic of road networks noted in the literature is their approximate planarity (Peng et al., 2014; Xie and Levinson, 2007). Road networks essentially lie in a plane such that when two roads intersect, a link between them is created. Few exceptions to this rule exist such as elevated highway bridges spanning other roads. Boeing (2018) investigated the planarity of 50 urban street networks worldwide, showing that many road networks can be described as approximately planar. However, the planar simplification can misrepresent intersection densities, street lengths and routing in certain cites that contain a non-negligible number of grade separations such as Moscow (Boeing, 2018).

Several authors (Rifaat et al., 2011; Southworth and Ben-Joseph, 2003) analysed and classified the patterns of urban road networks. Wang et al. (2017b) summarised these studies and classified all road networks as grid (four-legged intersections with right angles and parallel lines), warped parallel (straight lines mostly parallel to each other with curved or rectilinear formations and three-legged intersections), mixed (no dominant pattern), loops and lollipops (tree-like structure with cul-de-sacs, branches and three-legged intersections) and sparse (discontinuous and decentralised with a high proportion of cul-de-sacs). As an indication, according to Wang et al. (2017b), all of these patterns could be identified in community areas in Florida's Orange County (USA).

2.3.2 Road networks intersections

Network topologies are typically characterised by the distribution of the degree (i.e. the number of adjacent links) of their nodes. The studies of Cardillo et al. (2006), Masucci et al. (2009) and Wang et al. (2017a) evaluating the topology of network samples from 20 cities, London (UK) and Xiamen Island (China) respectively allow characterising the degree distribution in road networks. Undirected graphs representing road networks generally have very few six-or-more road intersections, few five-road intersections, a large number of four-road intersections and a very large number of three-road intersections except in cities presenting a dominant square-grid structure (e.g. San Francisco) where four-street intersections are more frequent than three-street intersections.

These empirical studies show that the number of connections of road intersections is limited. In road networks, two distant nodes are less likely to be directly connected due to the distance-dependence of the links travel costs (Buhl et al., 2004). Hence, although intersections connecting more than six roads exist (e.g. the roundabout at Place Charles de Gaulle in Paris connects 12 streets) they are very rare and can be treated as exceptions.

2.3.3 Road networks links

Another important characteristic of road networks noted in Xie and Levinson (2007) is the heterogeneity resulting from road hierarchy (i.e. roads are typically categorised into minor and major local streets, regional roads, and highways as discussed above) that differentiate between functional properties and operational performance of roads, which provide both property access and travel mobility. Local streets mainly serve the land access function while arterial roads (e.g. highways) provide a high level of mobility for through movement.

Road hierarchy results in heterogeneous link travel costs. It is, however, difficult to go

beyond this statement and define a general distribution for the link travel costs in road network models because these costs depend on dynamic factors such as the link travel time (which depends on a variety of parameters including the link length, speed limit and traffic conditions). Furthermore, even the distributions of static parameters like the length of the links present several configurations. Crucitti et al. (2006) found that self-organised cities (e.g. Cairo, Egypt) exhibited single-peaked distributions while planned cities (e.g. Los Angeles, USA) exhibited multimodal distributions due to their grid pattern. However, Crucitti et al. (2006) did not report any specific distribution. Masucci et al. (2009) fitted a power-law (with a cut off for the longest streets) to the London street network model. The study of Strano et al. (2013) that considered 10 European cities showed slightly different results as a power-law emerged in the distribution tails but the fitting worsened with decreasing link lengths. They observed that the percentage of streets failing inside the power-law region ranged from 4% (Barcelona, Spain) to 29% (Lancaster, UK) and suggested that cities may be composed of streets following two distributions.

2.3.4 Summary of the characteristics of road networks and their graph representations

Finally, the review of the different studies of real-world road networks topologies and patterns allowed identifying the main properties of road networks and their representations:

- road networks are not universally planar but many road graphs can be approximated as planar;
- road networks include patterns ranging from the regular grid and wrapped parallel structures to the more irregular loops, lollipops and sparse structures;
- road graphs have a negligible proportion of intersections with six or more connections;
- road graphs comprise a large majority of three or four road intersections;
- the functional properties and performance of road links are heterogeneous.

2.4 Random road network models

In this thesis (more specifically in Chapter 4), a novel random road graph model is developed and used to evaluate the correlation between road network properties and resilience. The present subsection surveys existing random road network models to provide a background to this topic.

Random road network models were developed for different purposes. Bai et al. (2003) used a grid model to evaluate the impact of mobility (e.g. connected vehicles on a freeway) on the performance of routing protocols for ad hoc networks. That model is very regular and does not hold many features of real road networks like the heterogeneity in nodal degrees. More sophisticated models for generating random road network models have been proposed by the research community in complex network theory. Gerke et al. (2007) proposed a planar variant of the classical Erdős–Rényi random graph model (in

complex network theory a "random network" refers to a network where each node pair is connected with a fixed probability). Masucci et al. (2009) built on this basis to propose the Growing Random Planar Graph (GRPG) that seeks to mimic the effect of urban sprawls. Unfortunately, both models tend to generate more high degree nodes (superior to six) than observed in real networks. Eisenstat (2011) also notes that the GRPG model results in an unrealistic abundance of acute-angled intersections.

Other works focused on developing models for road networks at a larger scale (e.g. national scale) that hence account for the diversity in road hierarchy. Kalapala et al. (2006) studied the topological and geometric structure of the national road networks of three countries (i.e. Denmark, England and the USA). The study revealed that all journeys from a postal code to another, regardless of their length, have an identical structure. Drivers seeking to optimise their travel time would typically start their journey in a local street close to their point of origin, and progressively move to larger and faster roads (which are higher in the road hierarchy) until reaching the fastest single road between their origin and destination. On this road, they cover as much distance as possible, and then progressively descend to smaller roads until their destination. This finding led Kalapala et al. (2006) to introduce a square-grid fractal model for road placement that reproduces both the observed hierarchical and scale-invariant structure of journeys. Noting that the basic fractal model was too regular to resemble real road networks, Eisenstat (2011) proposed the *quadtree* model, which employs the fractal model but uses a random tree to distribute the smaller square grids in the network. The drawback of both models is that the degree of the intersections in the networks generated is limited to four.

To overcome the shortcomings of the grid model, Peng et al. (2014) developed the Grid model with Random Edges (GRE). The main idea of this model is to randomly introduce the effects of obstacles and shortcuts in the basic grid model. Obstacles (e.g. buildings, parks and rivers) normally make a road network sparser as they prevent certain roads from being built while shortcuts (i.e. diagonal links in the grid) make a road network denser. Using an optimisation algorithm and six parameters (the area length and width, the average lengths of vertical and horizontal lines in the network model, a probability controlling the presence of horizontal and vertical lines to simulate obstacles, and a probability controlling the presence of shortcuts), they fit the model to real road network samples from 66 main cities in Europe and the USA. The topological characteristics (i.e. average nodal degree, average shortest path length, and density of nodes and links) of the abstract models and real networks were reasonably correlated especially in the case of the US cities (for which the fitting process was easier since they generally do not have shortcuts).

2.5 Disruptive events management

2.5.1 Disruptive events

Disruptive events can impact both the supply and the demand side of the transport system. The supply side (i.e. the network) is affected by the damage induced on the infrastructures, which in turn impacts traffic conditions through road unavailability as well as speed and capacity reductions. The demand side that represents the users' flow patterns, mode choice

and average speed is also impacted. The effects on the demand side include for example trip cancellations due to destinations being affected or re-routing due to congestion on usual routes.

According to the CEDR (2009) disruptive events are responsible for around 10% to 25% of the congestion experienced in Europe (i.e. 10-15% in Sweden and 25% in England) and are the largest single cause of journey unreliability. In the USA, the estimated loss due to disruptive events is 1.3 billion vehicle-hours of delay congestion each year costing almost US$10 billion (FEMA, 2012). Disruptive events can be categorised based on several factors: cause, scale, severity, etc. This section makes a distinction between man-made and natural events.

Man-made events

Man-made events range from small accidents leading to the closure of one lane in a local road to major accidents causing a motorway closure for several hours with cascading effects affecting the entire network. El-Rashidy (2014) gives the example of a five-vehicle crash on the westbound carriageway of the M26 motorway, which occurred in Kent (UK) on 16 April 2014 and led to the closure of M26 in both directions for over six hours. The motorway was then partially reopened (i.e. one lane was opened on the M26 eastbound) while the second eastbound lane and the westbound lanes between M20 and M25 remained closed for 12 hours (BBC, 2014). According to the BBC report (2014), two people died in the crash while others were seriously injured. The accident also led to a hundred vehicles being trapped on the motorway for several hours.

Sabotage and terrorist actions such as New York 9/11 and London 7/7 are also man-made events that can disrupt road traffic and cause widespread economic losses (Cox et al., 2011). Finally, infrastructure deterioration due to ageing and repair works can also lead to disruptions. For example, the road works carried out in London regularly lead to "significant congestion and reliability costs on road users and businesses" (Arter and Buchanan, 2010).

Natural events

Natural events (such as earthquakes, extreme temperatures, high winds, heavy rain and snowfall) affect road infrastructures and disrupt traffic flows. The impacts of natural events are manifold and include reductions in visibility, vehicles stability manoeuvrability, traffic speeds and road capacity as well as increases in maintenance costs, operations costs and accident rates (Maze et al., 2005; Pisano and Goodwin, 2004; UK Department for Transport, 2014). However, it is noted that accidents occurring during rain or winter conditions seem less severe as they involve fewer fatal crashes (Brown and Baass, 1997). This is mainly attributed to the decrease in vehicle speeds during adverse weather conditions.

Floods and winter conditions were found to cost Europe and the UK more than any other weather-related disruptive event (Enei et al., 2011). Chatterton et al. (2010) estimated the cost of the summer 2007 flood—caused by exceptional rainfall—at £191 million. Approximately half of this amount is due to road infrastructures damage whereas the over half is due to traffic delays. The authors recognised however that there is much uncertainty about the estimate of traffic delay and redirections.

Finally, natural events are expected to increase in severity and frequency due to climate change. Hence, numerous policy-makers and practitioners emphasise the need to protect transport infrastructures from climate change (Colin et al., 2016; DEFRA, 2011; Kiel et al., 2016).

2.5.2 Traffic incident management

When disruptive events occur congestion quickly builds and the likelihood of a secondary incident increases (Austroads, 2017). Depending on the incident location and traffic distribution, the travel time of road users may increase at the route, area or network level. From a safety perspective, Karlaftis et al. (1999) found that each minute of clearance time of the primary incident increases the likelihood of a second crash by 2.8%. Therefore, Traffic Incident Management—the process of detecting, responding to, and clearing traffic incidents (Austroads, 2017)—plays a key role in reducing the impacts of incidents on safety and traffic operation. A typical Traffic Incident Management process involves six operational stages: detection and verification, motorist information, response, site management, traffic management, and clearance (Austroads, 2017).

2.5.3 Risk analysis vs Resilience analysis

So far, the dominant approach used to inform the management of disruptive events in engineering systems has been risk analysis (Park et al., 2013). Typical risk analyses involve three stages: risk identification and characterisation, risk exposure analysis, and consequences analysis.

However, Park et al. (2013) challenge the applicability of risk analyses to complex systems. Complex systems such as transportation networks are in a a perpetual dynamic state because they involve engineering, human and natural systems interacting together while they are subject to both external and internal forces. Hence, a range of hazards occurring in complex systems are unpredictable. For instance, prior to the London 7/7 attacks, it was difficult to conduct comprehensive risk analyses of terrorist attacks since there was little information about the location, time and consequences of such events (El-Rashidy, 2014).

To overcome this limitation, addressing the resilience (ability to resist, recover from and adapt to shocks) of complex systems can be a more suitable approach since it is a dynamic property emerging and observable across a variety of disruption scenarios (Park et al., 2013). Resilience analyses accept the possibility that a wide range of disruptive events may occur but are not necessarily predictable, and focus on anticipating and protecting the performance of the disrupted system rather than preventing or mitigating the loss of assets due to specific events (ARUP, 2014).

2.6 The concept of system resilience

2.6.1 Definitions and concepts

The term resilience originates from the Latin word “resiliere” which means to bounce back (Henry and Ramirez-Marquez, 2012). The concept of resilience was extended to

systems by Holling (1973), as the ability of ecological systems to "absorb changes of state variables, driving variables, and parameters, and still persist." Since then, the word has been adapted and reinvented to refer to the capacity of systems to anticipate, sustain and recover from external shocks, as well as, the ability to cope with changes in general (IPCC, 2012; Martinson, 2017).

The growing interest in resilience led to confusion over its concept as several authors, (e.g. Ganin et al., 2017; Henry and Ramirez-Marquez, 2012), found a lack of consensus and rigour in the use of the term. For example, the concept of resilience overlaps other concepts such as robustness and reliability, often confused with resilience (Bruneau et al., 2003; Ganin et al., 2017). To provide more clarity, the different definitions available have been surveyed. The review highlighted the concepts connected to the word resilience.

The seminal framework introduced by Bruneau et al. (2003) associates system resilience with the following notions: (i) reduced failure probabilities (ii) reduced consequences from failures and (iii) reduced time to recovery. The framework includes two historical definitions of resilience. The first one, attributed to Holling (1973), refers to the perturbation that can be absorbed before the system is displaced from one state to another. The second definition describes resilience as the speed of the system to return to its initial equilibrium (Pimm, 1984). These definitions led to two distinct approaches to resilience (Reggiani, 2013). On the one hand, Pimm's definition (1984) marks the origin of the engineering resilience—in which the system has a unique equilibrium. On the other hand, the ecological resilience, accredited to Holling (1973), expects the system to move from a state of equilibrium into a new, different and stable state after a shock. In the latter, the focus shifts from the system itself to its function and output (Spaans and Waterhout, 2017).

Woods (2015) identified four concepts associated with resilience in the context of complex systems:

- Resilience as rebound from trauma and return to equilibrium;
- Resilience as a synonym for robustness i.e. capacity to absorb perturbations;
- Resilience as opposite of brittleness, i.e. ability to extend adaptive capacity in the face of unexpected events;
- Resilience as network architectures that can sustain the ability to adapt to future events as conditions evolve.

The first two categories match the historical definitions of resilience and the last two concepts of Bruneau et al. (2003). In the third and fourth categories Woods (2015) insists on the ability to "adapt" with the idea that the first two categories (i.e. resilience as rebound from trauma and return to equilibrium, and resilience as a synonym for robustness) are concerned with known or well-modelled perturbations only.

Ultimately, the two main concepts associated with resilience in the majority of the literature are the ability to absorb perturbation and recover quickly. The other resilience concept (i.e. "reduced failure probabilities") mentioned by Bruneau et al. (2003) has evolved to refer to the capacity to adapt to unexpected events and conditions. The confusion over the concept of resilience probably derived from the existence of these different notions and the tendency of researchers to focus on one of these notions when addressing

particular systems (Koliou et al., 2018). System resilience as a comprehensive concept can thus be summarised with three pillars: reducing (i) consequences (ii) recovery time (iii) and vulnerabilities to future expected and unexpected conditions.

2.6.2 Properties and related subjects

As explained above, the concept of resilience comprises three pillars: reduced consequences, reduced recovery time and reduced vulnerability to future unpredictable shocks. Therefore, a resilient system should exhibit these three abilities. A possible approach to assess the resilience of a system is to consider the properties of resilient systems.

Many researchers and practitioners took this approach, proposing conceptual frameworks desegregating resilience into several properties. Their studies provide further insights into the notion of resilience and help to determine the boundaries and relationships between resilience and other terms such as robustness, vulnerability, and reliability. Table 2.1 provides an overview of the different concepts and properties usually connected to system resilience.

Table 2.1: Overview of the properties often associated with system resilience

Properties (alphabetical order)	Definitions (adapted from reference data)	Relationship with resilience according to reference data (author, date)		
		Bruneau et al., 2003	Godschalk, 2003	Hosseini et al., 2016
Adaptability (or flexibility)	Capacity to change and adapt in response to changing circumstances	-	Property of resilient systems*	-
Rapidity (or Recoverability)	Capacity to meet priorities and achieve goals in a timely manner in order to contain losses	Resilience property	-	Resilience dimension
Redundancy	Extent to which elements exist that are substitutable (i.e. spare capacity purposely created within systems to accommodate disruption and surges in demand)	Resilience property	Property of resilient systems*	-
Reliability	Ability to maintain typical operation prior to a disruption	-	-	Resilience dimension
Resourcefulness	Capacity to identify problems, establish priorities, and mobilize resources when a disruption occurs	Resilience property	-	-
Robustness (or Strength)	Ability to withstand a given level of stress or demand without suffering degradation or loss of function	Resilience property	Property of resilient systems*	-
Vulnerability	Ability to stave off initial impacts after an adverse event	-	-	Resilience dimension

*The other properties mentioned by Godschalk (2003) are: Diversity, Autonomous components, Collaboration, Efficiency and Interdependence

Godschalk (2003) reviewed several studies of system resilience to identify the common

characteristics of resilient systems (Table 2.1). According to Godschalk (2003), resilient systems are composed of small *autonomous* (able to operate independently) components with *diverse functionalities* ("to protect the system against various threats"). They are also *efficient* (optimised input-output ratio), *redundant* ("so that the system does not fail when one component fails") and *strong* (able to withstand an adverse event). Furthermore, *collaboration* (shared information and resources among components or stakeholders) and *adaptability* (the capacity to learn from experience and change) are additional indicators of resilience.

Bruneau et al. (2003) associate resilience of both physical and social systems to the 4R's: *robustness, redundancy, rapidity and resourcefulness* (defined in Table 2.1). They also see robustness and rapidity as resilience "ends" (i.e. outcomes that deeply affect stakeholders), while redundancy and resourcefulness are resilience "means" by which system resilience can be improved. In other words, although adding redundant elements to a system can enhance resilience, robustness and rapidity are the key measures that should be used to evaluate the benefits of this strategy.

Subsequent studies draw on the work of Bruneau et al. (2003) and Godschalk (2003). For instance, Reed et al. (2009) mentioned the 4R's in a resilience assessment of a power supply network after Hurricane Katrina. Simonovic (2018) used them to assess the resilience of a railway network under flooding. Researchers and practitioners also supplemented these sets of properties to propose their own context-specific frameworks, e.g. Murray-Tuite (2006) in the context of transportation systems and ARUP (2014) in the context of cities.

Reliability and *vulnerability* are two other concepts often associated with system resilience. Referring to the approach of Henry and Ramirez-Marquez (2012), Hosseini et al. (2016) described them as part of a time-dependent process involving a disturbed system:

- Reliability is the "ability of the system to maintain typical operation prior to a disruption";
- Vulnerability is the "ability of the system to stave off initial impacts" after the disruptive event;
- Recoverability is the "ability of the system to recover in a timely manner."

In this framework, a resilient system encompasses these three abilities. The definitions of robustness and vulnerability are close (Table 2.1) such that vulnerability is often viewed as the opposite of robustness (Simonovic, 2018).

The seminal definition of reliability as the ability of a system to "perform its required functions under stated conditions for a specified period of time" (IEEE Computer Society, 1991) is compatible with the framework of Hosseini et al. (2016) where reliability focuses on the system pre-event performance. However, this focus on the system pre-event performance also suggests that reliability is not essential in resilience analyses as the latter focuses on the consequences of disruptive events. The focus on consequences allows resilience studies to consider unpredictable events while reliability studies often deal with probabilities and predictable events.

Finally, it is noted that there is no consensus on the definitions and relationships between the different concepts and properties mentioned above as the same terms can

be used with different definitions in different contexts. For instance, in the context of hazard mitigation, Cutter et al. (2008) view resilience and vulnerability as separate but often linked concepts, while some researchers consider resilience as an integral part of vulnerability. In the present thesis, system resilience is considered as a comprehensive concept that can be measured by the system robustness and rapidity—as proposed by Bruneau et al. (2003). The adaptability side of resilience is included in the present thesis by the consideration of a multitude of potentially unpredictable disruption scenarios.

2.7 Resilience modelling and quantification for road network management

The present section draws on the understanding of system resilience established above to analyse the literature on resilience modelling and quantification for road network management. This section discusses three aspects of the different studies and approaches available in the literature: the transport model, disruption model, and resilience quantification model.

2.7.1 Transport models

Transport models represent real-world transport and land use systems to predict and analyse their performance under different conditions. Two main types of transport models can be identified in road-network-resilience assessment studies: topological and traffic flow models.

Topological models

Topological studies root in graph theory and focus on measuring the resilience of road networks based on their structure (the arrangement of the roads and intersections). Road infrastructures are modelled as a graph $G(V, E)$ composed of a set of nodes or vertices (V) and a set of links or edges (E). The most intuitive and popular approach (called primal representation) is to model both intersections and dead-ends as nodes and the street segments between them as links. This approach "retains the geometric patterns and geographical properties of transportation systems" (Lin and Ban, 2013). Depending on the scope of the study, nodes can represent real-life intersections, major intersections or cities. The same principle applies to the links. The latter are attributed weights corresponding to their actual lengths, travel times, monetary costs, or a generalised travel cost combining the previous metrics.

Alternatively, the graph can represent the network intersections as edges and the road segments as vertices. This approach (called dual representation) reflects the functional structure of the transport network (Lin and Ban, 2013) in the sense that users generally navigate from one street to another (for example, GPS systems provide the name of the streets that we should follow not the name of the intersections). The dual representation provides a better picture of road hierarchy (Kalapala et al., 2006; Lin and Ban, 2013) and leads to graphs with higher degrees than that of the primal graphs. Therefore, the dual representation of a road network is comparable in its degree distribution with computer, ecological or social networks (Casali and Heinimann, 2020).

Considering the geographical nature of road disruptions, most of the studies on the resilience of road networks (Buhl et al., 2006; Casali and Heinimann, 2019; Hu et al., 2016; Zhang and Wang, 2016; Zhang et al., 2015) use the primal representation. These studies measure the impacts of disruptions on the distance between the nodes—or Origin-Destination (OD) zones—, the network connectivity (i.e. the number of nodes—or OD zones—that are connected), or the number of redundant alternative routes between the OD zones. However, topological models disregard traffic flows and link capacity constraints. Hence, these studies are unable to capture dynamic effects of the disruption such as increased congestion on alternative routes and the related behavioural responses (Mattsson and Jenelius, 2015).

Traffic-flow models

Traffic-flow models also represent roads into graphs but add another layer to the physical network representation: the distribution of the flow of vehicles through the network. As a result, traffic flow studies generally provide a more realistic assessment of the consequences of disruptions for the users and society (Mattsson and Jenelius, 2015). The resilience studies based on traffic-flow models generally measure the impact of the disruption on the users' travel time and sometimes consider the environmental (Omer et al., 2013) and economic implications (Kurth et al., 2020; Omer et al., 2013) of the disruptions.

However, in comparison to topological analyses, traffic-flow analyses present two major disadvantages: their data hungriness and computational complexity. These analyses require travel demand data (describing the origin and destination of the users) and calibrated behavioural models (describing the users' response to changes in their travel costs) that are often unavailable. Besides, considering the computational effort required for traffic simulations, it is currently unrealistic to perform thousands of disruption simulations that each require a traffic analysis as with topological analyses. This is especially true for large networks as the computational effort of traffic simulations exponentially increases with the size of the network model.

The traffic models used in the literature typically minimise the travel cost of all road users (Bhavathrathan and Patil, 2015a, 2015b; Omer et al., 2013), assume that users independently minimise their own travel cost (Ganin et al., 2017) or that only the users affected by the disruption modify their routes (Faturechi and Miller-Hooks, 2014). These assumptions are called as System-Optimum, User-Equilibrium, and Partial-User-Equilibrium traffic assignments respectively. The traffic assignment is the fourth stage of the seminal four-step (trip generation, trip distribution, modal split, and traffic assignment) transport model (Ortúzar and Willusem, 2011) that can be used to estimate the number of vehicles (or people) that will use a specific transport facility based on travel data that can be obtained through census information, surveys, and estimates. The assumptions related to the traffic model are however rarely validated against real-life data as the travel demand data required are often unavailable. More sophisticated traffic models are also used in the literature including dynamic models considering the evolution of the traffic flow over time (Gauthier et al., 2018; Nogal et al., 2016) and stochastic models considering the subjectivity of the users' response to the disruption (Nogal and Honfi, 2019). These features however increase the data requirements and computational complexity of transport

models.

2.7.2 Disruption models

As explained in Chapter 1, the resilience of road networks should characterise their ability to deliver this function under a multitude of potentially unpredictable conditions. However, assessments of the potential impact of disruptive events on road networks generally focus on a few scenarios illustrating the proposed methodology (Nogal et al., 2016; Omer et al., 2013; Zhang and Wang, 2016) or the worst-case scenario using a game theory approach (Alderson et al., 2017; Bhavathrathan and Patil, 2015a, 2015b, 2018). These studies do not uncover the potential impact of all possible disruption scenarios as suggested by the resilience paradigm.

A range of recent studies consider multiple disruption scenarios in the road transport context. For example, Zhou et al. (2017) and Wisetjindawat et al. (2017) proposed interesting frameworks to consider multiple hazards. Both studies, however, belong to the risk analysis paradigm, which relies on records of past disruptions (including road accidents, maintenance and disasters), that may overlook unpredictable events as explained above (Section 2.5).

Ganin et al. (2017) performed twenty realisations of disruption scenarios affecting a random and finite number of links on traffic flow models of 40 US cities. The purpose of the study was to compare efficiency (the annual delay in peak-periods under normal conditions) and resilience (the annual delay in peak-periods due to disruption) across different network topologies. Hence, the impacts of the different disruption scenarios were not studied in detail and the number of scenarios considered relatively limited. The other studies that consider multiple disruption scenarios can be divided into two groups: dismantling process studies and link criticality studies.

Dismantling process studies

The research community in complex network theory has studied robustness as the changes of some metric of the network functionality against the fraction of removed nodes (or links) to understand how many nodes (links) have to be removed to fragment a network into isolated components (Réka et al., 2000; Zanin et al., 2018). Applications of the "dismantling process" approach to road networks are available in (Buhl et al., 2006; Casali and Heinimann, 2020; Hu et al., 2016). Buhl et al. (2006) and Casali and Heinimann (2020) performed hundreds to thousands of realisations of different types of dismantling processes on self-organised street networks (e.g. Rome) and the Zurich road network, respectively. Hu et al. (2016) compared different types of dismantling processes and recovery strategies in square grids and the road network of the Hainan province (China).

These three studies made a distinction between *targeted* and *random* dismantling processes. The latter model damage to a random set of links (e.g. pavement maintenance, pipe bursting or police incidents amongst others can lead to random road closures) whereas targeted attacks imply a driving force seeking to maximise damage to the network (e.g. the bombing of a critical bridge). Besides random and targeted failures, Hu et al. (2016) considered *localised* failures (e.g. landslides, flooding). Unlike random and targeted failures that cause damage to network components distributed throughout the whole system, lo-

calised damage lead to aggregated destruction of adjacent components limited to a specific area. While random and targeted failures are commonly considered in complex network theory (Réka et al., 2000; Zanin et al., 2018), the consideration of their localised counterparts is more recent (Hu et al., 2016).

However, the focus on dismantling processes only is not necessarily appropriate for road network management. Dismantling-process analyses are useful to determine the critical number of failed components after which networks can no longer function. This information is important, for example, to address mutations and router problems in gene and computer networks respectively (Réka et al., 2000). For road networks, this information is relevant only when analysing major disasters (e.g. earthquakes or large floods) that can potentially damage many roads. This is because contrary to computer, ecological or social networks, road networks are composed of large physical infrastructures that are difficult to damage. Hence, dismantling processes lack applicability to a wide range of road perturbations such as car accidents, sabotage actions and landslides that disrupt a limited number of roads. Besides, experience showed that the unavailability of a small fraction of a transport network can lead to major consequences for society and the economy. For instance, the collapse of the I-35W Bridge in Minneapolis (USA) resulted in economic losses of US$71,000 to US$220,000 a day (Xie and Levinson, 2011). Hence, a better understanding of the potential impacts of events disrupting a limited number of links and intersections remains important in practice.

Link criticality studies

Another group of studies, that can be called link criticality studies, traditionally consider a full range of predictable and unpredictable disruption scenarios. These studies seek to identify the links whose failure would result in the highest impacts on the network performance. The rationale for such studies is that the most critical roads should be given top priority for pre-event reinforcement and post-event restoration.

To identify critical links in a network, Taylor et al. (2006) proposed an approach based on single-link failures (SLFs) where each link is removed from the network model and the corresponding effect on the network performance is estimated. The levels of impact are then ranked and the links demonstrating the most significant impacts are considered the most critical. This approach has been widely adopted and improved in subsequent studies (Gauthier et al., 2018; Omer et al., 2013; Sullivan et al., 2010) that also considered link capacity reductions rather than complete link removal. However, capacity reductions add to the already high computational cost of this approach since several scenarios need to be computed per link.

A growing concern in link criticality studies is that this approach disregards the effect of multiple-link disruptions. Wang et al. (2016) showed that the most critical links in multiple-link failures are not simply the combination of the most critical links with single-link failure. Hence, the consideration of single-link failures only is insufficient as this approach could lead to inefficient prevention and restoration measures in the advent of events disrupting several road segments or several events concurrently affecting different parts of the network.

2.7.3 Resilience quantification models

As discussed above, resilient systems are associated with two main properties: robustness—the ability to function despite disturbances—and rapidity (or recoverability)—the ability to recover its functionality quickly. In the context of road networks, most papers (e.g. Bhavathrathan and Patil, 2018; Ganin et al., 2017; Gauthier et al., 2018; Omer et al., 2013) focus on robustness while recovery processes have attracted less attention. The present subsection discusses the resilience quantification models that focus on robustness, before discussing the models that consider recovery processes.

Robustness quantification

Robustness measures (that do not address rapidity) are sometimes referred to as resilience measures in the literature e.g. in (Ganin et al., 2017; Omer et al., 2013). These resilience indicators are considered as robustness measures in this Chapter although they are not referred to as is in the references. Robustness metrics focus on the instantaneous loss of performance of the system following a disruption without considering the subsequent recovery process. The majority of these metrics compare the network pre- and post-event functionality. Depending on the transport and disruption models adopted (discussed in the previous subsections), the network functionality is measured by the network connectivity, the network redundancy, the users' travel time, etc. In reality, robustness indicators should compare the required- and disrupted-network performance to evaluate the ability of the system to provide functionality despite disruption. However, as the definition of the required performance is arbitrary (since it depends on the judgement of the transport operators, public authorises and users), the network pre-event performance is often used as a proxy for the required performance.

The robustness indicators available in the literature range from the simple difference (Ganin et al., 2017) or ratio (Bhavathrathan and Patil, 2015a, 2015b; Omer et al., 2013) of the network performance metrics to more complex indicators such as the indicator of Ip and Wang (2011) and Zhang and Wang (2016). Ip and Wang (2011) defines the resilience [*sic*] of a transport network as the weighted sum of the resilience of the nodes, the node resilience being the weighted average number of reliable routes to all other nodes. The index of Zhang and Wang (2016)—called Weighted average number of reliable Independent Path Ways ($WIPW$)—follows the same principle. $WIPW$ assesses the extent to which redundant alternative routes exist between the OD pairs (i.e. combinations of trips' starting and ending points):

$$WIPW = \sum_{i=1}^{n} w_i r_i \tag{2.1}$$

where w_i and r_i are the weighting factor associated to node i and the average number of reliable independent pathways (IPWs) between i and any other nodes in the network model, respectively. w_i reflects the importance of i being connected during a disaster (i.e. w_i is inversely proportional to the shortest distance from i to the nearest emergency centre). r_i is also computed using weighting factors that take into account:

- the number of IPWs between i and any other nodes

- the reliability (i.e. failure probability) of the IPWs
- the average daily traffic and length of the IPWs (which reflect the relative impact of the pathway on society).

This method differs from the other robustness quantification methods as it includes the reliability of the links in a network-level assessment. However, this assessment is hazard-specific, requires data on the link reliabilities, and is therefore appropriate for certain hazards only (e.g. earthquakes). With their indicator, Zhang and Wang (2016) attempt to take into account the fact that during and after disasters, users are likely to modify their usual routes to reach emergency services or evacuate the affected area. This topic is addressed in more details in a growing research area called "evacuation and emergency transport modelling". An overview of the research on highway-based evacuation modelling and simulation is available in (Murray-Tuite and Wolshon, 2013).

Resilience quantification

Several generic (i.e. applicable to any system using the appropriate context-specific functions) frameworks were developed to assess the resilience of engineering systems (Bruneau et al., 2003; Henry and Ramirez-Marquez, 2012; Sharma et al., 2018). These frameworks include the seminal work of Bruneau et al. (2003) that defines robustness and rapidity as the key measures that should be used to quantify resilience and introduces a graphical interpretation of the resilience concept where the latter is measured by the integral of the quality of infrastructure over time. This concept—called resilience triangle—is illustrated in Figure 2.2, where the quality of infrastructure is measured by the quantity $100 - Q(t)$, $Q(t)$ being the system performance expressed in percentage. As shown in Figure 2.2, a hazard causes a sudden drop in performance at t_0, after which the system gradually recovers its performance until t_1 when the system is completely repaired. The integral hence measures both the loss of performance and the time required to return to the pre-event performance. Henry and Ramirez-Marquez (2012) proposed a time-dependent system resilience measure alongside with a time-to-recover and a resilience-cost metric. More recently, Sharma et al. (2018) proposed a series of partial descriptors based on the analogy of the system recovery curve with a cumulative distribution function in probability theory including resilience "centre" and resilience skewness.

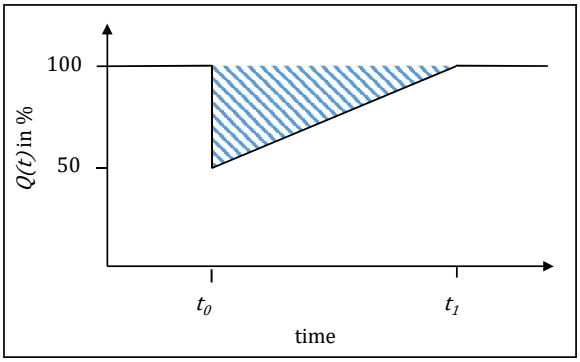

Figure 2.2: The resilience triangle—adapted from Bruneau et al. (2003).

In the context of road networks, the studies that consider recovery processes propose different approaches. Nogal et al. (2016) and Nogal and Honfi (2019) focus on the gradual adaptation of road users following both the perturbation and restoration phases. Tuzun Aksu and Ozdamar (2014) developed a model optimising the link-repair sequence to quickly recover the network connectivity to facilitate evacuations. Zhang et al. (2017) developed a model optimising the link-repair sequence to quickly improve the network performance under stochastic damage levels and repair durations. To this end, the authors added recovery processes to their robustness quantification method (Zhang and Wang, 2016). Finally, Hu et al. (2016), compare different repair strategies under random, localised, and targeted perturbations. However, the studies of Hu et al. (2016), Tuzun Aksu and Ozdamar (2014) and Zhang et al. (2017) rely on topological transport models that do not consider link capacity constraints (which are discussed above).

Noting that recovery processes are case-specific and depend on whether infrastructures are damaged, Murray-Tuite (2006) suggest that when the infrastructure is damaged, recovery could be measured by the amount of time, money, and outside assistance required to restore connectivity at an acceptable level of service. In the case where infrastructure is not damaged, the author proposes to measure recovery by the amount of time required to alleviate congestion.

2.8 Summary and concluding remarks

The present chapter provides a background to the research presented in this doctoral thesis. The literature survey covered several topics including road network management, road networks properties, random road network models, disruptive events management, and road network resilience. This chapter firstly highlighted the role of road agencies and their management practices (road classification and life cycle asset management) in road network resilience. Then, a review of studies examining real road networks topologies and patterns was conducted to identify the common properties of road graphs including approximate planarity, negligible proportion of intersections with six or more connections and heterogeneity in roads functionality and performance. This chapter also discussed the random graph models available in the literature. This discussion showed that the GRE model synthesizes most of the topological characteristics of road networks. This model is therefore used as a basis to build the random road graph model used in this thesis (Chapter 4).

The review subsequently focused on disruptive events management. It was shown that road networks are increasingly exposed to a wide range of disruptive events threatening their usability. These events were categorised into man-made and natural events. Figure 2.3 summarised this classification as well as the interactions between the different types of events.

The review showed that the management of disruptive events could be informed by two approaches: risk analyses and resilience analyses. Risk analyses focus on the probability of occurrence and consequences of disruptive events and therefore have limited applicability to complex systems (such as road networks) that often face unpredictable and unknown hazards. In contrast, resilience analyses accept the possibility that a range of disruptive events may occur but are not necessarily predictable, and focus on anticipat-

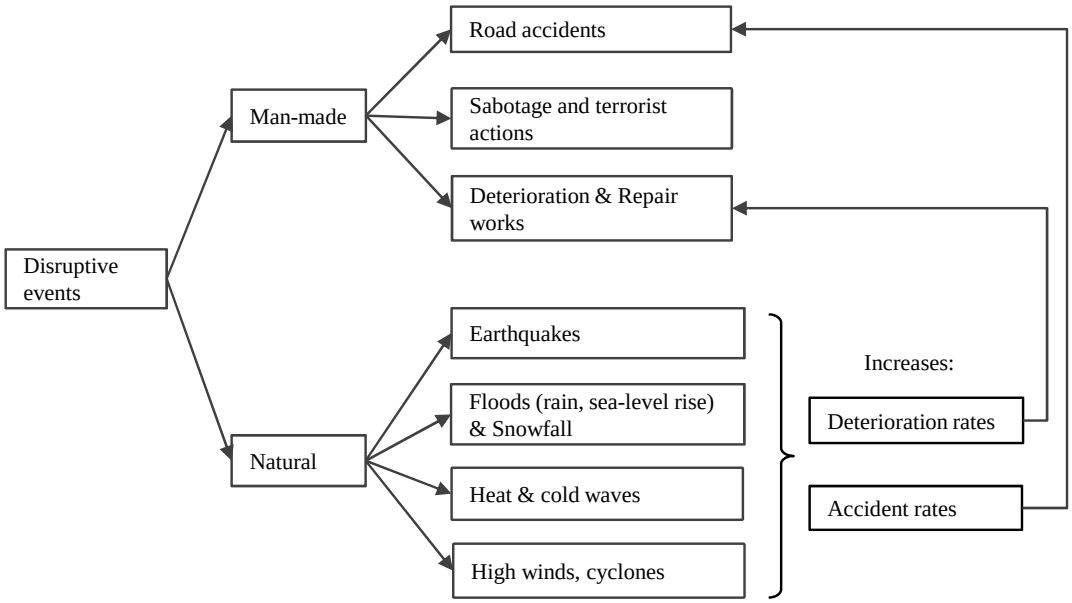

Figure 2.3: Classification of disruptive events and their interactions

ing and protecting the performance of the disrupted system. The remainder of the review focused on resilience and showed that the resilience concept was gradually stretched to incorporate several notions that can be summarised as reducing disruptions consequences, recovery time from disruptions, and vulnerabilities to future expected and unexpected conditions. Finally, the present chapter discussed the advantages and disadvantages of the road-network-resilience assessment approaches available in the literature. This allowed the identification of research gaps that will be addressed in the present thesis: lack of characterisation of the potential impacts of a full range of predictable and unpredictable disruption scenarios, lack of characterisation of the rapidity component (i.e. recovery strategies) in road network resilience, and limited understanding of the effects of road networks' characteristics (topology, travel demand distribution, congestion, etc.) on road network resilience (Section 1.2).

Chapter 3

Robustness of road networks to multiple disruption scenarios

3.1 Introduction

The literature review showed that system resilience can be measured by two key properties that resilient systems should exhibit under stress: robustness (the ability to absorb perturbations) and rapidity (the ability to recover quickly). This chapter focuses on road networks' robustness to multiple disruption scenarios. As the main function of road networks is to provide mobility (i.e. the ability to travel between trip origins and destinations in a timely manner) the robustness of road networks should characterise their ability to deliver this function under a multitude of potentially unpredictable conditions. However, assessments of the potential impact of disruptive events on road networks generally focus on a limited set of scenarios illustrating their methodologies (Nogal et al., 2016; Omer et al., 2013; Zhang and Wang, 2016) or the worst-case scenario using a game theory approach (Alderson et al., 2017; Bhavathrathan and Patil, 2015b, 2018). These studies do not uncover the potential impact of all possible disruption scenarios as suggested by the resilience paradigm. This is unfortunate as such findings could be useful to practitioners and public authorities. For example, considering that a wide range of events (e.g. pavement maintenance, road accidents, flooding, etc.) can unpredictably disrupt any parts of the network, the identification of multiple worst-case scenarios rather than the single worst-case scenario would be more useful in practice.

A range of recent studies consider multiple disruption scenarios in the road transport context. However, as shown in Chapter 2, these studies present one (or several) of the following shortcomings:

- disruptions are modelled based on records of past disruptions that may overlook unpredictable events (Wisetjindawat et al., 2017; Zhou et al., 2017).

- full dismantling processes are used to model disruptive events in road networks (Buhl et al., 2006; Casali and Heinimann, 2020). Dismantling-process analyses are useful to determine the critical number of failed components after which networks can no longer function. This information is relevant when analysing major events (e.g. earthquakes or floods) but less relevant for a wide range of road perturbations such

as car accidents, sabotage actions and landslides that disrupt a limited number of roads only.

- Disruptions are limited to single-link failures (Omer et al., 2013; Sullivan et al., 2010; Taylor et al., 2006). However, multiple-link failures are not the simple combination of the most critical links with single-link failure (Wang et al., 2016). Consequently, the consideration of single-link failures only may lead to inefficient prevention and restoration measures in the advent of events disrupting several road segments or several events concurrently affecting different parts of the network.

Besides, some of these studies (Buhl et al., 2006; Casali and Heinimann, 2020) rely on network topological models that take into account the network topology but disregard traffic flows, capacity constraints and congestion.

Therefore, although research has extensively contributed to the understanding of road network robustness, characterisation of the potential impacts of a full range of predictable and unpredictable disruption scenarios is still lacking. To increase this understanding, the present thesis adopts a hazard-independent approach that considers all possible scenarios disrupting multiple links (more specifically up to a certain number of links). The maximum number of concurrently disrupted links is limited by computational effectiveness. The threshold for the maximum number of disrupted links is chosen depending on the network studied to understand the effect of the damage extension (number of disrupted links) on the network performance. Besides, the present chapter uses traffic modelling techniques accounting for traffic flows and congestion to provide a more realistic assessment of the impacts of the disruptions on the network.

To assess road network robustness to multiple disruption scenarios, this chapter develops and uses a robustness indicator suitable to discriminate between the impacts of a wide range of disruptive events. The proposed indicator based on the demand-weighted average increase in travel time along the OD pairs of the disrupted network is compared to a total travel time change indicator, which is representative of the robustness indicator used in the literature (Chapter 2). The comparison is based on the application of both indicators to two case studies: a four-node highway network model and the Sioux Falls road network model.

This chapter is organised as follows. Section 3.2 presents the methods and case studies. Section 3.3 and 3.4 describe and discuss the results, respectively. Section 3.5 provides some concluding remarks.

3.2 Methods

3.2.1 Disruption model

Disruptive events can impact both the supply and the demand side of the transport system. The supply side (i.e. the network) is affected by the damage induced on the infrastructures, which in turn impacts traffic conditions through road unavailability as well as speed and capacity reductions. The demand side representing the flow of users can also be impacted as trips may be cancelled or delayed due to usual routes and destinations being affected. As this study seeks to evaluate how the availability of alternate routes and capacity helps

remediate the consequences of network disruptions, travel demand was considered fixed to effectively compare the network performance under different disruption scenarios (all other things being equal).

As road disruptions are rarely predictable, an "all-hazard" approach in line with the resilience paradigm was adopted. All possible combinations of link failures disrupting up to a certain number of links at the same time were simulated. The maximum number of concurrently disrupted links was chosen depending on the case study.

3.2.2 Robustness indicators

Demand-weighted average increase in travel time along the OD pairs

Robustness metrics should compare the required- and disrupted-network performance to evaluate the ability of the system to provide functionality despite disruptions. As the definition of the required performance is arbitrary (since it depends on the judgement of the transport operators, public authorises and users), the network pre-event performance is often used as a proxy for the required performance. The network performance can be measured by the users' travel time (TT) since the main function of road networks is to allow road users to reach their chosen destination within a reasonable travel time.

This chapter presents a novel robustness indicator that measures the demand-weighed average increase in travel time along the OD pairs of the disrupted network. This indicator was developed as part of the present thesis. It is computed in two steps. Firstly, a TT relative change index (TTC_w) is computed for each OD pairs:

$$TTC_w = \left(1 + \frac{TT_d^w - TT_0^w}{TT_0^w}\right)^{-1} \tag{3.1}$$

where TT_0^w and TT_d^w are the undisrupted and disrupted travel times on the OD pair w, respectively. The travel time change index decreases as the travel time increases, being equal to 1 if the TT remains unaltered despite the disruption. TTC_w can also exceed 1 for OD pairs whose road users experience a decreased TT due to reduced congestion on some roads that they share with users who had to reroute due to the disruption.

The network robustness indicator (RO) then combines the travel time change indices of all OD pairs using a weighted average:

$$RO = \sum_w k_w TTC_w \tag{3.2}$$

where w and k_w are an OD pair and the associated weighting factor, respectively. k_w is given by the ratio between the demand for w and the total demand in the network. As disruptions cause an increase in travel time in most OD pairs, the network robustness indicator (RO) remains between 0 and 1. $RO = 100\%$ indicates that despite the disruptive event the TT remains roughly equal to the initial travel time on all OD pairs. Otherwise, the network robustness decreases as TT_d^w increases, the drop being more important when highly demanded routes are impacted.

To complement RO, several measures of the spread of the impacts across the OD pairs can be used. Among these measures, the most meaningful could be the proportion of road users unable to reach their chosen destination following the disruption. These users wish

to travel between disconnected OD pairs whose TTC_w tend to zero (as the travel time between the trip origin and destination becomes infinite). Hence, the proportion of users unable to reach their chosen destination—also called unsatisfied demand (USD)—is given by:

$$\begin{aligned} &USD = \textstyle\sum_w k_w \delta_w \\ &\text{where } \delta_w = \begin{cases} 0, & \text{if } TTC_w < 0.001 \\ 1, & \text{otherwise} \end{cases} \end{aligned} \tag{3.3}$$

where $TTC_w < 0.001$ means that the disrupted travel time on w is 1000 higher than the initial travel time on w. This threshold proved to be low enough to distinguish between the OD pairs where the TT naturally increases and the OD pairs where the TT unrealistically increases (as the latter use failed roads that are assigned a very high and unrealistic cost of travel in the model) in the case studies of this thesis. Moreover, it seems reasonable to consider that an OD pair where the travel time is multiplied by 1000 is blocked. Depending on the networks operators' and users' level of acceptance, this threshold could be modified to consider OD pairs where the travel time is multiplied by 50, 100, etc. as failed.

For a more detailed assessment, the travel time in equations 3.1-3.3 can be replaced by a generalised travel-cost metric considering other route choice factors such as distance, tolls, and scenery. The weighting factors (k_w) can also be adapted to give more importance to critical routes used by emergency services, for example.

Total travel time change indicator

Most robustness indices described in the literature consider the change in total travel time in the network (Bhavathrathan and Patil, 2015b; Ganin et al., 2017; Omer et al., 2013). This metric seems however unable to discriminate between scenarios leading to few or many Origin-Destination pair disconnections as these scenarios all lead to very high increases in total travel time. When an OD pair (w) is disconnected (i.e. destination D can no longer be reached from origin O), transport models assume that the travel time is infinite (or takes a very high value), which arbitrarily increases the total (or average) travel time. The robustness indicators based on the total TT may hence arbitrarily and unfairly decrease towards 0% even when a large proportion of the demand is still satisfied. In comparison, the demand weighted average used in the proposed robustness indicator (RO, Eq. 3.2) ensures that the decrease in performance due to w being disconnected is proportional to the importance of w.

To demonstrate the ability of RO to discriminate between a wider range of perturbation scenarios than total TT based indicators, the relative change of the total travel time ($ToTTC$) was computed and compared with RO.

$$ToTTC = \left(1 + \frac{ToTT_d - ToTT_0}{ToTT_0}\right)^{-1} \tag{3.4}$$

where $ToTT_0$ and $ToTT_d$ are the undisrupted and disrupted total travel times, respectively. $ToTTC$ provides a measure of the change in system-wide travel time scaled in [0,1].

3.2.3 Case studies

Four-node highway test network

The indicators were firstly tested on a very simple highway network with four nodes and six links (Prescott, 2017). For the sake of simplicity, the link-travel times were assumed to be linearly dependent on the link flow (Figure 3.1). The travel times (tt_i) are in minutes and the flows (x_i) in thousands of vehicles per hour. Two OD pairs are considered: from O1 to D1 and from O2 to D2 with peak-hour demand for travel $d_1 = 4000$ and $d_2 = 5000$ vehicles per hour respectively. The traffic assignment model used is a user equilibrium that minimises the travel time of all road users. This model is the fourth stage of the seminal four-step (trip generation, trip distribution, modal split, and traffic assignment) transport model (Ortúzar and Willusem, 2011) that can be used to estimate the number of vehicles (or people) that will use a specific transport facility based on travel data that can be obtained through census information, surveys, and estimates.

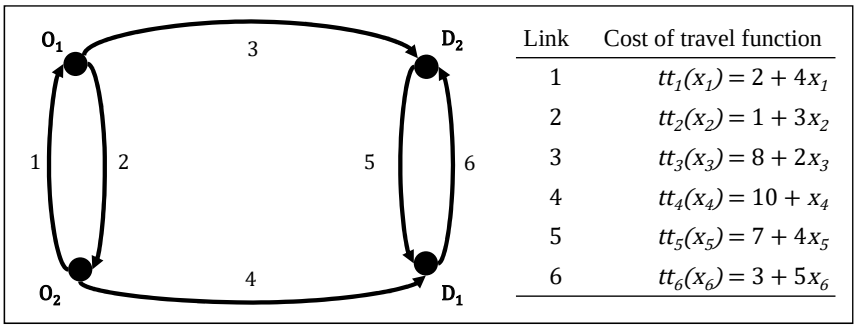

Link	Cost of travel function
1	$tt_1(x_1) = 2 + 4x_1$
2	$tt_2(x_2) = 1 + 3x_2$
3	$tt_3(x_3) = 8 + 2x_3$
4	$tt_4(x_4) = 10 + x_4$
5	$tt_5(x_5) = 7 + 4x_5$
6	$tt_6(x_6) = 3 + 5x_6$

Figure 3.1: Four-node highway test network model.

Two damage extension levels were considered in this case study: single-(SLFs) and two-(2LFs) link failures. These disruptions led to the unavailability of one or several routes, which was modelled by assigning a very high cost of travel (10,000 min) to the disrupted routes. SLFs and 2LFs were sufficient to assess the potential impacts of all possible failure scenarios in this network as the results showed that certain 2LFs cause 99.3% decreases in network performance measured by travel time increases. A *Python 3.6* code was develop (as part of the present thesis) to compute both the traffic equilibrium and the robustness indicators.

The Sioux Falls network

The second case study is the Sioux Falls (USA) network. Firstly introduced in LeBlanc et al. (1975), the Sioux Falls network (Figure 3.2) has been extensively used as a case study in the literature (Bhavathrathan and Patil, 2018; Mitradjieva and Lindberg, 2013; Wang et al., 2016). This network consists of 24 nodes, 76 directed links, and 24 OD zones. The datasets describing this case study were obtained from the Transportation Networks for Research repository (Transportation Networks for Research Core Team, 2019). These datasets provide the network structure, link characteristics (including capacity, length, and free-flow travel time) and the origin-destination trip matrices.

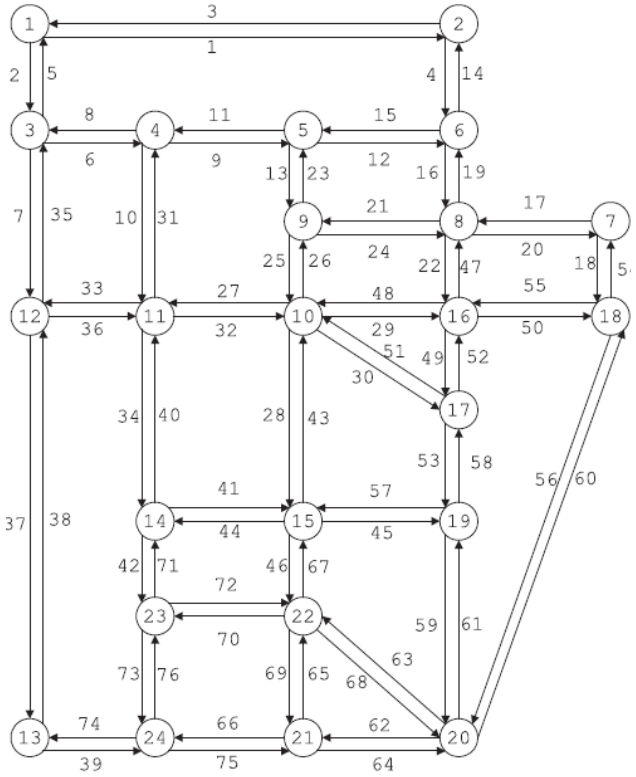

Figure 3.2: Sioux Falls network model.

Transport model A standard transport model (Ortúzar and Willusem, 2011) was used to compute and compare the travel time of road users in the initial and disrupted conditions. Using the demand matrix available at the Transportation Networks for Research repository (Transportation Networks for Research Core Team, 2019), traffic was assigned to the network assuming that users independently minimised their travel time. Although individual driving habits may vary (D'Lima and Medda, 2015), this assumption seems reasonable in the absence of more detailed data as it was adopted in a traffic model validated against traffic data from 40 US urban areas (Ganin et al., 2017).

The travel time of link a (tt_a) is defined by the standard BPR function (Bureau of Public Roads, 1964):

$$tt_a(x_a) = tt_a^f \left[1 + 0.15\left(\frac{x_a}{c_a}\right)^4\right] \tag{3.5}$$

where x_a, c_a and tt_a^f are the link flow, capacity and free-flow travel time, respectively.

Disruption simulations The simulations were performed in Julia language (v.1.2) using the packages *Distributed*, *LightGraphs* and *TrafficAssignement* for parallel processing, network analysis and traffic assignment computation, respectively. The latter implements three methods to find the user equilibrium: the original, conjugate, and bi-conjugate Frank-Wolfe (FW) algorithms (Mitradjieva and Lindberg, 2013). FW algorithm is one of the most popular methods used to solve traffic assignment problems while the conjugate and bi-conjugate versions of this algorithm improve its convergence speed. The fast bi-conjugate FW algorithm was used here with a relative convergence gap of 10^{-4}, which is

a sufficient criterion for equilibrium stability (Boyce et al., 2004). To model link closures, a very high free-flow travel time (10,000 min) was assigned to unavailable links.

Five damage extension levels were considered in this case study: single-, two-, three- (3LFs), four- (4LFs) and five- (5LFs) link failures. It was assumed that single- to five-link failures could provide enough data points to understand the effect of the damage extension (number of disrupted links) on the Sioux Falls network. This seems true as certain two-link failures already fragmented the Sioux Falls network model and certain five-link failures (that disrupt 13% of the undirected links in the Sioux Falls network) caused 87% decreases in performance, measured by travel time increases.

The links of the Sioux Falls network (Figure 3.2) were disrupted in both directions at the same time leading to 38 single-, 703 two-, 8436 three-, 73,815 four- and 501,942 five-link failures. Hence, the robustness and link criticality indicators measured the impact caused by the unavailability of both directions. For consistency, the link flows refer to the sum of the flows in both directions in this paper. However, as the demand in the Sioux Falls network is not totally symmetric a link might be more critical in one direction than the other. For the original Sioux Falls network, the simulations took 41 hours using parallel processing on an *Intel i3-7100* 3.9GHz and 8GB memory workstation. The simulation code was developed as part of this research.

3.3 Results

3.3.1 Comparison of the robustness indicators in the Four-node network

The impacts of all single- and two-link failures on the Four-node test network (Figure 3.1) were evaluated using the network robustness indicator, RO (Eq. 3.2), which measures the demand-weighted average increase in travel time along the OD pairs. The impacts were also evaluated using the total travel time change indicator, $ToTTC$ (Eq. 3.4), which measures the relative change of the total travel time (often used as a robustness indicator in the literature). The results are shown in Table 3.1, where they are ordered in increasing number of routes unavailable and OD pairs disconnected, which can be used as an indicator of disruption severity.

In the undisrupted network, two routes connect each OD pair and the average travel time per driver is 27.5 min. Single-link failures either blocked one route or two routes serving different OD pairs (as shown in Table 3.1). Hence, none of the SLF resulted in network disconnection as at least one of the routes connecting each OD pair remained available. Most of the scenarios of 2LF (8/15) caused the unavailability of two routes serving different OD pairs, which did not affect the network connectedness. The other scenarios blocked two routes serving the same OD pair or three routes, which, in both cases, disconnected one OD pair. Finally, the simultaneous failure of road 3 and 4 resulted in the unavailability of all routes (Table 3.1).

Table 3.1 shows that the network robustness indicator reflects the impact of the hazards on the network as it gradually decreased with the number of routes unavailable. Besides, the values spread in a large range (from 0.3% to 96%), showing that RO is suitable to compare several scenarios. In comparison, the total travel time change indicator ($ToTTC$) gradually decreased with the number of unavailable routes when OD pairs were

not disconnected (first three rows in Table 3.1) but reached a close to zero value for all scenarios leading to OD-pair disconnections (last three rows in Table 3.1). Therefore, this indicator was unable to differentiate between the cases where one or two OD pairs were disconnected.

Table 3.1: Evaluation of the impacts of all possible single- and two-link failures in the four node test network.

No. of routes unavailable	No. of OD pairs disconnected	Single-link failures	Two-link failures	Network robustness (RO)*	Total travel time losses ($ToTTC$)*
0	0	-	-	100%	100%
1	0	1,2,5,6	-	[79.2%, 96.0%]	[75.7% , 96.0%]
2	0	3,4	1&2, 1&3, 1&5, 2&4, 2&6, 3&5, 4&6, 5&6	[56.8%, 82.6%]	[56.8% , 80.4%]
2	1	-	1&6, 2&5	[51.8%, 60.8%]	[0.5% , 0.6%]
3	1	-	1&4, 2&3, 3&6, 4&5	[29.6%, 42.6%]	[0.5% , 0.6%]
4	2	-	3&4	0.3%	0.3%

*[min, max]

3.3.2 Comparison of the robustness indicators in the Sioux Falls network

The impacts of all possible single- to five-link failures on the Sioux Falls network were evaluated using the network robustness indicator, RO (Eq. 3.2), which measures the demand-weighted average increase in travel time along the OD pairs. The impacts were also evaluated using the total travel time change indicator, $ToTTC$ (Eq. 3.4), which measures the relative change of the total travel time (often used as a robustness indicator in the literature). The results are shown in Figure 3.3, where the values and kernel density of the network robustness indicator are compared to that of the total TT relative change indicator for the five damage extension groups. In Figure 3.3.b, the unsatisfied demand indicator, USD (Eq. 3.3), is used to distinguish between the disruption scenarios that lead unsatisfied demand (grey points) and the scenarios that do not lead to unsatisfied demand (yellow points).

In Figure 3.3.a, both indicators present single-peaked distributions, however, the distributions of the total TT change indicator have less pronounced peaks than the network-robustness-indicator distributions. Furthermore, it can be observed in Figure 3.3.a that $ToTTC$ progresses more quickly towards zero than RO as the damage extends. Some 2LF, 3LF, 4LF and 5LF scenarios have $ToTTC$ values close to zero while their RO values remain superior to 0.475, 0.322, 0.223 and 0.126, respectively.

Three domains appear in Figure 3.3.b regardless of the damage extension group. On the left side of the plots ($ToTTC \leq 0.10$), RO is independent of $ToTTC$ (vertical lines). On the right side ($ToTTC > 0.5$), the two indicators appear linearly correlated ($R^2 = 0.80$). Between these two domains, the linear model is less relevant ($R^2 = 0.42$).

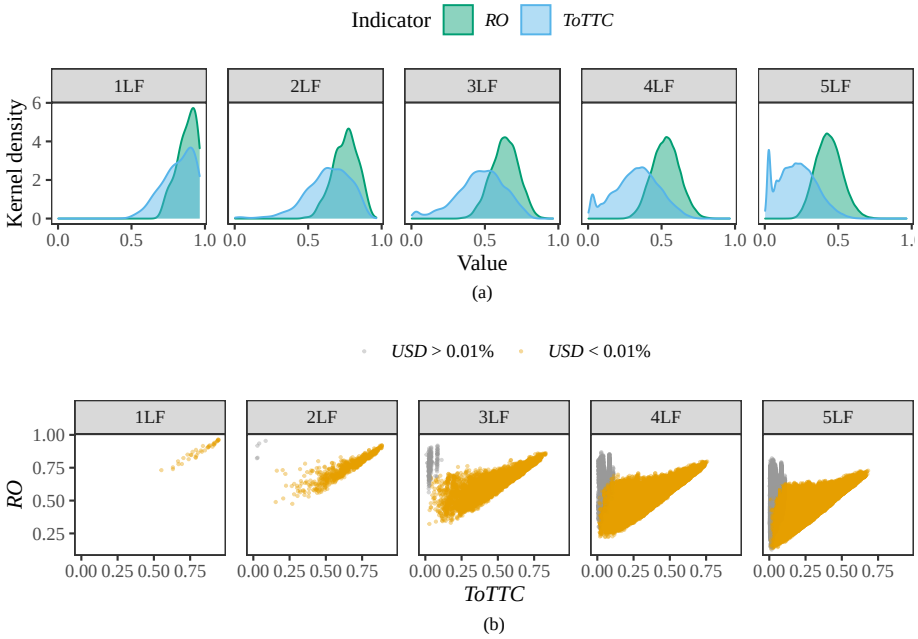

Figure 3.3: Comparison of the network robustness (RO) and total travel time change ($ToTTC$) indicators under single- (1LF), two- (2LF), three- (3LF), four- (4LF) and five- (5LF) link failures in the original Sioux Falls network

The $ToTTC$ values close to zero correspond to link combinations whose failure cause OD-pair disconnections measured by a non-zero USD value (grey points in Figure 3.3.b). For example, the simultaneous disruption of (1,2) and (1,3) isolates node 1 from the rest of the network and disconnects all OD pairs involving this node as suggested by the network structure (Figure 3.2). Besides, none of the 1LFs lead to OD pair disconnections, which explains why none of the 1LFs have a $ToTTC$ value close to zero).

Extended impact of single- and multiple-link failures in the Sioux Falls network

The simulations considered five levels of damage extension (from single- to five-link failures) that had an increasing impact on the Sioux Falls network performance. Figure 3.4 shows the evolution of the mean and minimum, and mean and maximum values of RO and USD across the damage extension groups, respectively.

In Figure 3.4.a, the mean robustness indicator value quickly decreases as the damage extension increases (from 86.7% in 1LFs to 43.6% in 5LFs), while the standard deviation of RO remains steady (between 6.50% and 9.30%). A regression analysis showed that the relationship between the mean robustness indicator value and the damage extension could be captured by a linear model ($R^2 = 1$). The relationship between the minimum robustness indicator values and the damage extension could be captured by a piecewise linear model ($R^2 = 1$), where the minimum value of RO linearly decreases as the damage extension increases, the slope being sharper before the breakpoint (≈ 2.32). This breakpoint is close to two, which is the minimum number of links required to fragment the Sioux Falls network and cause unsatisfied demand (as shown in Figure 3.4.b).

In Figure 3.4.b, the mean USD value barely increases with the damage extension (from

0% in 1LFs to 0.1% in 5LFs), which shows that most scenarios do not disconnect OD pairs. In comparison, the maximum value of USD increased in steps (from 0% in 1LFs and 2LFS to 1.7% in 2LFs to 7.3% in 3LFs and 4LFs, etc.). The standard deviation of USD increased with the damage extension, meaning that the heterogeneity of the potential impacts of the failure scenarios on the proportion of stranded users increased with the number of failed links.

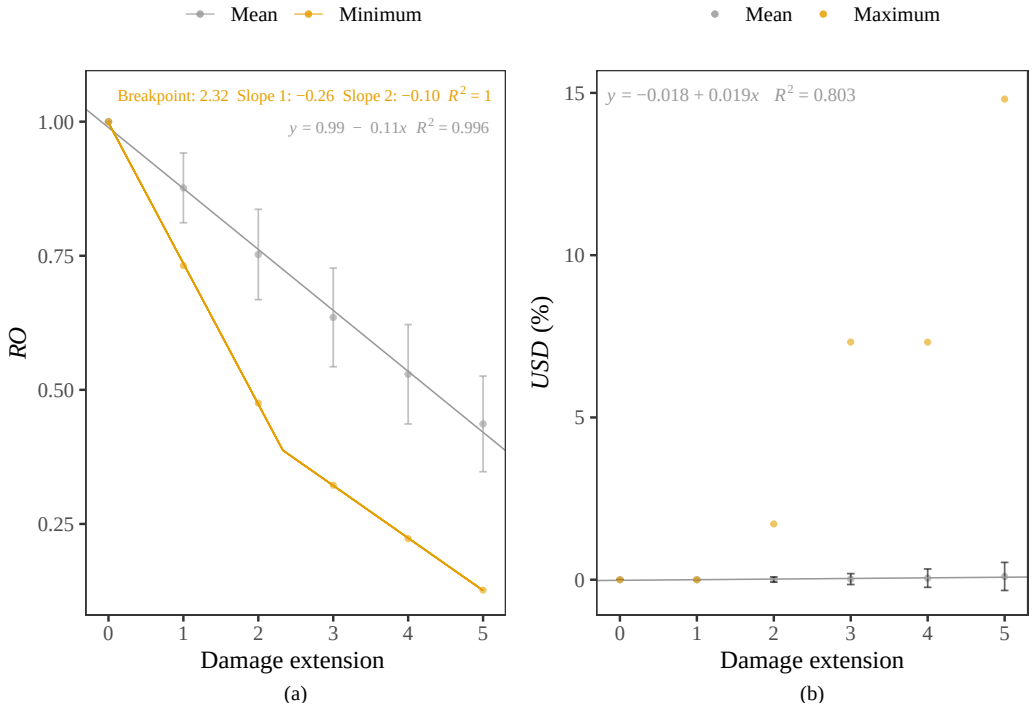

Figure 3.4: Evolution of the network robustness (RO) and unsatisfied demand (USD) indicators depending on the damage extension (number of failed links) in the original Sioux Falls network. Error bar = mean ± sd

3.3.3 Most critical disruption scenarios in the Sioux Falls network

The network robustness indicator was used to identify the top-5 most critical scenarios in all damage extension groups. These scenarios are presented in Table 3.2 along with their RO and USD values. Table 3.2 excludes the most critical 5LF scenarios for the sake of brevity. The top-5 most critical 5LF scenarios in the Sioux Falls network are discussed in Chapter 5, which explores the relationship between the most critical scenarios and links.

Table 3.2 shows that none of the top-5 most critical scenarios led to unsatisfied demand ($USD = 0\%$). This Table also shows that the most critical combinations of 2LFs, 3LFs and 4LFs did not necessarily involve the most critical links with SLF as links outside of this group, for example (10,11) and (17,19), appeared in these combinations.

Table 3.2: Top-5 most critical combinations of single-, two-, three-, and four-link failures in the original Sioux Falls network

Link combination	RO (USD)	Link combination	RO (USD)
(10,15)	73.2 % (0 %)	(10,15) (17,19) (18,20)	32.2 % (0 %)
(18,20)	74.0 % (0 %)	(9,10) (10,11) (18,20)	33.2 % (0 %)
(9,10)	75.3 % (0 %)	(10,15) (16,17) (18,20)	34.0 % (0 %)
(12,13)	77.7 % (0 %)	(5,9) (10,11) (10,15)	34.3 % (0 %)
(6,8)	77.8 % (0 %)	(9,10) (10,15) (18,20)	34.5 % (0 %)
(9,10) (10,11)	47.5 % (0 %)	(9,10) (10,11) (10,15) (18,20)	22.3 % (0 %)
(10,15) (18,20)	48.9 % (0 %)	(9,10) (10,11) (12,13) (18,20)	22.3 % (0 %)
(5,9) (10,11)	51.6 % (0 %)	(10,15) (10,17) (16,17) (18,20)	22.6 % (0 %)
(9,10) (18,20)	53.0 % (0 %)	(5,9) (10,11) (10,15) (15,19)	22.6 % (0 %)
(12,13) (18,20)	53.5 % (0 %)	(3,12) (9,10) (10,11) (18,20)	22.8 % (0 %)

RO = Network robustness indicator (Eq. 3.2); USD = Unsatisfied demand indicator (Eq. 3.3)

3.4 Discussion

3.4.1 Measuring road network robustness

In the first case study (the Four-node test network), the comparison between the values derived from the network robustness indicator (measuring the demand-weighted average increase in travel time along the OD pairs) and the total TT change indicator clearly showed that the former was able to discriminate between a wider range of scenarios than the latter (Table 3.1).

In the second case study (The Sioux Falls network), the comparison between the values derived from the two indicators showed conflicting results. The distributions of the total TT change indicator in the damage extension groups presented less pronounced peaks (Figure 3.3.a), which suggests that this indicator provided a finer distinction between the impacts of the disruption scenarios than RO. As the ability to discriminate between the impacts of different scenarios—which helps towards the allocation of the limited resources to the most critical scenarios—is a desirable feature of robustness indices, $ToTTC$ may appear to be a better indicator.

However, the comparison also showed that contrary to RO, $ToTTC$ provides a zero value for all disruption scenarios that lead to OD-pair disconnections despite the variability of the resulting unsatisfied demand. In Figure 3.3.b, most of the scenarios causing OD-pair disconnections appear on the left side of the plots where $ToTTC$ remains inferior to 10% while RO ranges between 12% and 95%. $ToTTC$ is unable to discriminate between the impacts of scenarios causing OD-pair disconnections because these scenarios all result in very high total travel time values. This is because link unavailability is usually modelled by assigning a very high cost of travel to the damaged link such that when an OD pair is disconnected the users along this OD pair experience a very high and unrealistic travel cost. RO differentiates between the impacts of scenarios involving OD-pair disconnections because this indicator aggregates the values of the travel time change indices (TTC_w, Eq. 3.1) of all OD pairs, which include disconnected OD pairs with TTC_w values close to zero

and non-disconnected OD pairs with higher TTC_w values.

Subsidiary indicators quantifying the spread of the impacts among the OD pairs and users can be used to complement the assessment including an indicator measuring the share of unsatisfied demand. The latter could even be combined with one of the conventional indicators based on the increase in total TT to provide an aggregated indicator able to consider the scenarios that lead to OD-pair disconnections as proposed by Bagloee et al. (2017). However, as shown in Table 3.2, several perturbation scenarios lead to the same proportion of unsatisfied demand. This would limit the ability of the aggregated indicator to discriminate between the impacts of these scenarios. In contrast, RO provides a single measure of the impacts and can discriminate between the impacts of most scenarios.

3.4.2 Network robustness and damage extension

The first case study considered disruption scenarios concurrently affecting up to two links with the assumption that single- and two-link failures could provide enough data points to understand the effect of the damage extension on the Four-node test network. The results validated this assumption as single- and two-link failures allowed the evaluation of the effects of the two main mechanisms behind the loss of performance in disrupted networks: travel time increases and network (or OD pairs) disconnections. The later could be observed as certain two-link failures fragmented the four-node network (Table 3.1). Besides, the concurrent failure of link 3 and 4 disconnected the two OD pairs of this case study and led to a robustness indicator value of 0.3%. Hence, the impacts of the scenarios considered covered the full range of possible robustness values.

The second study considered disruption scenarios concurrently affecting up to five links with the assumption that single-, two-, three-, four- and five-link failures could provide enough data points to understand the effect of the damage extension on the Sioux Falls network. The results partly validated this assumption. Single- to five- link failures allowed the evaluation of the effects of the two main mechanisms behind the loss of performance in disrupted networks: travel time increases and network (or OD pairs) disconnections. The later could be observed as certain two-link failures already fragmented the Sioux Falls network while some five-link failures led to larger disconnections. This is evidenced by the range of the maximum value of the unsatisfied demand indicator (USD) that increased from 0% in 1LFs to 15% in 5LFs. As this indicator mainly depends on the network connectivity, it is comparable to the network robustness indicators used in topological studies measuring road network robustness by the reduction in the size of the giant (or largest connected) component of the network under dismantling processes (Buhl et al., 2006; Casali and Heinimann, 2020). The data points obtained for the maximum values of USD (Figure 3.4.b) are consistent with the first points of the plots shown in these studies. In the later, the size of the giant components under targeted dismantling processes decreases in two—for small networks composed of few hundred nodes in Buhl et al. (2006)— or three—for large networks composed of thousands of nodes in Casali and Heinimann (2020)—main stages. In small networks, the most detrimental stage to the network performance (or transition phase) occurs in the first stage (when 0% to 30% of the links are disrupted) while in large networks the transition occurs in the second stage (when 10% to 40% of the links are disrupted). The Sioux Falls network being small, the

transition phase started with 2LFs and it can be expected that the maximum value of USD will continue to rapidly increase reaching a value of approximately 90% when up to 30% of the links ($\approx$ 11 links in the Sioux Falls network) will be disrupted as reported in Buhl et al. (2006).

However, the present results also showed that certain five-link failures (that disrupt 13% of links in the Sioux Falls network) can cause 87.4% decreases in network performance measured by the demand-weighted average increase in travel time along the OD pairs (RO) as shown in Figure 3.4.a. This value means that the travel time of most road users would be multiplied by eight. Therefore, single- to five- links failures provided sufficient data points to understand the full range of potential impacts caused by multiple-link failures on the travel time in the Sioux Falls network. Besides, the present results showed that the evolution of the mean and minimum robustness indicator values with respect to the damage extension could be represented by linear and piecewise linear models, respectively (Figure 3.4.a). The extra data points could hence be predicted using these models.

Ultimately, the present results show that the same disruption scenario can lead to major consequences in terms of travel time increases but minor consequences in terms of network (or OD pairs) disconnections. This shows that topological studies, which disregard traffic flows and potential congestion to focus on the network structure can overestimate the robustness of road networks.

3.4.3 Most critical scenarios and links

In the Four-node test network the combination of the most critical links with single-link failures, 3 and 4, lead to the most critical two-link failures (Table 3.1). In addition, 3 and 4 appeared in all of the top-5 most critical 2LF combinations (last two rows in Table 3.1). In the Sioux Falls network, this pattern could not be verified as (10,11), which does not belong to the top-5 most critical links with SLF, is part of the most critical 2LF combination (Table 3.2). The latter results are in accordance with the findings of Wang et al. (2016) that show that the most critical links when multiple-link failures occur are not simply the combination of the most critical links with single-link failure. However, the present results also indicate that the validity of this pattern depends on the network studied. The next chapters of this thesis (Chapters 4 and 5) investigate the role of the network characteristics in the realisation of this pattern.

3.5 Summary and concluding remarks

The research presented in this chapter was conducted to increase the understanding of the potential impacts of a full range of predictable and unpredictable disruption scenarios in road networks. In line with the hazard-independent approach suggested by the resilience paradigm, this chapter investigated the impact of all possible scenarios disrupting multiple links (more specifically up to a certain number of links) in two case studies. The thresholds chosen for the maximum number of disrupted links (two in the Four-node network and five in the Sioux-Falls network) allowed the observation of the two key mechanism behind the loss of performance in disrupted networks (travel time increases and OD-pair disconnections). These thresholds also provided sufficient data points to understand the

effect of the damage extension (number of failed links) on the performance of the networks considered. Therefore, the approach adopted allowed understanding the potential impact of a wide range of disruptive events, including unpredictable events that could be overlooked by risk analyses focusing on a few predictable scenarios. This research led to two key conclusions:

- The widely adopted robustness-quantification approach that measures network robustness by the total travel-time losses cannot discriminate between the impacts of the scenarios causing OD-pair disconnections. The discrimination between these scenarios remains important as they are manifold and lead to different proportions of stranded road users. Hence, this discrimination could help transport practitioners and public authorities in the allocation of the limited resources available for road infrastructures construction and maintenance to the most critical scenarios and links.
- To discriminate between the impact of scenarios that lead to OD-pair disconnections, it is necessary to consider the impacts on the OD pairs (or users) separately rather than the total travel-time losses in the network. This can be achieved by measuring the relative change of the travel time along the OD pairs. The proposed robustness indicator uses a demand-weighted average to aggregate these relative change values into one indicator.

The present research provided a disruption model and a robustness indicator suitable to assess the impacts of multiple disruption scenarios in road networks. These tools hence define a theoretical framework for assessing the role of network topology, demand variations and recovery strategies in network resilience, which are the objectives of the subsequent chapters of this thesis.

Chapter 4

Role of network topology and demand variations in network robustness

4.1 Introduction

In Chapter 3, a robustness assessment framework for road networks was developed to increase the understanding of the potential impacts of a full range of disruption scenarios on road network performance. This framework was tested on two case studies. Although these case studies provide interesting conclusions the generality of these conclusions remains unclear. Similarly, several road network robustness studies available in the literature including (Cats et al., 2016; Wang et al., 2016; Zhang et al., 2015) provided interesting findings but focused on a small set of networks. As such, their findings may only be valid for the specific networks studied. Further investigations are thus required to evaluate the effectiveness of these approaches and the generality of their findings.

Wang et al. (2016) showed that the most critical links when multiple-link failures occur are not simply the combination of the most critical links with single-link failure. Their study was however limited to two different networks of up to 24 nodes, which seems insufficient to justify the generality of the statement. Hence, it remains unclear how the most critical links can be identified considering multiple-link failures, how different are the criticality rankings when only single-link failures are considered as opposed to when multiple-link failures are considered and how sensitive are these results to different network characteristics.

Besides, robustness studies commonly distinguish between targeted and random failures (as discussed in Chapter 2). However, most of these studies conclude that transport networks are less robust to targeted attacks than random ones but do not attempt to quantify the extended impact of targeted attacks (Zanin et al., 2018). As explained in Zanin et al. (2018), the simple conclusion that a network is more vulnerable to targeted attacks does not provide any novel insights since it is inherent to the definition of both kinds of attacks. A more interesting question is how much more vulnerable a network is to targeted attacks compared to random failures. In other words, the objective is rather to quantify the difference of impacts and subsequently determine if a particular network

is well protected against targeted attacks or not.

The present chapter aims at answering these questions by performing a robustness analysis on a variety of abstract road networks. These networks result from a model that randomly generates graphs presenting the topological and operational characteristics of real road networks. This random network model is used because contrary to real maps its characteristics are controllable and should (hypothesis) allow for a sound sensitivity analysis of network robustness, which in turn can provide practical insights for network planners and operators. This novel approach allows the analysis of a large set of networks resulting in a clearer understanding of the generality of the results and conclusions, which are ultimately validated on a set of real network samples from *OpenStreetMap* (www.openstreetmap.org).

The research presented in this chapter adopts a topological transport model. Although topological models disregard capacity constraints and can overestimate network robustness (as shown in Chapter 3), they have the advantage of not requiring detailed travel-demand data. Topological analyses are also less computationally expensive than traffic analyses (as discussed in Chapter 2). These two qualities of topological models allow the analysis of a large set of potential disruption scenarios and road networks.

This chapter has four research objectives: (i) develop a random road network model, (ii) use this model to evaluate the correlation of topological and operational network characteristics with robustness to single-, multiple-, random- and targeted-link failures as well as (iii) the correlation between single- and multiple-link-failure based link criticality rankings, and (iv) validate the results using real road network samples. This chapter is organised as follows. Section 4.2 presents the methods including the random road graph model. The results are presented in section 4.3 and discussed in section 4.4. Finally, some conclusions and recommendations are provided in Section 4.5.

4.2 Methods

This section describes the research method adopted. Firstly, the abstract road network model is introduced. The network attributes and the robustness metrics used are then presented, followed by the experimental procedure. Finally, the road network samples used for validation are presented.

4.2.1 Grid network with Random Edges and Regional Edge Costs (GREREC) model

The model used to generate random road networks is an improvement of the GRE model (Section 2.4) since this model synthesizes most of the topological characteristics of road networks (identified in the literature review of Section 2.3). Four modifications were introduced to the GRE model to better fit the purpose of the present analysis:

- the removal of the links at the rim of the network is allowed;
- the unconditional removal of vertical and horizontal links is allowed;
- the generation of all types of diagonals (i.e. shortcuts) is possible;

- the geometric lengths of the edges are not considered instead the links are directly assigned a random travel cost depending on the link position in the network.

The first three modifications allow the generation of a larger spectrum of network topologies. To ensure that the graphs generated by the original GRE model are connected (i.e. a path exist between every pair of nodes), the model always keeps the edges at the rim of the area and allows the removal of a vertical edge only if its adjacent bottom left horizontal edge exists. The elimination of these two constraints allows the generation of sparser and more irregular topologies. In addition, keeping the edges at the rim of the area means that for any pair of nodes in the network there is a path connecting them through the network periphery, which may not always be the case in real networks. This assumption may be especially problematic for robustness analyses, which aim at evaluating the consequences of link failures in the network. One implication of these two modifications is however that the graphs generated can be disconnected. An analysis of the connectedness of GREREC model is provided in Appendix A.1. This analysis shows that the values of p and q for which the graphs depend on m and n and that p plays a more important role than q because the shortcuts alone are not sufficient to connect the network nodes since they only depart from certain nodes (see rule 3) and 4) in the procedure below.

Besides, the GRE model generates only shortcuts departing form specific nodes to ensure planarity (two diagonals cannot intersect without creating a node). In the present model, the construction of both diagonals was made possible by allowing the construction of one diagonal providing that the other one does not exist (see rule 3) and 4) in the procedure below).

The fourth modification increases the flexibility of the model and allows the introduction of road hierarchy effects in the network. To this end, travel-cost values are randomly assigned to the links depending on their origin node. The area around a node hence describes a "region" where roads are likely to present the same characteristics (length, speed limits, etc.). This modification implies that contrary to the original GRE model, the present model does not generate geometric grid networks with straight lines. The networks generated have a "grid" topology but their spatial representation may include curved roads to respect the geometric distances between the nodes.

This new model is called the Grid network with Random Edges and Regional Edge Costs (GREREC). The procedure used to generate a graph with the GREREC model is described below:

1. Generate a graph with a rectangular grid topology. The dimensions m and n of the rectangle (i.e. the number of nodes per row and columns respectively) are the only parameters necessary to define the grid. The graph generated has $N = m \cdot n$ nodes and the vertex on the i-th column and j-th row is denoted as $v_{i,j}$.

2. Check and remove the existing edges by the order "left to right, bottom to top" with probability $(1 - p)$.

3. For each vertex $v_{i,j}$ where both i and j are odd numbers, generate the four diagonal edges departing from $v_{i,j}$ with probability q.

4. For each vertex $v_{i,j}$ where i is an even number (regardless of j), generate the four diagonal edges departing from $v_{i,j}$ with the probability q providing that the diagonal is not intersecting an existing one.

5. Randomly assign a travel cost to the edges by the order "left to right, bottom to top" with the following rule: all the links departing from the same node have the same cost of travel.

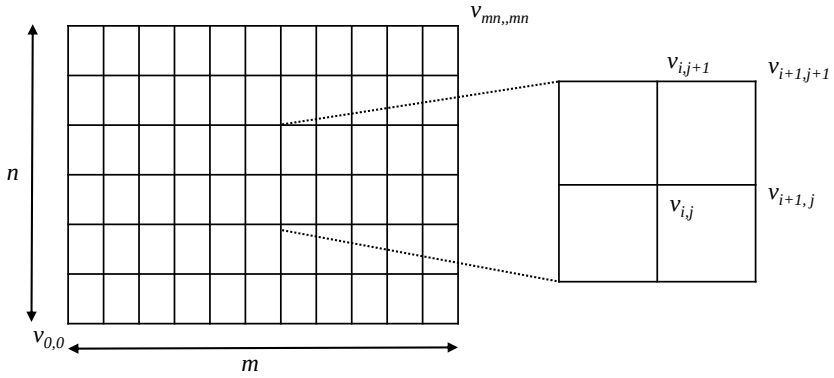

Figure 4.1: Grid network used in the procedure to build the GREREC model

The grid network model used in the procedure is shown in Figure 4.1. The sequences of travel costs assigned to the links in rule 5 were generated as normally distributed random numbers in the discrete interval $[1, max(n, m)]$ to ensure that the costs diversity was proportional to the network size. In other words, a larger network is more likely to be composed of a more diverse range of road types. Considering the huge variety of link cost distributions observed in real road networks (Section 2.3), the standard normal distribution was arbitrarily adopted to generate random sequences of link costs that at least were unlikely to result in uniform distributions since none of the distributions observed in real road networks was uniform.

The GREREC model hence uses four parameters: m and n (the dimensions of the rectangular grid), p (the probability of keeping horizontal and vertical edges in the grid) and q (the probability of generating shortcuts in the grid) to generate random road graphs. The standard deviation of the link costs in the network can also be used to measure the link cost heterogeneity (h_{lc}) in the network. Figure 4.2 shows examples of graphs generated by the GREREC model. The topologies generated range from relatively sparse and decentralized structures (Figure 4.2.a) to very compact structures (Figure 4.2.f) but also include the very ordered grid-like structure (Figure 4.2.d) and more irregular structures (Figure 4.2.b).

4.2.2 Network topological and operational characteristics

Network topological characteristics

To characterise the topology of the graphs generated, five topological measures with potential relevance to network robustness were selected: the network alpha, beta and gamma

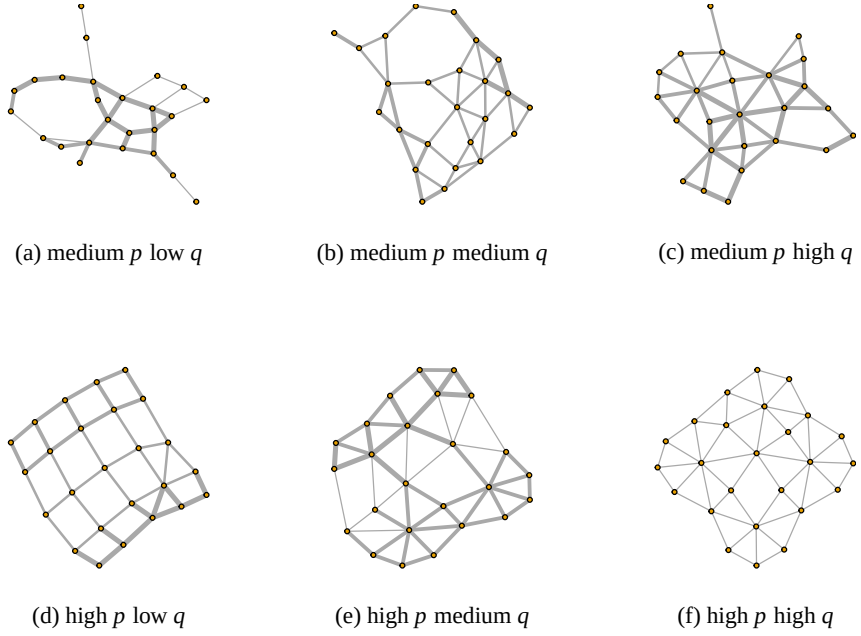

(a) medium p low q (b) medium p medium q (c) medium p high q

(d) high p low q (e) high p medium q (f) high p high q

Figure 4.2: Examples of graphs generated by the GREREC model depending on p (probability of keeping horizontal and vertical edges) and q (probability of generating shortcuts). Low p means $p < 0.33$, medium p means $0.66 > p > 0.33$, high p means $p > 0.33$. The edge thickness indicates a higher cost of travel. $m = n = 5$

indices, as well as the average and standard deviation (heterogeneity) of the degree distribution in the network.

The alpha, beta and gamma indices are measures of the connectivity (or density) of planar graphs presented in Kansky (1963). The alpha index (α) is the ratio of the number of cycles (i.e. path wherein a node is reachable from itself without using the same link more than once) to the maximum possible number of cycles ($2N - 5$):

$$\alpha = \frac{L - N + \mu}{2N - 5} \tag{4.1}$$

where L, N and μ are the numbers of links, nodes and sub-graphs in the graph respectively. The case when $\mu = 1$ (the graph is connected) is referred to in Buhl et al. (2004) as the meshedness coefficient, which varies from zero (tree structures) to one (complete planar graph, which is a triangulation).

The beta index (β) is the ratio between the number of links and the number of nodes.

$$\beta = \frac{L}{N} \tag{4.2}$$

Minimally connected networks (where the links form a cycle) have a beta value close to one while denser networks have a higher β. A network composed of mostly four-legged intersections (e.g. the grid pattern) would present a value of β close to two. The average degree and β are equivalent in undirected graphs (i.e. $\beta = 2 < Degree >$, $< Degree >$ being the average value of the nodal degree distribution) since in these graphs the total number of links equals two times the sum of the node degrees (Barabási and Pósfai, 2016).

The gamma index (γ) is the ratio of the number of links to the maximum possible number of links in a planar graph $3(N-2)$:

$$\gamma = \frac{L}{3(N-2)} \tag{4.3}$$

All of these indices (i.e. α, β, γ) increase with the network connectivity.

Operational characteristics

The main function of road networks is to provide mobility i.e. connect origin-destination pairs in a timely manner. In the graphs representing road networks, some of the nodes don't serve as origin-destination points. To take this specificity into account, it is assumed that the bottom-left ($v_{0,0}$) and top-right ($v_{mn,mn}$) nodes of the original grid (Figure 4.1) were OD points and randomly selected additional OD points in the network with probability r. When $r = 0$ only these two nodes were considered as OD points, while when $r = 1$ all the nodes in the network served as OD points.

Therefore, besides their topological characteristics, the GREREC networks have two operational characteristics: r_{OD}, the ratio between the number of OD points and the number of nodes, and h_{lc}, the heterogeneity of the link travel costs (standard deviation of the links cost distribution).

4.2.3 Robustness, link-criticality and attack-extended-impact indicators

Robustness indicator

The robustness indicator (RO, Eq. 3.2) developed in Chapter 3 was used to assess the disruption impacts on the networks considered. In the present chapter, the transport model does not consider link capacity constraints and potential congestion for computational reasons as hundreds of networks are analysed and compared. This implies that the present chapter mainly concerns uncongested road networks. The OD pairs were considered to be of equal importance (i.e. $k_w = 1/N_{OD}$, N_{OD} being the number of OD pairs), and TT_0^w and TT_d^w are the undisrupted and disrupted travel costs on the least-cost path along w in Eqs. 3.1-3.2.

Link criticality indicator

The present chapter considers a full range of predictable and unpredictable disruption scenarios using the hazard-independent disruption model proposed in Chapter 3. All possible single-, two- and three-link failures were simulated. The maximum number of concurrently disrupted links was limited to three for the sake of computational effectiveness.

To identify the most critical links with regards to multiple-link-failures, the following method was adopted. A criticality index was computed for each link depending on the effect of its degradation on the network performance in all of the scenarios considered. The criticality index (Cr_a) of link a is:

$$Cr_a = \sum_t \frac{1}{L_t} \langle 1 - RO_s \rangle_t^a \tag{4.4}$$

where RO_s is the network robustness to the hazard s as defined in Equation 3.2. The notations t and L_t indicate a damage extension group (e.g. 2LF) and the number of links damaged by the hazards of this group, respectively. The division by L_t means that failed links were assumed to equally contribute to the loss of performance. $\langle 1 - RO_s \rangle_t^a$ means that $1 - RO_s$ is averaged over the scenarios of the same size t in which a is damaged. The averages per scenario size ensure that the contributions of the different scenario sizes to the link criticality are in the same range. Indeed, there are more scenarios of multiple-link failures than SLFs. If L is the number of links in the network, there is one, $(L-1)$ and $(L-1)(L-2)$ scenarios of SLF, 2LFs and 3LFs per link, respectively, hence a simple sum would inherently give more importance to multiple-link failures. The criticality index of a non-critical link would tend to zero as the network robustness to the hazards involving the failure of this link will be close to 1, causing Cr_a to increase with the link criticality.

Comparison of the link criticality rankings derived from different scenarios

To compare the rankings derived from the criticality index (Cr_a) when only single-link failures are considered as opposed to when multiple-link failures are considered, Spearman's rank-order correlation coefficient was used. Spearman's and Kendall's coefficients are the most popular indicators to evaluate the correlation of non-parametric measures and have equivalent performances (Puth et al., 2015). The choice of Spearman's coefficient has been motivated by the fact that Puth et al. (2015) found better results when the data contain ties, which is the case in the present study. This coefficient provides a measure in [-1,1], where -1 and 1 indicate a very strong negative and positive correlation respectively while zero indicates no correlation.

Measurement of the extended impact of targeted attacks

In this section, an indicator is developed to quantify the difference in impact between random and targeted attacks. The "dismantling process" approach found in complex network theory studies (Réka et al., 2000; Zanin et al., 2018) is used to develop a single measure of road networks robustness to a mode of attack (e.g. targeted attacks) that does not present the arbitrariness of the indicator used in (Buhl et al., 2006) and accounts for the increased TT. This measure is called "cumulative" robustness (CRO_z) and is given by the expression:

$$CRO_z = \frac{1}{L}\int_0^L RO_z(x)dx \tag{4.5}$$

where z is the attack mode considered and L the total number of links in the network. $RO_z(x)$ is the road network robustness indicator (Eq. 3.2) when x links failed. As $RO_z(x)$ is scaled between 0 and 1, the division by L also scales CRO_z between 0 and 1. The value obtained can hence be used to compare the robustness of networks of different sizes.

The computation of the network cumulative robustness to targeted attacks requires a sequence of failed links resulting in rapid and severe robustness losses. Criticality-based attacks were excluded because of their computational costs, as these require the analysis of $L!$ SLF scenarios in a network containing L links. Instead, the betweenness centrality (i.e. the number of shortest paths that go through an edge) first introduced by Freeman

(1979) were used to identify important links in the networks. The betweenness centrality of link a is given by

$$BETW(a) = \sum_{x \neq y} \frac{\sigma_{xy}(a)}{\sigma_{xy}} \tag{4.6}$$

where σ_{xy} and $\sigma_{xy}(a)$ are the number of shortest paths between the nodes x and y and the number of shortest path between x and y that contain a respectively (De Meo et al., 2012). The link betweenness can be used as an indicator of the link importance (Cats et al., 2016) as an edge with a high betweenness score connects many pairs of nodes through the shortest path between them.

In the interactive (or dynamic) betweenness attack, the links with the highest betweenness scores are iteratively removed while the betweenness of the links is recomputed after each removal. Dynamic betweenness attacks hence target potentially highly critical links in each step, making the attack more harmful to the network than attacks based on initial estimations of link importance in the original network. Interactive betweenness attacks were selected to model targeted attacks in this chapter since they have been reported as the most detrimental attack among different attacks (Holme et al., 2002; Zanin et al., 2018).

To evaluate the extended impact of targeted attacks in a specific network, the cumulative robustness of the network to an interactive betweenness attack (CRO_{BETWI}) and a representative random attack (CRO_{RAND}) were compared. The latter was obtained by averaging the impact of 1000 random attacks. The extended impact of targeted attacks (TA_{EI}) is defined as the difference between both values:

$$TA_{EI} = CRO_{RAND} - CRO_{BETWI} \tag{4.7}$$

The concepts described in this section are illustrated in Figure 4.3 where CRO_{BETWI} corresponds to the area under the dashed curve and CRO_{RAND} is the mean area under the solid curves.

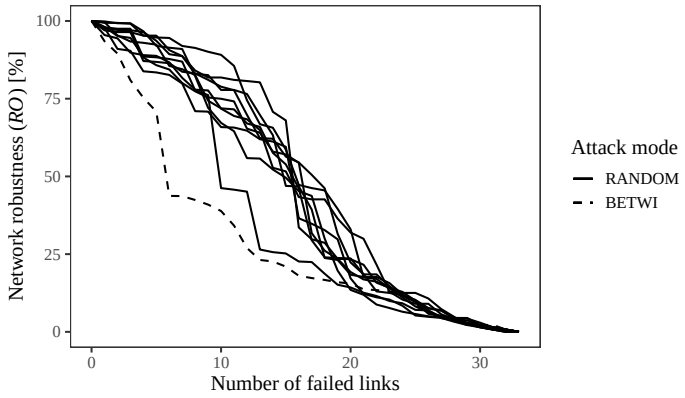

Figure 4.3: Comparison of the impact of a targeted dismantling process (BETWI) and 10 random dismantling processes (RANDOM) on a 33-link GREREC network.

4.2.4 Experimental procedure and simulations

To identify the characteristics that influence network robustness to single, multiple, random and targeted link failures in the GREREC model, quasi Monte-Carlo (QMC) simulations were employed to obtain 300 samples that are as different from each other as possible. Contrary to standard Monte-Carlo methods based on pseudo-random numbers, QMC methods use sequences of quasi-random numbers providing values that are better equidistributed in a given volume than pseudo-random numbers (Dalal et al., 2008). These methods were originally designed for integration but were used here to ensure that the results covered a large parameter space with limited samples and thus save computation time. Sobol's algorithm was adopted as one of the most popular and effective algorithms for generating quasi-random sequences (Bratley and Fox, 1988).

The parameters values (n, m, p, q, r) were chosen in [2,15]×[2,15]×[0,1]×[0,1]×[0,1] each parameter being uniformly sampled from its interval (n and m were discretely sampled). The values of n and m were limited to 15 for computational cost reasons. As an indication for $n = m = 15$, the basic grid network has 420 links leading to 12,225,940 scenarios of three-link failures to analyse.

For each set of parameter values, the simulations were performed as follows:

1. Use the parameter values to generate an undirected graph using the GREREC model (section 4.2.1)
2. Check whether the graph is connected; if the graph is not connected go to the next iteration.
3. Select a random set of OD pairs in the network with probability r.
4. Perform an analysis of the network robustness to single-, multiple-, random- and targeted-link failures as well as an analysis of the link-criticality rankings correlation.

4.2.5 Validation using real road maps

To validate the results of the analysis of the GREREC networks, the same analysis was performed on 30 real network samples. These samples were extracted from the road networks of six urban areas around the world: Johannesburg, London, New York, Paris, San Francisco and Seville. Five samples were arbitrarily extracted in each of these areas using bounding boxes defined by latitude and longitude bands of 0.01 width (≈ 1.11 km) to obtain graphs of the same order of magnitude as the GREREC networks analysed. To acquire the samples, the Python package *OSMnx* (Boeing, 2017) was used to download drivable street network data within the chosen boundaries from *OpenStreetMap* (www.openstreetmap.org) and automatically processed into length-weighted nonplanar graphs. In *OpenStreetMap* intersections of two divided roads, small roundabouts and sometimes intersections where opposite streets are not perfectly aligned create clusters of nodes that correspond to single intersections in the real world. Hence, these network samples slightly underestimate the number of high degree intersections. For the sake of reproducibility, it was however decided to keep the existing models unaltered. Figure 4.4 shows examples of the graphs analysed. The 30 graphs analysed are shown in Appendix B.

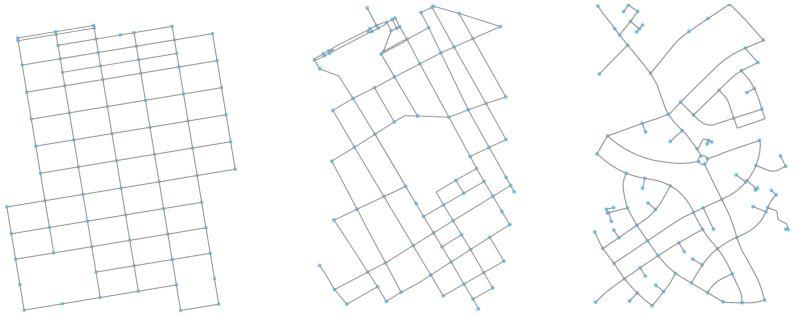

Figure 4.4: Examples of road network samples extracted from *OpenStreetMap* and analysed: (a) Pacific Heights, San Francisco, (b) Levallois-Perret, Greater Paris and (c) West Kensington, London

4.3 Results

The simulations were performed in **R** 3.4.4 and used the libraries *randtoolbox* and *igraph* for quasi-random number sequence generation and network analysis respectively. The **R** script was run in seven days on the University of Nottingham's high-performance computer, using in parallel twelve compute nodes with 2×20 core processors (Intel Skylake 6138 2.0GHz) and 192 GB memory each. The simulations resulted in 161 connected GREREC networks analysed in the following subsections.

4.3.1 Evaluation of the GREREC networks topology and patterns

The topological indices presented in section 4.2.2 were computed to evaluate the topology of the networks generated. The networks were also categorised into structural pattern groups based on the division of the values of p and q into three equally spaced intervals (Table 4.1). As only one connected network was generated with a value of p inferior to 0.33 (low values of p are highly likely to result in disconnected networks), this network was excluded from the structural pattern analysis since it could not support a statistical analysis. The distributions of the nodal degree in each of these structural pattern groups are summarised in Figure 4.5. Figure 4.2 shows examples of networks belonging to each group.

α, β, γ and the average degree provided the same information as the correlation between these different values ranged from 0.98 to 1. Hence, regardless of the index considered, the two extremes structures are the sparse structures of B1 and the very compact structures of C3 (i.e. lowest and highest connectivity values respectively in Table 4.1).

The low degree heterogeneity of B1 and C1 (0.98 and 1.02 respectively) suggest that both structures are rather homogeneous compared to the other ones. Indeed, B1 and C1 present a dominant frequency (median superior to 35%) of 3-legged and 3- and 4-legged intersections respectively, whereas the frequency peaks are less pronounced in the other groups (Figure 4.5). B1 represents sparse structures with a high proportion of 3-legged intersections that provides some "regularity" to the structure. This group is close to the warped parallel structure in Wang et al. (2017b)). B2 and B3 represent more organic structures with a mixture of vertical and horizontal links and shortcuts. C1 is the very

Table 4.1: Topological characteristics of the GREREC networks generated depending on p (probability of keeping horizontal and vertical edges) and q (probability of generating shortcuts).

Network group	p	q	α index	β index	γ index	$\langle Degree \rangle$	h^*_{Degree}
B1	[0.33, 0.66]	[0, 0.33)	0.291(0.11)	1.51(0.26)	0.538(0.066)	3.02(0.53)	0.969(0.32)
B2	[0.33, 0.66]	[0.33, 0.66]	0.446(0.14)	1.82(0.31)	0.637(0.090)	3.64(0.62)	1.413(0.15)
B3	[0.33, 0.66]	(0.66, 1]	0.543(0.11)	2.01(0.24)	0.699(0.068)	4.02(0.48)	1.753(0.20)
C1	(0.66, 1]	[0, 0.33)	0.476(0.09)	1.88(0.21)	0.655(0.058)	3.77(0.41)	1.021(0.19)
C2	(0.66, 1]	[0.33, 0.66]	0.612(0.11)	2.14(0.26)	0.745(0.070)	4.26(0.51)	1.336(0.15)
C3	(0.66, 1]	(0.66, 1]	0.713(0.11)	2.32(0.29)	0.812(0.067)	4.64(0.58)	1.619(0.30)

mean(standard deviation); * Degree heterogeneity

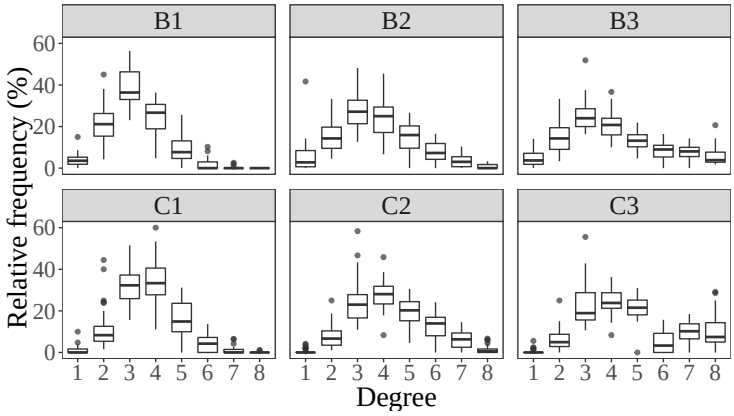

Figure 4.5: Nodal degree frequencies in the GREREC network structural pattern groups (box = 25th and 75th percentiles).

ordered grid-like structure with a majority of vertical and horizontal links. Finally, C2 and C3 are more compact structures where an increasing proportion of shortcuts are introduced in this grid-like structure.

4.3.2 Correlation between the network characteristics and robustness metrics in the GREREC networks

To model single- and multiple-link failures, three damage extension groups were considered: single-, two- and three-link failures. The robustness of the networks generated to the disruption scenarios was assessed using Eq. 3.2. The mean robustness indicator values of each network to the scenarios of the same damage extension group was used as a general measure of the network robustness to this damage group. The robustness values were also used to compute the link criticality indicators using Eq. 4.4. SLF, 2LF and 3LF based criticality rankings were compared to the rankings derived from the combination of all of these scenarios (ALL) using Spearman's correlation coefficient. These correlation values evaluate the extent to which SLF (or 2LF, etc.) based criticality measures repre-

sent the overall link criticality. The indicators related to the impacts of targeted attacks (CRO_{BETWI}, CRO_{RAND} and TA_{EI}) were computed using Eqs. 4.5-4.7.

All of these robustness metrics were evaluated against three types of network characteristics: the network size (i.e. the number of nodes in the network), topology (i.e. α, β, γ and the degree distribution) and operational characteristics (i.e. the proportion of nodes serving as OD pairs and heterogeneity of the link costs). Spearman's coefficient was used to assess whether a monotonic relationship existed between these variables (Table 4.2). An analysis of the distributions of the network attributes in the sample analysed is provided in Appendix A.2.

Table 4.2: Correlation (R_S) between the network characteristics and robustness metrics in the set of GREREC networks analysed. ^{ns}, *, ** and *** denote the significance at $p > 0.05$, $p < 0.05$, $p < 0.005$ & $p < 0.001$ respectively.

	Network characteristics				
	Network size (N)	Network connectivity (α, β, γ)	Degree heterogeneity	Link costs heterogeneity	Proportion of nodes being OD points
Mean robustness to SLF	0.92^{***}	$[0.72, 0.83]^{***}$	0.38^{***}	-0.33^{***}	-0.10^{ns}
Mean robustness to 2LF	0.93^{***}	$[0.72, 0.83]^{***}$	0.38^{***}	-0.33^{***}	-0.10^{ns}
Mean robustness to 3LF	0.93^{***}	$[0.72, 0.83]^{***}$	0.39^{***}	-0.33^{***}	-0.10^{ns}
SLF vs ALL[(1)]	0.16^{*}	$[-0.04, 0.00]^{ns}$	-0.19^{*}	-0.16^{*}	0.86^{***}
2LF vs ALL	0.41^{***}	$[0.19, 0.24]^{*}$	-0.05^{ns}	-0.16^{*}	0.66^{***}
3LF vs ALL	0.73^{***}	$[0.63, 0.71]^{***}$	0.45^{***}	-0.26^{***}	-0.35^{***}
Robustness to a BETWI[(2)]	-0.28^{***}	$[0.29, 0.43]^{***}$	0.16*	0.06^{ns}	0.20^{*}
Robustness to a RAND[(3)]	0.20^{*}	$[0.78, 0.87]^{***}$	0.58^{***}	-0.10^{ns}	0.17*
Targeted attack extended impact	0.59^{***}	$[0.68, 0.74]^{***}$	0.63^{***}	-0.15^{ns}	-0.00^{ns}

[(1)] Correlation of the link criticality rankings derived from single- (SLF), two- (2LF) and three- (3LF) link failures, and the combination of all three (ALL); [(2)] Interactive betweenness attack; [(3)] Representative random dismantling process.

Concerning the network connectivity, the highest correlation value in absolute was systematically obtained with β (or its equivalent the average degree). β is hence the preferred connectivity indicator for the plots of this chapter except for the robustness to random and targeted attacks that had the strongest correlation with γ.

Mean robustness of the networks to single-, two- and three-link failures

The proportion of nodes serving as OD points was not correlated with the network mean robustness to SLFs, 2LFs and 3LFs ($|R_S| < 0.20$ and p-value > 0.05). The degree and link cost heterogeneities both showed weak correlations with the network mean robustness to

SLFs, 2LFs and 3LFs (Table 4.2). The network characteristics that exhibited the strongest correlation with the mean network robustness were the network size and connectivity (Table 4.2) suggesting a potential relationship between these values shown in Figure 4.6.

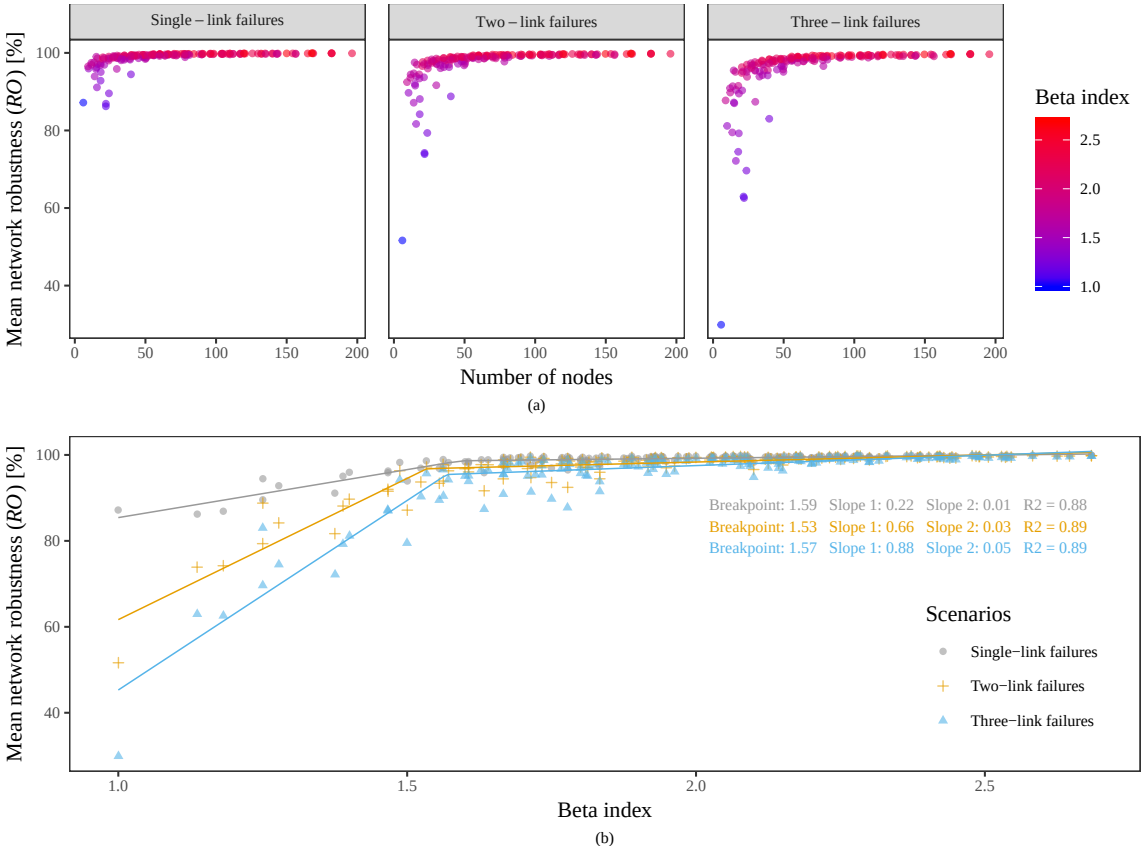

Figure 4.6: Mean robustness of the GREREC networks to single-, two- and three-link failures depending on their (a) size and connectivity and (b) connectivity.

Two domains appear in the plots of Figure 4.6.a. On the left side, the smallest networks exhibit a large variability in their mean robustness to SLFs, 2LFs and 3LFs while on the right side, the mean robustness of the largest networks seems independent of N. A visual assessment suggested that the change points for SLF, 2LF and 3LF were approximately $N = 30$, $N = 35$ and $N = 40$, respectively. Furthermore, the assessment of the results across the different damage extension groups shows that the average mean robustness of the small networks (less than 30 nodes) went from 96% (sd = 0.04) in SLFs to 87% (sd = 0.14) in 3LFs. In contrast, the average mean robustness of the large networks ($N > 30$) slightly decreased from 99% (sd = 0.01) in SLFs to 98% (sd = 0.02) in 3LFs.

Two domains are also present in the data of Figure 4.6.b that could be well represented by a piecewise linear model ($R^2 \approx 0.89$). Hence, the mean network robustness linearly increased with β, the slope being sharper before the breakpoint ($\beta \approx 1.55$). Besides, the gaps between the mean robustness of the networks to SLFs, 2LFs and 3LFs gradually decreased with β. The average mean robustness of the weakly connected networks ($\beta \leqslant 1.55$) went from 93% (sd = 0.04) in SLFs to 77% (sd = 0.16) in 3LFs while in the highly connected networks it slightly decreased from 99% (sd = 0.01) to 98% (sd = 0.02).

Correlation between the link-criticality rankings

The distributions of the link ranking correlation values are summarised in Table 4.3. These results indicate that SLF-based criticality rankings were generally very strongly correlated with the rankings based on all scenarios (the mean correlation value being 0.934) however low correlation values were also observed (e.g. 0.460). 2LF and 3LF based rankings showed even stronger mean correlations with the rankings based on ALL (0.983 and 0.995 respectively).

Table 4.3: Correlation (R_S) between the link criticality rankings derived from different scenarios: single- (SLF), two- (2LF) and three- (3LF) link failures and the combination of all three (ALL)

	SLF vs ALL	2LF vs ALL	3LF vs ALL
Min	0.460	0.698	0.878
Median	0.985	0.999	0.999
Mean	0.934	0.983	0.995
Max	1.000	1.000	1.000

Table 4.2 shows that SLF vs ALL was not correlated with the network attributes ($|R_S| < 0.20$) except for the proportion of nodes serving as OD points ($R_S = 0.86$). The correlations between 2LF vs ALL and the network attributes were weak at best ($|R_S| < 0.40$) except for the proportion of nodes serving as OD points ($R_S = 0.66$). In the case of 3LF-based criticality rankings, the correlation with the ratio of OD points to nodes became weak and negative ($R_S = -0.35$) while other network attributes started to play a role (i.e. the correlation of 3LF vs ALL with N and β were 0.73 and 0.71 respectively).

The influence of the network size on the rankings correlation is shown in Figure 4.7.a, where it can be seen that there were no significant relationship between the number of nodes in the network and both SLF vs ALL and 2LF vs ALL. In contrast, the minimum value of 3LF vs ALL increased with N. The influence of the proportion of nodes being OD points on the rankings correlation is shown in Figure 4.7.b, where the accuracy of SLF-based rankings increased with r_{OD}. When $r_{OD} \leq 0.5$ the mean value of SLF vs ALL is 0.87 (sd = 0.12) but reaches 0.99 (sd = 0.01) when $r_{OD} > 0.5$.

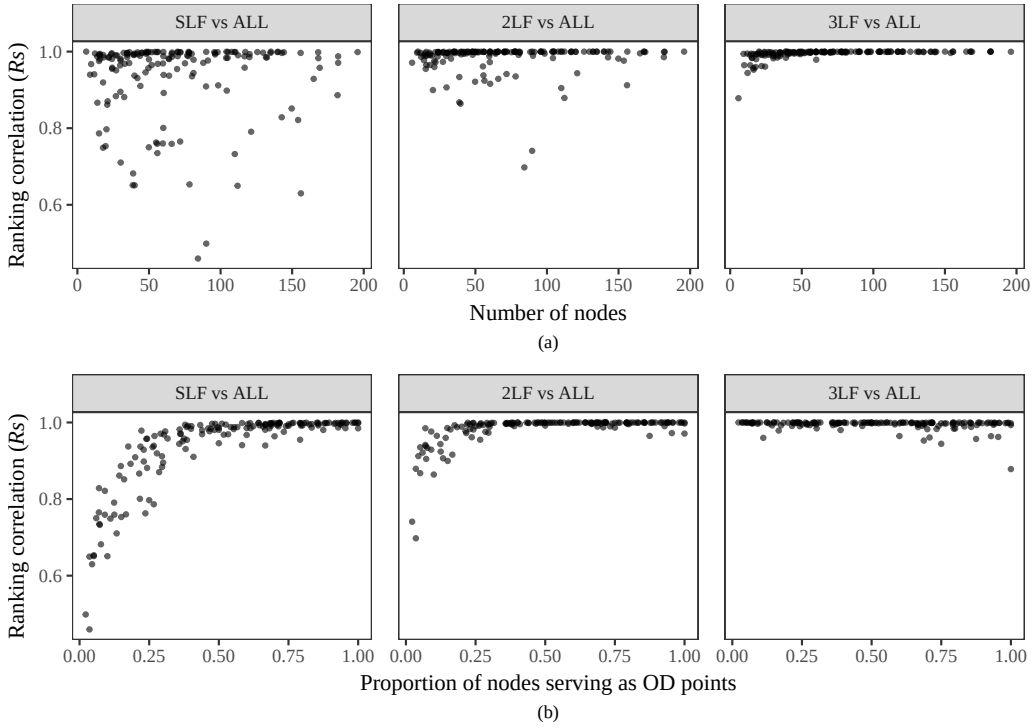

Figure 4.7: Correlation of the link criticality rankings derived from single- (SLF), two- (2LF) and three- (3LF) link failures and the combination of all three (ALL) depending on (a) the network size and (b) the proportion of nodes serving as OD points in the GREREC networks

Extended impact of targeted attacks

None of the network attributes demonstrated a strong correlation with the network robustness to a dynamic betweenness attack ($|R_S| < 0.43$). In contrast, the network robustness to random attacks demonstrated a strong correlation with the network connectivity ($0.78 \leqslant R_S \leqslant 0.87$), a moderate correlation with the degree heterogeneity ($R_S = 0.58$) and no correlation or an uncertain weak correlation with the other attributes (p-value > 0.001). The results are similar for the targeted attack extended impact except that the network size demonstrated a moderate correlation with TA_{EI} ($R_S = 0.59$).

Figure 4.8 shows the influence of the network connectivity, size and structural pattern group membership on both CRO_{RAND} and TA_{EI}. In Figure 4.8.a the largest networks seemed to follow a linear model relatively supported by a regression performed on the networks with more than 10 nodes ($R^2 = 0.76$). In contrast, the linear model appeared less relevant for TA_{EI} ($R^2 = 0.45$).

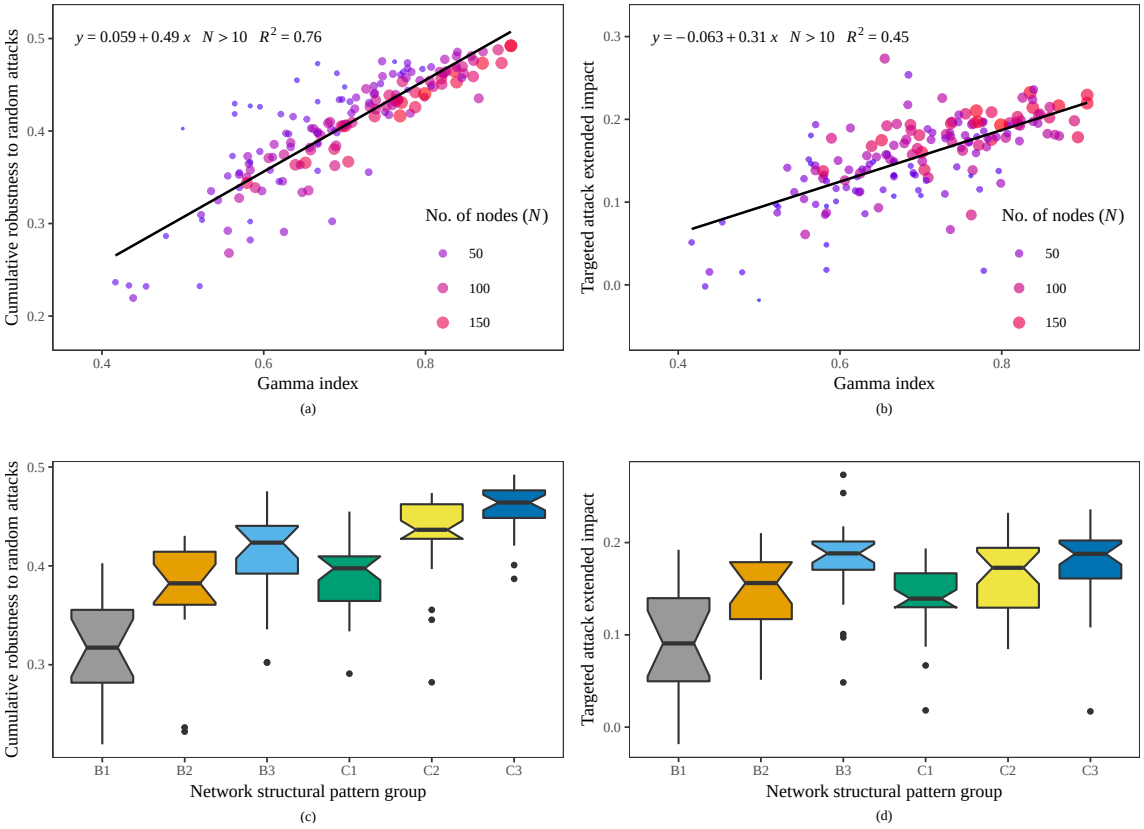

Figure 4.8: Relation between the "cumulative" robustness to random attacks—i.e. robustness to random dismantling processes—(CRO_{RAND}, Eq. 4.5) and the extended impact of targeted dismantling processes (TA_{EI}, Eq. 4.7) and three networks attributes: (a and b) the network connectivity and size and (c and d) the structural pattern group membership. box = 25th and 75th percentiles, notch = $\pm 1.58 IQR/\sqrt{n}$

.

4.3.3 Comparison with the real road networks

Topology of the road network samples

As the topology of a network can be characterised by its degree distribution, the average and standard deviation of the degree distributions in the GREREC and real networks (Figure 4.9) were used for comparing their topology. The real network topologies ranged from tree-like structures (Figure 4.4.c) to more compact and ordered grid-like structures (Figure 4.4.a) with average degrees of 2.33 and 3.32 respectively. In Figure 4.9, it can be seen that the topology of the real networks was close to the topology of some of the GREREC networks but that the latter also contained a large range of networks with higher average degree and degree heterogeneity values. Furthermore, the comparison with Table 4.1 and Figure 4.5 suggests that B1, B2, C1 and C2 were the GREREC structural pattern groups that are the closest to the real networks, while B3 and C3 present higher proportions of high degree nodes (superior to six) than real networks. Hence, the GREREC model better represents real road networks when the probability of generating shortcuts is low ($q < 0.66$).

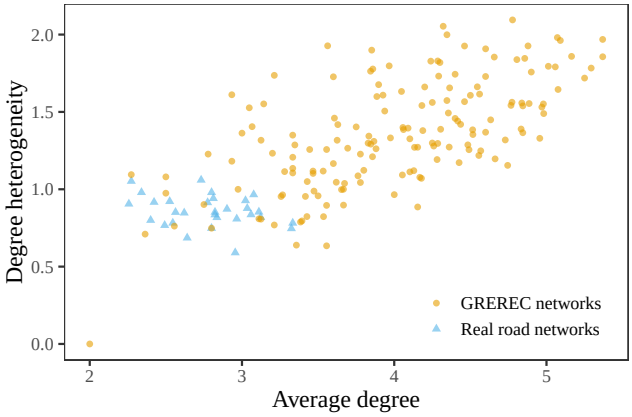

Figure 4.9: Comparison of the topology of the GREREC and real networks analysed. The degree heterogeneity is the standard deviation of the degree distribution in the network.

Correlation of the network robustness metrics with the network characteristics in the real network models

The correlation between the networks attributes and robustness metrics was also evaluated in the real network models (Table 4.4). These correlations were generally consistent with the correlations observed with the GREREC networks (Table 4.2) as they often had the same signs, ranges and p-values.

Although the correlations of the network mean robustness in SLFs, 2LFs and 3LFs with the network size were lower in the real networks (0.67 on average) than in the GREREC networks (0.93 on average), the network size and connectivity remained the only parameters strongly correlated to the mean network robustness. Furthermore, the smallest real networks also exhibited a large variability in their mean robustness to SLFs, 2LFs and 3LFs while the robustness of the largest networks seemed independent of N. The average mean robustness of the small real networks ($N \leqslant 30$) went from 91% (sd = 0.04) in SLFs to 73% (sd = 0.10) in 3LFs, while the average mean robustness of the large networks ($N > 30$) slightly decreased from 98% (sd = 0.01) in SLFs to 95% (sd = 0.04) in 3LFs.

However, in the real networks, the correlation of the mean robustness to single and multiple link failures with the degree heterogeneity was uncertain (p-value > 0.05) while the correlation with the link cost heterogeneity appeared stronger (-0.57 on average). Besides, the piecewise linear model connecting the network mean robustness and connectivity (Figure 4.6.b) remained relevant for the real networks but less accurate ($R^2 \approx 0.59$ in Figure 4.10.a).

In the real networks, the correlation of the robustness to the interactive betweenness attack with the network parameters remained weak or moderate at best (Table 4.4). The GREREC and real network correlation results were also similar for the robustness to random dismantling processes except that the latter was now uncorrelated with the degree heterogeneity. In contrast, the correlation of the extended impact of targeted attacks with the network size, connectivity and degree heterogeneity went from being strong in the GREREC networks to being not significant, moderate and not significant, respectively.

The linear model connecting network connectivity and robustness to random dismantling processes remained relevant ($R^2 = 0.87$ in Figure 4.10.b) for the real networks but

Table 4.4: Correlation (R_S) between the network characteristics and robustness metrics in the road network samples analysed. ^{ns}, *, ** and *** denote the significance at $p > 0.05$, $p < 0.05$, $p < 0.005$ & $p < 0.001$ respectively.

	Network characteristics				
	Network size (N)	Network connectivity (α, β, γ)	Degree heterogeneity	Link costs heterogeneity	Proportion of nodes being OD points
Mean robustness to SLF	0.66^{***}	$[0.74, 0.83]^{***}$	-0.20^{ns}	-0.55^{**}	-0.17^{ns}
Mean robustness to 2LF	0.67^{***}	$[0.73, 0.82]^{***}$	-0.20^{ns}	-0.57^{**}	-0.17^{ns}
Mean robustness to 3LF	0.68^{***}	$[0.72, 0.81]^{***}$	0.17^{ns}	-0.59^{***}	-0.16^{ns}
SLF vs ALL[(1)]	0.28^{ns}	$[0.20, 0.21]^{ns}$	-0.08^{ns}	-0.29^{ns}	0.59^{***}
2LF vs ALL	0.41^{*}	$[0.22, 0.24]^{ns}$	-0.10^{ns}	-0.39^{*}	0.40^{*}
3LF vs ALL	0.35^{ns}	$[0.01, 0.02]^{ns}$	-0.00^{ns}	-0.30^{ns}	-0.25^{ns}
Robustness to a BETWI[(2)]	-0.43^{*}	$[0.53, 0.67]^{**}$	-0.11^{ns}	0.43^{*}	0.01^{ns}
Robustness to a RAND[(3)]	0.27^{ns}	$[0.70, 0.83]^{***}$	-0.18^{ns}	0.31^{*}	0.11^{ns}
Targeted attack extended impact	0.30^{ns}	$[0.48, 0.52]^{**}$	-0.22^{ns}	-0.18^{ns}	0.24^{ns}

[(1)] Correlation of the link criticality rankings derived from single- (SLF), two- (2LF) and three- (3LF) link failures, and the combination of all three (ALL); [(2)] Interactive betweenness attack; [(3)] Representative random dismantling process.

with a steeper slope of 1.1 compared to 0.49 for the GREREC networks.

Table 4.5 shows that SLF vs ALL, 2LF vs ALL and 3LF vs ALL were at best weakly correlated with the network attributes ($|R_S| < 0.40$ and p-value > 0.005) apart from the proportion of nodes serving as OD points that was strongly correlated with SLF vs ALL ($R_S = 0.59$). This is also consistent with the GREREC results except that 3LF vs ALL was also strongly correlated with the network size and connectivity in the GREREC networks.

The results of the link criticality rankings comparisons in the real network models are summarised in Table 4.5. As with the GREREC networks (Table 4.3), SLF-based criticality rankings were generally very strongly correlated with the rankings based on all scenarios (the mean correlation being 0.973) while 2LF and 3LF based rankings showed even stronger mean correlations with the rankings based on ALL (0.999 and 0.995 respectively).

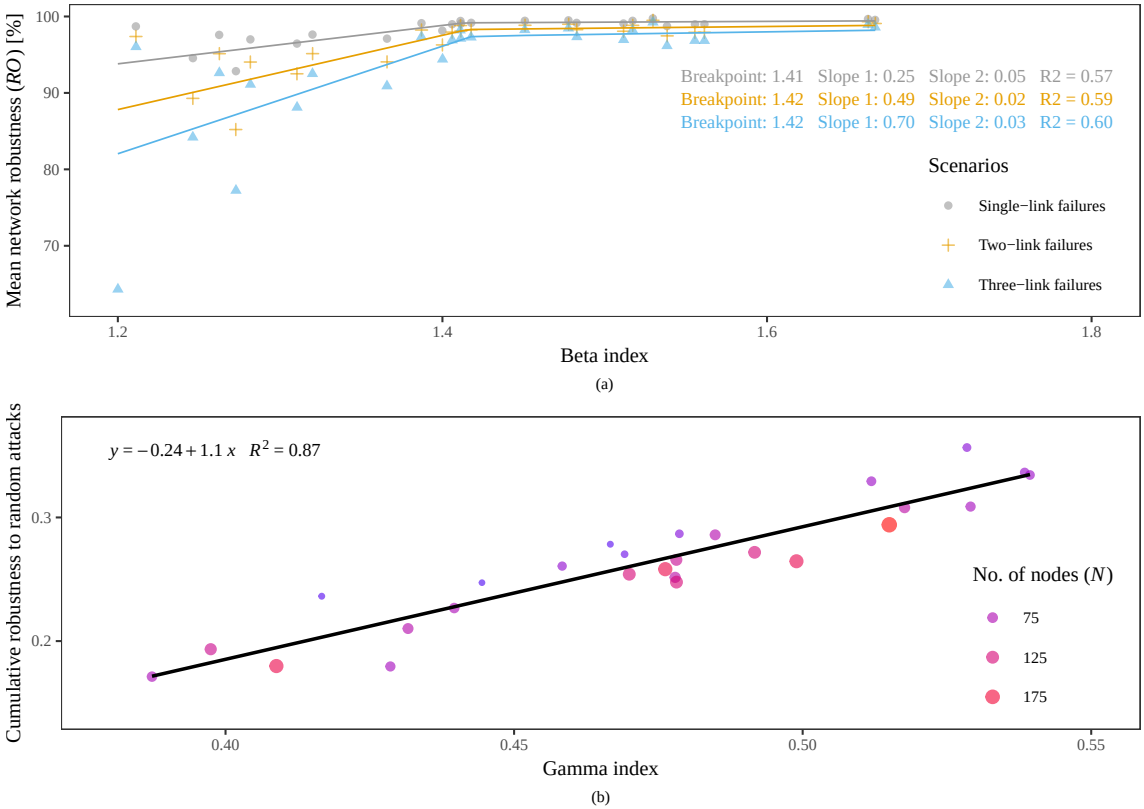

Figure 4.10: Influence of the network connectivity (beta and gamma) on the (a) mean robustness (RO, Eq. 3.2) to single-, two- and three-link failures and (b) "cumulative" robustness to random attacks—i.e. robustness to random dismantling processes—(CRO_{RAND}, Eq. 4.5) in the real road network models

Table 4.5: Correlation (R_S) between the link criticality rankings derived from single- (SLF), two- (2LF) and three- (3LF) link failures and the combination of all three (ALL) in the real road network samples

	SLF vs ALL	2LF vs ALL	3LF vs ALL
Min	0.803	0.998	0.974
Median	0.993	0.999	0.995
Mean	0.973	0.998	0.995
Max	1.000	1.000	1.000

4.4 Discussion

The comparison of the topology of the GREREC and real road networks suggest that the former contain a larger set of topologies. For example, the structural-pattern groups B3 and C3 have higher proportions of six-to-eight degree nodes than real networks. Although these networks may be rare in the real world due to costs and land-use constraints, their inclusion in this analysis remains useful to assess the benefits in terms of robustness of designing and building networks with a higher proportion of intersections connecting more than six streets.

The robustness analysis performed on both sets of networks allowed determining the influence of certain network attributes on network robustness as well as the generality of these findings. Firstly, the variations of the correlation between the robustness metrics and the network attributes (Table 4.2 and 4.5) depending on the aspect of robustness considered (mean robustness, link criticality, and extended impact of targeted attacks) reflect the fact that network robustness is a complex and multidimensional problem in which different network characteristics play more or less important roles depending on the aspect of robustness considered. Hence, none of the network attributes on its own is sufficient to explain road network robustness.

4.4.1 Influence of the degree and link-cost distributions on network robustness

Among the indicators considered, the link cost heterogeneity (i.e. the standard deviation of the link cost distribution) was the only indicator that showed no significant correlation with the robustness metrics of the GREREC networks. It is, however, difficult to conclude that the road network robustness is generally independent of the link cost heterogeneity as this could be specific to the indicator tested or to the process used to generate the link costs in the GREREC model. Indeed, the link cost heterogeneity of the real networks had a stronger (but still moderate) correlation with the mean robustness to single-, two- and three-link failures. Hence, the present results show that the link cost heterogeneity has a weak to moderate influence on the network robustness and more importantly that the links travel costs are much less important than the other parameters considered (i.e. the network topology and proportion of nodes serving as OD points) in terms of robustness.

In the GREREC networks, the degree heterogeneity (i.e. the standard deviation of the degree distribution) was positively and moderately correlated with network average robustness (i.e. mean robustness to SLFs, 2LFs and 3LFs and robustness to random dismantling processes). This correlation could not be verified in the real network samples. Considering the strong correlation between the network connectivity and robustness in both sets of networks, this difference may be explained by the fact the degree heterogeneity and connectivity were correlated in the GREREC networks ($R_S = 0.64$, p-value $< 10^{15}$) but uncorrelated in the real graphs ($R_S = -0.21$, p-value $= 0.256$). This highlights one of the weaknesses of the GREREC model where higher degree heterogeneity is often paired with higher connectivity while it may not always be the case in the real-world.

The present results may explain why previous research found that the degree heterogeneity positively impacted road network robustness. Considering the tail of degree distribution as an indicator of the degree heterogeneity, Buhl et al. (2006) noticed that the latter was positively correlated with the network robustness to random dismantling processes. The suitability of this indicator to reflect the degree heterogeneity is however problematic for two reasons. Firstly, the accuracy of this index depends on whether degree distributions tails (for degrees superior to three) can be approximated by exponential decays. This is not the case, for example, in cities presenting a dominant square-grid structure (e.g. San Francisco) where four-street intersections are more frequent than three-street intersections. Secondly, tails also contain information about the network connectivity as lower-decay rates also imply that more high-degree nodes are present in the network and

therefore that the network connectivity and robustness are higher.

4.4.2 Influence of the network size and connectivity on the network robustness to single-, multiple-, random- and targeted-link failures

The analysis showed that a linear model connected the network density and robustness in both the GREREC (Figure 4.8.a) and the real (Figure 4.10.b) networks. These observations are consistent with the conclusions of Buhl et al. (2006) who also found a linear relationship between those metrics although they considered a different robustness indicator. The steeper slope observed in the real networks can be explained by the smaller range of γ in this set of networks [0.38, 0.58] compared to [0.41, 0.91] in the GREREC networks since the data in Figure 4.8.a suggests that the slope of the linear model would also be steeper in this range. Hence, the network robustness to a random dismantling process linearly increases with the density (i.e. the proportion of possible links or cycles that are actually present in the network).

In both the GREREC and the real networks, the weak to moderate correlation observed between the network robustness to a dynamic betweenness attack (CRO_{BETWI}) and the connectivity indicators (α, β and γ) contrasts with the strong correlation found between the network connectivity and its mean robustness to SLFs, 2LFs, 3LFs and random dismantling processes. This may be because CRO_{BETWI}—like any other measure of the impact of a targeted attack—essentially looks at the impact in the worst-case scenario. As two networks can perform similarly under a targeted attack but differently under a wider range of disturbances, such measures may not be sufficient on their own to compare the robustness (ability to maintain functionality despite various disturbances) of different networks. It is, therefore, more meaningful to study and quantify the impact of targeted attacks in comparison with other attacks in the same network.

The positive correlations observed between the network connectivity, CRO_{RAND} and the extended impact of targeted attacks (TA_{EI}) suggest that although highly-connected networks are likely to be more robust to random failures than sparse networks, the extended impact of a targeted attack would also be larger in the former. Highly connected networks hence offer more opportunities for malicious attacks to be more detrimental than random attacks. In practice, this means that in sparse networks most of the links should be equally protected as the impacts of random and targeted attacks are close, whereas high-betweenness links should be given a higher priority for protection in complex networks.

However, network dismantling processes and the related robustness indicators lack applicability as real-life perturbations (car accidents, floods or sabotage actions) rarely follow this mechanism. Hence, the present study also considered single- and multiple-link failures to determine the influence of the network size (number of intersections) on the network robustness. Like the network connectivity, the network size was strongly correlated to the mean robustness to SLFs, 2LFs and 3LFs in both the GREREC and the real networks. These strong correlations can be explained by the fact that both parameters increase the number of alternatives routes available to substitute the disrupted ones. Furthermore, the correlation of the network size with the robustness to SLFs, 2LFs and 3LFs but lack of correlation with the robustness to random dismantling processes

suggests that most of the MLFs scenarios had a local impact.

The present results also showed that the relationship between the network connectivity and mean robustness tends to follow a piecewise linear model in the case of SLFs, 2LFs and 3LFs (Figure 4.6.b and 4.10.a), in which the effect of the network density on the mean robustness decreases to almost zero after the breakpoint. The value of this breakpoint slightly increased from 1.41 in the real networks to 1.55 in the GREREC graphs and should, therefore, be around those values.

Finally, if the conclusion that single- and multiple-link failures are more harmful in small and sparse networks was expected, the present research still provided quantitative estimates showing that the impact of SLFs and 3LFs are comparable in large networks (more than 30 nodes) while their impacts differ of 9% (18% in the real networks) in robustness on average in the small networks. Similarly, in the sparse networks ($\beta < 1.55$) the mean impact of SLFs and 3LFs differed of 16% (7% in the real networks) in robustness but of only 1% in the compact networks.

Similar behaviours could be expected for scenarios involving a greater number of failed links (four-link failures, etc.) although the size and connectivity thresholds may slowly increase with the number of failed links considered. Therefore, when designing or upgrading a road network, the addition of redundant routes in the network (by building additional roads and intermediate intersections) is an efficient way to improve the network mean robustness up to a certain size ($N \approx 40$) and connectivity ($\beta \approx 1.5$) threshold after which the robustness enhancement is limited.

4.4.3 Influence of the ratio of OD points to nodes on the link criticality rankings

The comparison of the link criticality rankings derived from single-, two- and three-link failures and the combination of all three showed that these rankings depend on the scenarios and network considered in both the GREREC and the real networks. The low correlation values obtained in some cases (e.g. the minimum value was 0.460 in the GREREC networks) indicate that SLFs and ALL can provide substantially different lists of links which are most critical to the network performance in case of disruption. The minimum value (0.803) obtained in the real networks was certainly higher than in the GREREC model because the set of real networks (30) was smaller than the set of GREREC networks (161). These results hence confirm and give more depth to the conclusions of Wang et al. (2016): the most critical links when multiple-link failures occur are not simply the combination of the most critical links with single-link failures.

The present study showed that SLF vs ALL was significantly positively correlated with the proportion of nodes being OD points in both the GREREC and real networks. Furthermore, SLF-based rankings were well correlated with the rankings based on all scenarios in networks with a high proportion of nodes serving as OD points ($r_{OD} > 0.5$). In such networks, OD pairs are more likely to be originally connected by direct routes for which the alternatives routes are much more costly or do not exist. In these networks, SLFs are hence very critical while the contribution of MLF scenarios to the link criticality is limited. In contrast, SLF-based rankings are likely to misrepresent the overall link criticality in networks with a low ratio of OD points to nodes where SLFs are less relevant

due to the availability of several "equivalent routes".

Although the correlation between 3LF and ALL based rankings remained generally high (above 0.878 in the GREREC networks), the variability of the correlation between both rankings further decreased with the network size. This may be explained by the fact that most 3LF scenarios are likely to be very critical in small networks resulting in more difficulty in distinguishing between the impacts of these scenarios on the network performance and thus in ranking the links.

One practical implication of these findings is that the classical method assessing link criticality based exclusively on SLFs is likely to misrepresent the overall link criticality in road networks where the population (demand) is not homogeneously distributed among all the intersections. The application of this method outside of this case could lead to inefficient prevention and restoration measures in the advent of events disrupting several road segments (e.g. flooding) or several events affecting different parts of the network at the same time (e.g. a car accident could cause the unavailability of a road while a bridge is closed for repair work in another part of the network).

On the other hand, the brute-force approach—testing all possible scenarios of MLFs—is limited by its computational cost and appropriate for small to medium (sub)networks only. Considering this, two-link failures seemed to provide a possible solution balancing accuracy and computational cost (the mean values of 2LF vs ALL being 0.981 and 0.998 for the GREREC and real networks respectively compared to 0.933 and 0.973 for SLF vs ALL) at least to represent the overall link criticality in failures of up to three links. Future research could seek to determine more precisely when it is necessary to consider 2LF, 3LF, 4LF, etc. and accordingly develop less computationally expensive methods for link criticality ranking.

4.5 Summary and concluding remarks

The present chapter focused on finding universal insights into road networks robustness to single-, multiple-, random- and targeted-link failures. To this end, the GREREC model was developed to randomly generate a variety of abstract networks presenting the topological and operational characteristics observed in real road networks, on which a robustness analysis was performed. This analysis was also reproduced on a set of real network samples for validation.

The results showed that the GREREC model can generate networks with topologies similar to real maps (ranging from tree-like structures to more compact and ordered grid-like structures) but also more diverse topologies presenting, for example, higher proportions of intersections connecting six to eight streets than real maps. Hence, the analysis performed on both sets of networks allowed to assess the robustness of real networks but also networks that could be designed and built for greater resilience. As the scenarios considered model a large range of disruptive events leading to the closure of sets of roads (e.g. serious car accidents, bridge failures and repair works), the results provide a framework to understand the potential influence of different network attributes on different aspects of road network robustness to such events.

The network size and connectivity strongly influenced the network mean robustness to multiple-link failures and allowed to distinguish small (sparse) networks where the im-

pact of MLFs heavily depend on the attack size from large (compact) networks where the increased attack size has a negligible effect. The results also showed that the addition of redundant routes in road networks (through additional roads and intermediate intersections) is an efficient way to enhance the network robustness to multiple-link failures up to a certain size and connectivity threshold.

As the construction of new roads requires significant investments, the proposed link criticality indicator can be used as a tool to identify and prioritise the road segments for which alternatives connections should be built. This indicator should, however, be used carefully as the present research shows that link criticality rankings are sensitive to the type of disruption scenarios considered (i.e. single or multiple link failures) and that the network attribute controlling the correlation between SLF-based rankings and the rankings based on all scenarios is the ratio of OD points to nodes. The classical method assessing link criticality based exclusively on single-link failures is hence likely to misrepresent the overall link criticality in road networks where the population (demand) is not homogeneously distributed among all the intersections, which could lead to inefficient prevention and restoration measures in the advent of events disrupting several road segments or several events affecting different parts of the network at the same time.

The comparison of the impact of targeted and random attacks showed that highly-connected networks are more robust but also offers more opportunities for malicious attacks to be more harmful than random failures. The identification and protection of the most critical road segments are hence more crucial in compact road networks than in sparse networks where most links are equally important to the network performance.

Ultimately, the GREREC model and the results presented here could be used as a relevant null model to benchmark the robustness of road networks. As stated above, the present chapter adopted a topological transport model, which disregards capacity constraints, for computational effectiveness. Therefore, to complement the present results, Chapter 5 investigates the sensitivity of the network robustness, the difference between single- and multiple-link based link criticality rankings, and extended impact of targeted attacks to capacity constraints and travel demand variability.

Chapter 5

Role of demand variations and capacity constraints in network robustness

5.1 Introduction

Chapter 4 assessed the effects of different network characteristics (the network size, topology and demand distribution) on the robustness of road networks to single-, multiple-, targeted- and random-link failures. This research also assessed the effects of the network characteristics on the difference between the link criticality rankings based on single- and multiple-link failures and the difference between the impacts of targeted and random failures. However, this assessment relied on a topological model and therefore did not consider capacity constraints and potential congestion. To complement this research and assess the role of capacity constraints in road network robustness, the present chapter analyses the robustness of the Sioux Falls network (Chapter 3) under different travel demand conditions and disruption types.

To this end, the present chapter uses and adapts the hazard-independent disruption model developed in Chapter 3 (which considers all possible scenarios disrupting multiple links without considering disruption probabilities as explained in Section 1.3.2). This adaptation allows the comparison of the impacts of three types of damage, namely, random (damaging random sets of links), localised (damaging adjacent links), and targeted (seeking to maximise the damage to the system performance). The robustness analysis of the Sioux Falls network is also used to explore the predictability of the link combinations whose failure would lead to the highest impacts on the system performance, and the difference between the link criticality rankings when only SLFs are considered as opposed to when MLFs are considered. Finally, the effects of demand intensity and distribution variability (and therefore congestion) on the network robustness and link criticality metrics are assessed by repeating the robustness analysis under different travel demand conditions.

This chapter is structured as follows. Section 5.2 presents the methods and case studies. In Section 5.3 and 5.4, the results of the network robustness assessment are presented and discussed, respectively. Sections 5.5 provides concluding remarks.

5.2 Methods

5.2.1 Disruption model

The present chapter considers a full range of predictable and unpredictable disruption scenarios using the hazard-independent disruption model proposed in Chapter 3. All possible combinations of link failures disrupting up to five links at the same time were simulated. This resulted in a dataset that combined five levels of damage extension: single-, two-, three-, four- and five-link failures.

The disruption scenarios in this dataset were then categorized into three types of disruptions, that are, localised-, targeted- and random-link failures. Localised scenarios disrupt adjacent links. These scenarios can be identified using the following procedure:

1. Identification of all localised two-link combinations

   (i) for each link, a_1, in the network, search for all links, $a_2 \neq a_1$, adjacent to a_1 (i.e. connected to the same node) and store (a_1, a_2) in a dataset

   (ii) remove duplicates from the dataset

2. Identification of all localised three-link combinations

   (i) for each link combination, (a_1, a_2), search for all links, $a_3 \neq a_1 \,\&\, a_2$, adjacent to a_1 and for all links, $a_3 \neq a_1 \,\&\, a_2$, adjacent to a_2, and store (a_1, a_2, a_3) in a dataset

   (ii) remove duplicates from the dataset

3. Identification of all localised four- and five-link combinations

   (i) repeat step 2 using the localised three- and four-link combination datasets, respectively

It is noted that localised disruptions are normally specified in terms of hazard-prone areas derived from climate models (Casali and Heinimann, 2019; Demirel et al., 2015; Hu et al., 2016; Wisetjindawat et al., 2017). In this thesis, localised failures refer to a range of events that may differ in nature (flooding, landslide, or large demonstrations) but lead to similar consequences, that is, the unavailability of adjacent network components. Again, this approach is used to reduce the dependency of the robustness assessment on empirical data, which may overlook unpredictable events.

Unlike localised disruptions that lead to aggregated destruction of components in a limited area, targeted- and random-link failures can damage network components distributed throughout the whole system. The latter damage a random set of links (e.g. pavement maintenance, pipe bursting, or police incidents amongst others can lead to random road closures) whereas targeted attacks imply a driving force seeking to maximise damage to the network performance (e.g. the bombing of a critical bridge). Robustness studies—especially in the context of complex network theory—commonly distinguish between these two types of failures (Buhl et al., 2006; Réka et al., 2000; Zanin et al., 2018), while localised failures are increasingly considered (Hu et al., 2016).

In this chapter, targeted attacks correspond to the 5% scenarios in each damage extension group (dataset) that cause the highest increases in travel time, measured by the network robustness indicator (RO, Eq. 3.2). The random failures correspond to the scenarios that are neither localised nor targeted.

Table 5.1 presents the definitions, models and real-world events associated with the three types of scenarios. The events presented in Table 5.1 could lead to partial speed or capacity reductions rather than complete road obstructions. However, the inclusion of such effects would add to the already high computational cost of the hazard-independent approach since several scenarios need to be computed per link.

Table 5.1: Classification and model of disruptive events affecting road networks

Name	Definition	Model	Real-word events represented
Localised	Failure of adjacent links	Failures identified by the iterative procedure (above)	Flooding, Landslides, Large demonstrations
Targeted	Failure with a maximum impact on network performance	Failures leading to the bottom 5% robustness indicator values	Targeted bombing, Sabotage, Industrial actions
Random	Failure of randomly selected links in the network	Failures that are neither critical nor localised	Serious car accidents, Road works, Police incidents

5.2.2 Network robustness and link criticality assessment

To assess the impacts on the disruption scenarios, the present chapter uses the network robustness (RO, Eq. 3.2) and unsatisfied demand (USD, Eq. 3.3) indicators developed in Chapter 3. To identify the most critical links with regards to multiple-link failures, the present chapter adopts the method and link criticality indicator (Cr_a, Eq. 4.4) developed in Chapter 4. As in Chapter 4, Spearman's correlation coefficient was used to compare the rankings derived from the criticality index when multiple-link failures are considered with the rankings that can be derived from less computationally expensive approaches (e.g. the SLFs and the link flow in the undisrupted state).

5.2.3 Case studies

The original Sioux Falls network

The present chapter analyses the robustness of the Sioux Falls network, which is presented and studied in Chapter 3. The assumptions, transport model and disruption simulations used in Chapter 3 are also adopted here.

Effect of travel demand on the network robustness

To provide a clearer understanding of road network robustness dependency on travel demand conditions, the effect of the demand intensity and distribution on the Sioux-Falls-network robustness and link-criticality metrics was evaluated. In the original Sioux Falls network, the travel demand is heterogeneously distributed across all intersections as every

node is both an origin and a destination point (Figure 5.1). To evaluate the effect of the demand distribution, two extreme cases were considered. Firstly, a case where the travel demand between all OD zones of the Sioux Falls network was removed from the network and homogeneously distributed among six arbitrarily chosen nodes: 1, 8, 10, 12, 20, and 23 (Figure 3.2). Secondly, a case where the demand was homogeneously distributed to all nodes in the network was considered.

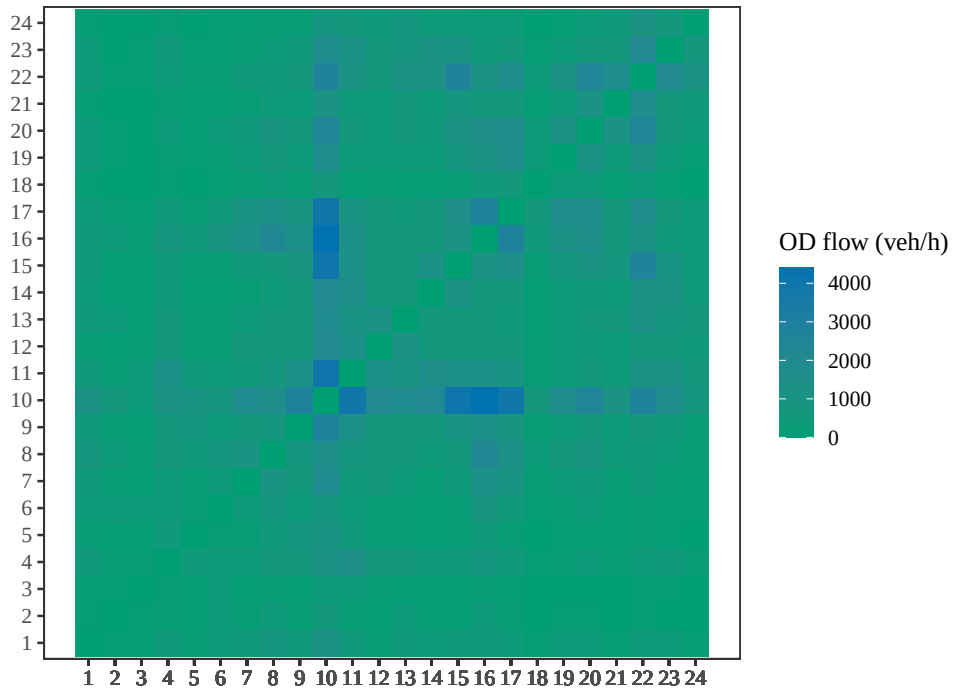

Figure 5.1: Demand distribution in the original Sioux Falls network (OD = Origin-Destination)

To evaluate the effect of the demand intensity, both extreme cases were computed under three levels of demand: low, medium, and high. The high level corresponds to the total demand in the original Sioux Falls network (360,600 vehicles/hour) that is already congested. The low (72,120 vehicles/hour) and medium (180,600 vehicles/hour) levels correspond to 20% and 50% of the total demand in the original network, respectively. These demand levels were chosen to obtain uncongested, congested, and highly-congested case studies.

5.3 Results

Impact of localised, random and targeted link failures

Subsets of the 2LF, 3LF, 4LF and 5LF scenario sets were considered to assess the difference between the impacts of localised, targeted, and random damage using the disruption model described in Section 5.2. The impacts of the three types of scenarios are compared in Figure 5.2. Figure 5.2.a shows the relationship between the network robustness indicator measuring the average increase in TT along the OD pairs and the unsatisfied demand indicator measuring the proportion of road users unable to reach their chosen destination.

Figure 5.2.b and c show the distributions of RO and USD across the damage type and extension groups.

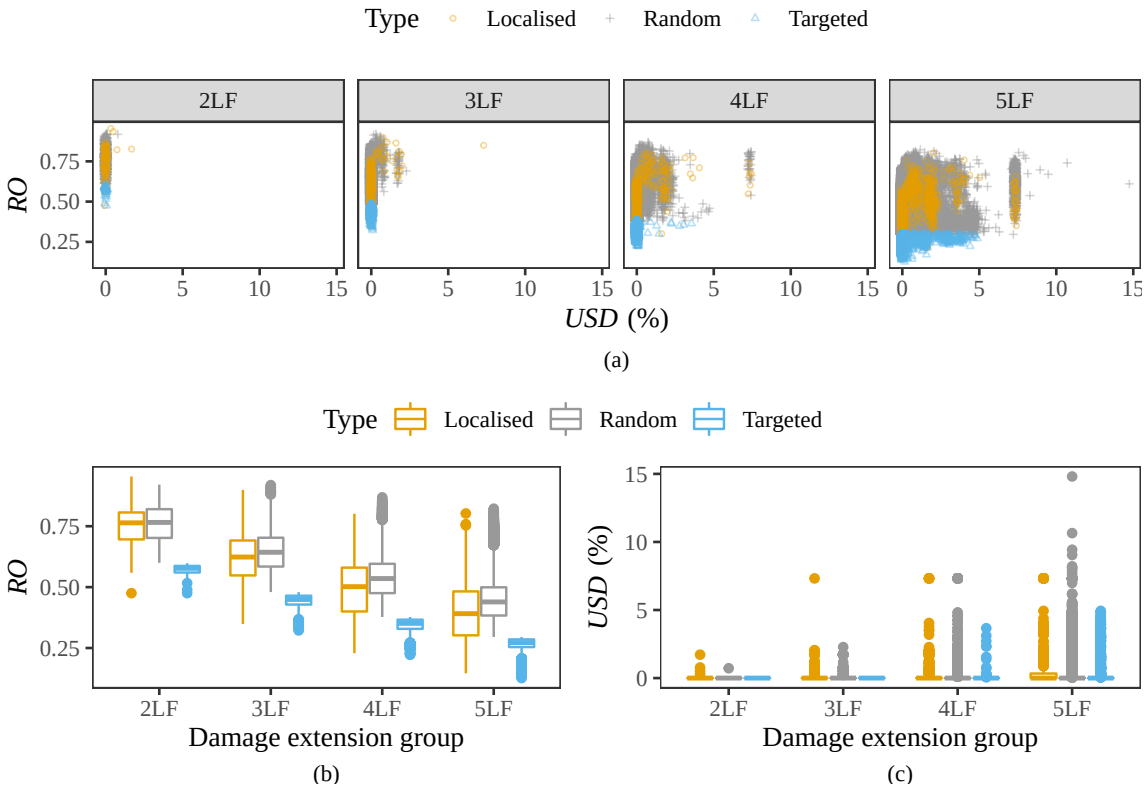

Figure 5.2: Impact of localised, random and targeted two- (2LF), three- (3LF), four- (4LF) and five- (5LF) link failures in the original Sioux Falls network. (RO = Network robustness indicator, USD = Unsatisfied demand indicator, box = 25th and 75th percentiles)

The results indicate that targeted attacks were much more critical to the network performance than random failures (the difference between the mean robustness to random and targeted failures being 19.4%, 20.3%, 19.5% and 17.9% in 2LFs, 3LFs, 4LFs and 5LFs, respectively in Figure 5.2.b) while localised failures were only slightly more critical than their random counterparts (the difference between the mean robustness to random and localised failures being 1.6%, 2.9%, 4.0% and 4.3% in 2LFs, 3LFs, 4LFs, 5LFs respectively in Figure 5.2.b). In addition, the difference between the mean robustness in localised and random failures increased with the damage extension while the difference between targeted and random failures seemed relatively constant.

Although the differences between the mean USD values in the three damage types were insignificant ($< 1.0\%$), it can be seen in Figure 5.2.a and c that the highest values of the unsatisfied demand indicator appeared among the localised scenarios four all damage extension groups except 5LFs. In contrast, the targeted attacks presented the lowest USD values.

5.3.1 Most critical disruption scenarios

The network robustness indicator was used to identify the five most critical scenarios in all damage extension groups. These scenarios are presented in Table 5.2 along with their RO and USD values.

Table 5.2: Top-5 most critical combinations of single-, two-, three-, and four-link failures in the original Sioux Falls network

Link combination	RO (USD)
(10,15)	73.2 % (0 %)
(18,20)	74.0 % (0 %)
(9,10)	75.3 % (0 %)
(12,13)	77.7 % (0 %)
(10,15)	77.8 % (0 %)
(9,10) (10,11)	47.5 % (0 %)
(10,15) (18,20)	48.9 % (0 %)
(5,9) (10,11)	51.6 % (0 %)
(9,10) (18,20)	53.0 % (0 %)
(12,13) (18,20)	53.5 % (0 %)
(10,15) (17,19) (18,20)	32.2 % (0 %)
(9,10) (10,11) (18,20)	33.2 % (0 %)
(10,15) (16,17) (18,20)	34.0 % (0 %)
(5,9) (10,11) (10,15)	34.3 % (0 %)
(9,10) (10,15) (18,20)	34.5 % (0 %)
(9,10) (10,11) (10,15) (18,20)	22.3 % (0 %)
(9,10) (10,11) (12,13) (18,20)	22.3 % (0 %)
(10,15) (10,17) (16,17) (18,20)	22.6 % (0 %)
(5,9) (10,11) (10,15) (15,19)	22.6 % (0 %)
(3,12) (9,10) (10,11) (18,20)	22.8 % (0 %)
(7,15) (8,16) (9,10) (10,11) (10,15)	12.7 % (0.1 %)
(9,10) (10,11) (10,16) (16,17) (18,20)	13.7 % (0.0 %)
(9,10) (10,11) (10,15) (16,17) (18,20)	13.9 % (0.0 %)
(5,9) (10,11) (10,15) (15,19) (18,20)	14.2 % (0.0 %)
(2,6) (4,5) (9,10) (10,11) (18,20)	14.2 % (0.0 %)

RO = Network robustness indicator (Eq. 3.2); USD = Unsatisfied demand indicator (Eq. 3.3), Bold font = localised scenario.

In accordance with the results presented in Figure 5.2, it can be seen in Table 5.2 that none of the top-5 most critical scenarios led to unsatisfied demand ($USD = 0$). Besides, among the top-5 most critical scenarios only one was a localised scenario that is (9,10) & (10,11) in bold in Table 5.2.

The most critical combinations of 2LFs, 3LFs, 4LFs and 5LFs did not necessarily involve the most critical links with SLF as links outside of this group, for example (10,11) and (17,19), appeared in these combinations. However, all top-5 most critical 2LF scenarios involved the disruption of at least one of the top-6 most critical links with SLF, (5,9) being the 6th most critical link with SLF. Similarly, the top-5 most critical 3LFs and 4LFs all contained one of the top-5 most critical combinations of 2LFs and 3LFs, respectively.

Four of the top-5 most critical 5LF combinations - except the first one i.e. (7,15) (8,16) (9,10) (10,11) (10,15) – contained one of the top-8 most critical 4LF combination, (4,5) (9,10) (10,11) (18,20) being the 8th most critical 4LF combinations. The critical combinations of 2LFs, 3LFs, 4LFs and 5LFs hence involved at least one of the most critical links with SLF.

This pattern suggests that to identify and evaluate the impact of the top-5 most critical MLF scenarios it might not be necessary to consider all possible scenarios. Instead, an iterative procedure could be used as follows (in a network composed of L links):

(i) Evaluate the impact of all SLFs [L simulations]

(ii) Rank the impacts and select the top-10 most critical links (and not the top-5 to reduce the probability of missing critical scenarios)

(iii) Compute all 2LF scenarios involving the top-10 most critical links with SLF [$10(L-1)$ simulations]

(iv) Rank the impacts and select the top-10 most critical 2LFs

(v) Compute all 3LF scenarios involving the top-10 most critical 2LFs [$10(L-2)$ simulations]

(vi) Repeat the two previous steps until reaching the desired number of failed links

Therefore, to identify the top-5 most critical scenarios concurrently disrupting M links, this procedure would require $L + 10\sum_{k=1}^{M-1}(L-k)$ disruption simulations (= 1,118 in the Sioux Falls network for 4LFs), which is far less computationally expensive than the $\binom{L}{M}$ simulations required to test all possible scenarios (= 78,315 in the Sioux Falls network for 4LFs).

5.3.2 Critical links

As the most critical failure scenarios involve a multitude of links including links that are only critical when they concurrently fail with a specific set of other links (Table 5.2), it is difficult to rank links using the top-5 most critical scenarios only. Therefore, the link criticality was assessed using the link criticality indicator, Cr_a (Eq. 4.4), which combines the robustness indicator values of all single and multiple-link failure scenarios into one indicator.

According to Cr_a, the most critical links in the Sioux Falls network were in criticality order, (10,15), (18,20), (9,10), (12,13), and (6,8), which is consistent with the SLF results (Table 5.2). To verify if the ranking provided by Cr_a was totally consistent with the SLF-based criticality ranking, the relation between the two rankings was evaluated using Spearman's correlation coefficient. The correlation between the two rankings was very strong ($R_s = 0.993$).

5.3.3 Effects of demand variations on the network robustness and link criticality results

To evaluate the effects of demand variations on the aforementioned results, the analysis was repeated on versions of the Sioux Falls network with different demand distribution

and intensity conditions (Section 5.2). For computational effectiveness, the disruption simulations were limited to single-, two- and three-link failures in these six case studies. The results are presented in Table 5.3, where the original Sioux Falls network is included for comparison. This table shows the mean and standard deviation of the flow/capacity ratio of the links in the network to provide a general measure of the congestion level. The low-, medium-, and high-demand levels correspond to uncongested (mean flow/capacity ratio < 0.5), congested (mean flow/capacity ratio ≈ 1), and highly congested (mean flow/capacity ratio > 1.5) conditions, respectively.

The mean robustness indicator values of each network—computed over SLFs, 2LFs and 3LFs— were used as a general measure of the network robustness. The comparison of this value across the different case studies (Table 5.3) shows that higher demand and congestion reduce robustness. Furthermore, for the same congestion level, the networks where the demand was better distributed across the nodes were more robust.

To compare the impact of localised-, random-, and targeted-link failures in the case studies, the differences between the mean robustness indicator values in these three types of damage were computed (Table 5.3). The results suggest that the impact of localised and random failures were similar in all case studies (the absolute difference between the two means being inferior to 5%). Localised failures were more critical than random failures in some networks as the sign of the difference changed. However, this sign seemed correlated to neither the demand intensity nor the distribution. The difference between the impacts of targeted and random failures remained significant in all case studies ($\geq$ 7%). The differences were higher in the networks with concentrated demand (between 21.9% and 30.2%) than in the networks with distributed demand (between 7% and 21%).

Spearman's correlation coefficient was used to quantify the difference between the link criticality rankings derived from multiple- and single-link failures. The correlation coefficients (presented in Table 5.3) showed that the two rankings were always very strongly ($R_s \geq 0.80$) correlated. The correlation was stronger in the networks where the demand was distributed to all the nodes and increased further with the congestion level in both demand distribution cases. The correlation between the criticality rankings based on the link flow, flow/capacity ratio and multiple-link failures were also examined, and discussion of these results is available in Appendix C. These results were not included in Table 5.3 for brevity.

The standard deviation of the link criticality values in each network was computed to evaluate the heterogeneity of the link criticality distributions in the networks. The results (presented in Table 5.3) showed that the heterogeneity was higher in the networks with concentrated demand. Moreover, the heterogeneity of the link criticality distribution increased with the demand intensity in both demand distribution cases.

The top-5 most critical links in all case studies were identified based on SLFs, 2LFs and 3LFs using the criticality indicator. The lists of these critical links are presented in Table 5.3, where it can be seen that the criticality ranking depends on the demand distribution and intensity as all lists were different.

The accuracy of the iterative procedure proposed to identify and predict the impact of the top-5 most critical scenarios of MLFs (Section 5.3.1) was evaluated by computing the proportion of top-5 2LFs and 3LFs that could be predicted in the case studies (Table 5.3). This procedure was more accurate when the demand was distributed (the minimum

proportion of scenarios identified was 50% when the demand was concentrated and 70% when it was distributed). This accuracy increased in congested networks (90% to 100% of the scenarios identified).

Table 5.3: Effect of the demand distribution and intensity on the network initial state, robustness, and link-criticality

	Demand concentrated in six nodes			Original Sioux Falls network	Demand distributed to all nodes		
Network initial state							
Demand level	Low	Medium	High	High	Low	Medium	High
Link flow/capacity ratio	0.40(0.40)	1.08(0.57)	2.19(0.99)	1.47(0.57)	0.41(0.30)	0.93(0.43)	1.79(0.62)
Network robustness							
Mean robustness[(1)]	0.923	0.781	0.663	0.755	0.950	0.859	0.704
Difference between mean robustness to random and localised failures[(2)]	-0.006	-0.021	-0.033	0.022	0.001	-0.004	-0.012
Difference between mean robustness to random and targeted failures[(2)]	0.219	0.302	0.270	0.199	0.070	0.190	0.212
Link criticality							
SLF vs ALL[(3)]	0.971	0.991	0.998	0.993	0.994	0.996	0.998
Standard deviation of the link criticality values	0.083	0.168	0.191	0.108	0.026	0.078	0.142
Top-5 most critical links according to ALL (in criticality order)	(1,3) (6,8) (13,24) (12,13) (3,12)	(3,4) (1,3) (3,12) (4 5) (6,8)	(3,4) (3,12) (6,8) (4,5) (13,24)	(10,15) (18,20) (9,10) (12,13) (6,8)	(6,8) (12,13) (13,24) (1,3) (18,20)	(5,9) (3,4) (6,8) (1,3) (9,10)	(5,9) (3,12) (12,13) (13,24) (6,8)
Proportion of top-5 most critical 2LFs and 3LFs predicted by the iterative procedure	1.000	0.500	0.900	1.000	0.700	1.000	0.900
Run time[(4)]	4min	25min	56min	33min	2min	8min	2h41min

mean (standard deviation); [(1)] mean computed over single- (SLF), two- (2LF) and three- (3LF) link failures; [(2)] mean computed over 2LFs and 3LFs; [(3)] Correlation between the link criticality rankings based on single-(SLF) and multiple- (ALL) link-failures, ALL = SLF + 2LF +3LF ; [(4)]; Time taken to perform the SLF, 2LF and 3LF simulations using parallel processing on an *Intel i3-7100* 3.9GHz and 8GB memory work station.

Figure 5.3 shows the spatial distribution of link criticality values in the different demand intensity and distribution conditions. For the sake of brevity, only the low and high demand concentrated in six nodes and distributed across all nodes are shown. In Figure 5.3, the link criticality values seem more heterogeneous in the networks with high and distributed demand, which is confirmed by the evolution of the standard deviation of the link criticality values in Table 5.3. Furthermore, it is interesting to note that in the uncongested networks (Figure 5.3.a and c) the most critical links—(1,3), (6,8), (12,13) and (13,24)— were in the network periphery while in the congested networks (Figure 5.3.b and d) some inner links—(4,5) and (5,9)—appeared among the top-5 most critical links (Table 5.4).

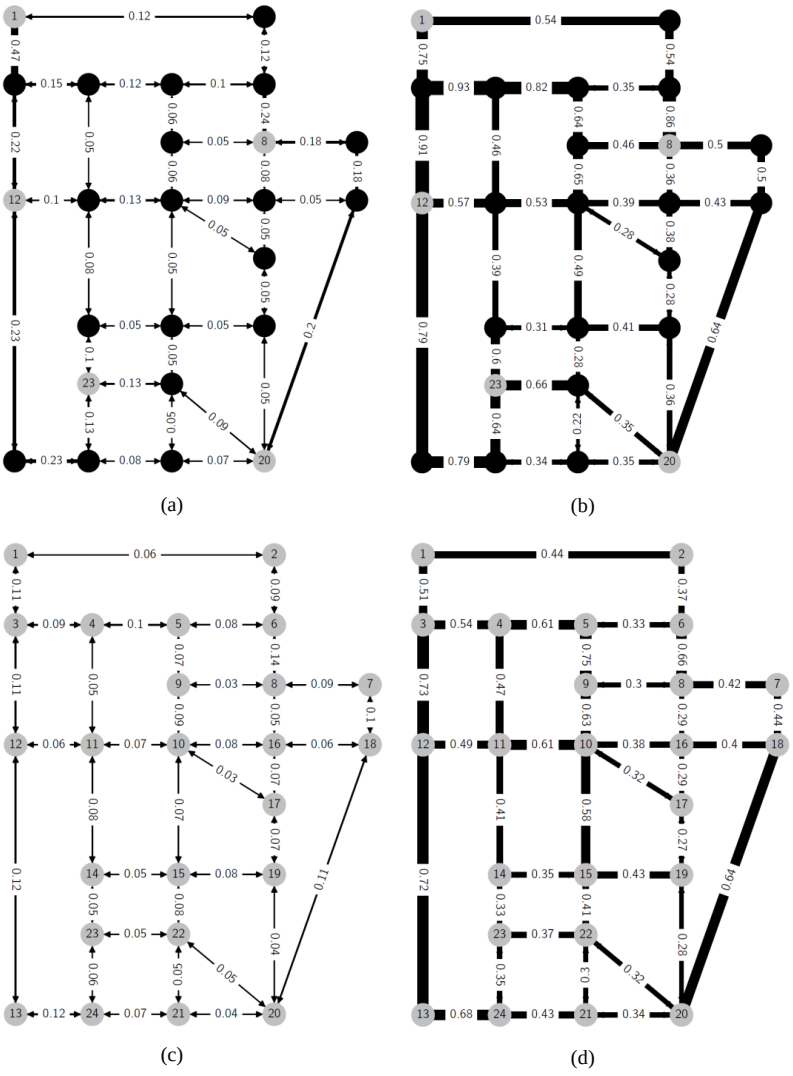

Figure 5.3: Most critical links in the Sioux Falls network under different conditions: (a) low demand concentrated in six nodes, (b) high demand concentrated in six nodes, (c) low demand distributed to all nodes, and (d) high demand distributed to all nodes. The nodes in silver are OD points; the link labels and thickness indicate the values of the link criticality indicator, Cr_a, which combines the link criticality derived from single-, two-, and three-link failures into one indicator.

The correlation between the link criticality rankings derived in the different demand intensity and distribution conditions was evaluated (Table 5.4) to determine which rankings were the closest to each other. Inside the demand distribution groups, the link criticality rankings were strongly correlated as the value of the correlation coefficient within the networks with concentrated and distributed demand remained above 0.767 and 0.698, respectively. Inside both groups, the correlation between the medium and high-level demand conditions increased further ($R_S > 0.90$). In contrast, the correlation between the rankings derived from the networks with concentrated and distributed demand was moderate to strong ($0.565 \leq R_s \leq 0.748$) and the correlation of the ranking in the original network with the other cases was moderate at best ($|R_S| \leq 0.575$).

Table 5.4: Correlation (R_S) between the link criticality rankings derived in different demand intensity and distribution conditions

		Demand concentrated in six nodes			Demand distributed to all nodes		
	Demand level	Low	Medium	High	Low	Medium	High
Demand concentrated in six nodes	Low						
	Medium	0.824					
	High	0.767	0.948				
Demand distributed to all nodes	Low	0.663	0.618	0.565			
	Medium	0.565	0.718	0.703	0.777		
	High	0.610	0.753	0.748	0.698	0.918	
Original Sioux Falls network	High	0.113	0.225	0.267	0.507	0.575	0.532

5.4 Discussion

5.4.1 Impact of random, localised and targeted damage

The comparison of the impacts of the three types of damage in the original Sioux Falls network (Table 5.2 and Figure 5.2) showed that the most critical types of scenarios were targeted, localised, and random failures (in that order); and that targeted attacks were significantly more detrimental to the network performance than random failures (20% difference in robustness) while localised failures were only slightly more critical than random failures (3% difference in robustness in average). These results are consistent with the findings of Hu et al. (2016) that however considered full dismantling processes rather than failure scenarios disrupting a limited number of roads.

Furthermore, the comparison of the difference between the mean robustness in localised and random failures across the different demand intensity and distribution conditions (Table 5.3) showed that their impacts were very close (the mean difference being inferior to 5%) and that one could be slightly more detrimental than the other in different conditions. This suggests that although random scenarios damage infrastructures distributed throughout the whole network (and therefore potentially impact more users) the resulting impact is in general equivalent to the impact of localised failures. Hence, the impact may

be significant in only one of the locations disturbed.

The analysis of the unsatisfied demand resulting from the different types of damage (Figure 5.2) showed that localised failures lead to higher proportions of unsatisfied demand than their targeted counterparts. Hence, localised damage cause a maximum impact on a limited number of road users. In contrast, targeted attacks strategically damage network components that are apart (as shown in Table 5.2 where the top-5 most critical combinations of link failures rarely involved adjacent links) but whose simultaneous failures cause important and widespread impacts (the mean difference between the impact of targeted and random failures remained superior to 7% in robustness in all case studies in 5.3). The difference was greater in the networks where the demand was concentrated in a few nodes compared to networks where the demand was distributed to all nodes. This is because in the former it is easier to cause important and widespread impacts with limited resources (number of disrupted links) as more vehicles share the same routes. This explanation is confirmed by the relatively high heterogeneity of the link criticality values observed in the networks with concentrated demand compared to the other cases (Table 5.3). In contrast, in the networks with distributed demand, most links tend to be equally critical, which explains why the extended impact of targeted attacks (i.e. the difference between the impact of targeted and random damage) is reduced when the demand is well distributed.

The demand intensity has a similar impact on the network as the heterogeneity of the link criticality values and the extended impact of targeted attacks increased with the demand intensity for both demand distribution conditions (except that in the network with concentrated demand the extended impact of targeted attacks was higher with medium demand than high demand). Therefore, it is more crucial to identify and protect the most critical links in networks that are congested and where the demand is not well distributed among the intersections.

5.4.2 Identification and sensitivity of the most critical scenarios and links

Predictability of the scenario- and link-criticality rankings

Wang et al. (2016) showed that the links involved in the most critical multiple-link failures are not simply the combination of the most critical links with single-link failure. The present results went further to show that the most critical links and scenarios are not completely random. The top-5 most critical scenarios of different sizes (i.e. SLFs, 2LFs, etc.) were related to each other as the top-5 most critical scenarios of size M tented to appear in the top-5 most critical scenarios of size $M+1$. This led to an iterative procedure (described in section 5.3.1) providing a heuristic to identify and predict the impact of these scenarios with a decreased computational effort.

This pattern and therefore the accuracy of the procedure seemed stronger and higher, respectively, in congested networks. This may be because all links are used in congested networks since road users along the same OD pairs use several routes to minimise their respective travel times. Therefore, in congested networks there is a limited spare capacity available to accommodate the users that need to re-route following a disruption such that disruptions mainly lead to additional congestion. The most critical scenarios of size M are

hence likely to appear in the most critical scenarios of size $M+1$. Whereas in uncongested networks, travellers along the same OD pairs tend to use the same route such that some links may be unused and provide a good alternative for re-routing when disruptions occur, leading to limited network performance losses. Hence, the combined effect of the link failures seems more difficult to predict in uncongested networks.

For the same reason, the proposed procedure can also provide a satisfying approximation of the link criticality ranking in congested networks as this procedure requires the computation of all SLFs, which according to the present results were very strongly correlated to the rankings based on MLFs in congested networks ($R_S > 0.990$). These results complement the findings of Chapter 4 that show the influence of the network size, topology, and demand distribution on the correlation between SLF- and MLF-based criticality rankings but does not consider the influence of congestion.

The limited accuracy of the iterative procedure in uncongested networks is not bad news considering that traffic simulations are individually less computationally expensive in uncongested networks than in congested networks as shown by the run times reported in Table 5.3. This is because the user equilibrium is easier to compute in uncongested networks. Indeed, the Frank-Wolfe algorithm seeks to find the equilibrium traffic flows where the travel time of each user is minimum. To this end, the algorithm incrementally assigns the OD demand in multiple steps such that in each step a fraction of the OD matrix is loaded to the shortest paths and the resulting link travel time calculated (depending on the link flow). The re-calculated link travel times are used in the following step to find new shortest paths for the OD pairs. In uncongested networks, the equilibrium search is rapid as the link travel times are independent of link flows such that most travellers along an OD pair use the same route. Whereas in congested networks, travellers along an OD pair use several routes to reduce their travel time as congestion builds up, leading to a greater number of iterations required to reach the equilibrium.

Finally, it is interesting to note that the pattern found between the top-5 most critical link combinations suggests that, in practice, the protection or rapid repair of the top-5 most critical links with SLF can also help towards the protection of the network performance against the most critical MLF scenarios as the latter tend to involve at least one of the top-5 most critical links with SLF.

Influence of the demand intensity and distribution on the link criticality rankings

The results showed that the link criticality rankings are sensitive to the demand intensity and distribution (Tables 5.3 and 5.4). The significant difference observed between the criticality rankings in the demand distribution conditions considered (demand heterogeneously distributed in the original Sioux Falls network, concentrated in six nodes, and homogeneously distributed to all nodes) was expected since the demand distribution modifies the network usage. The difference observed between the demand intensity (low, medium, and high) conditions was more interesting. The very strong correlation found between the medium- and high-demand conditions regardless of the demand distribution (Table 5.4) showed that the ranking of the links significantly changes as the network moves from uncongested to congested conditions but remains similar when congestion further increases.

In addition, the analysis of the spatial distribution of the link criticality values in the network (Figure 5.3) showed that the main difference between the uncongested and congested conditions was the fact that in the former the most critical links belonged to the network periphery while some inner links appeared among the top-5 most critical links in the congested networks. In uncongested networks, when an inner link is unavailable the network structure naturally provides several alternatives routes that lead to reasonable increases in travel time for the affected users, whereas, in congested networks, these alternative routes are already congested and therefore lead to greater TT increases.

To conclude, this shows that the accuracy of the demand distribution model is important for robustness assessments as this will significantly impact the resulting link criticality rankings. In contrast, the accuracy of the demand intensity evaluation seems less crucial if the network is accurately defined as uncongested or congested in its undisrupted state. Hence, practitioners should carefully think about the conditions that they wish to consider when performing road network robustness assessments. They may, for example, choose to consider the peak-hour conditions that should represent the worst-case scenarios in terms of demand intensity; or prioritise the demand going from/to critical locations (for example hospitals, fire stations and airports) that may lead to a different demand distribution than the dominant peak-hour home-work trips; or consider and combine both. This sensitivity analysis also provides some insights into the potential effect of the travel demand alteration caused by disruptions on the present assessment. Following a major disruption, work and leisure trips are likely to be cancelled or delayed while emergency trips (e.g. evacuation and transport from/to hospitals) are likely to increase. Hence, the travel demand is likely to concentrate in a few zones while the total demand intensity decreases. The low- and medium- demand intensity concentrated in six nodes may represent such conditions in the Sioux Falls network. In these conditions, the network robustness increased and the link criticality rankings completely changed (Table 5.3).

5.5 Summary and concluding remarks

The present chapter analysed in more detail the robustness of the Sioux Falls network (Chapter 3) to understand the difference between the impacts of localised, targeted and random disruptions but also the effect of demand variations and capacity constraints on road networks robustness. This analysis led to three key conclusions:

- The demand distribution (i.e. how the demand for travel, or population, is distributed among the network intersections) and intensity (i.e. whether the network is congested in the undisrupted state) significantly influence the robustness assessment results especially the link criticality rankings. Hence, practitioners need to carefully consider the traffic conditions for which the resilience assessment is made and also the possible evolution of these traffic conditions.

- Random and localised damage (disrupting the same number of links) generally lead to similar consequences while intentional attacks target links that may be apart and not critical on their own but whose combined disruptions create a maximised and widespread impact. Besides, targeted attacks are even more detrimental to the

network performance in comparison to random failures when the demand for travel (or population) is high and concentrated among a few nodes.

- In congested networks, it may not be necessary to simulate all possible disruption scenarios to identify and assess the impact of the most critical scenarios of multiple-link failures. Instead, a procedure that requires the computation of all SLF scenarios, followed by the computation of the top-10 most critical scenarios of 2LFs, 3LFs, etc. can be used. In uncongested networks, the proposed procedure may not provide satisfactory results. However, the lower computational time of the traffic simulations in uncongested networks reduces the need for such procedures. Hence, the full-scan approach that simulates all possible scenarios of multiple-link failures may be used in this case.

Chapter 6

Role of recovery strategies in network resilience

6.1 Introduction

Chapters 3 to 5 focus on road network robustness (the ability to absorb perturbations), which is one of the two main properties of resilient systems (the other being rapidity i.e. the ability to recover quickly). This focus on robustness allowed to evaluate how the availability of alternate routes and capacity helps remediate the consequences of initial disruptions to the network. These consequences mainly depend on the network topology, capacity and travel demand, and on the disruption type, extension and impacts on the system performance, which were all considered. However, to fully capture the resilience of a transport system, the speed of the network-performance recovery should also be considered.

In the context of road networks, most works (Bhavathrathan and Patil, 2018; Ganin et al., 2017; Gauthier et al., 2018; Omer et al., 2013) also focus on robustness while rapidity has attracted less attention. Still, considering the socio-economic consequences of road disruptions, recovery processes can have an important influence on the welfare of society as they can help alleviate disruption consequences in the early stage recovery. The studies that consider recovery processes propose different approaches. Nogal et al. (2016) and Nogal and Honfi (2019) focus on the gradual adaptation of road users following both the perturbation and restoration phases. Tuzun Aksu and Ozdamar (2014) develop a model optimising the link-repair sequence to quickly recover the network connectivity to facilitate evacuations. Zhang et al. (2017) develop a model optimising the link-repair sequence to quickly improve the network performance under stochastic damage levels and repair durations. Finally, Hu et al. (2016), compare different repair strategies under random, localised, and malicious perturbations. However, the studies of Hu et al. (2016), Tuzun Aksu and Ozdamar (2014), and Zhang et al. (2017) rely on topological network models and performance metrics that do not consider link capacity constraints. As shown in Chapter 3, this approach can significantly overestimate the resilience of road networks, particularly when analysing congested networks, as those in most major cities worldwide.

Hence, the understanding of the role of rapidity and therefore recovery strategies in the resilience of congested road networks is currently limited. To increase this understanding,

the present chapter compares the performance of several recovery strategies across a full range of disruption scenarios in the Sioux Falls network. This chapter has two objectives: (i) evaluate how recovery strategies can help reduce disruption consequences, and (ii) characterise the optimal recovery strategy.

In the traffic context, network resilience mainly depends on the consequences of the initial disruption to the network performance, the immediate response (in terms of closing lanes or reducing speed limits on affected roads) and the speed of restoring full functionality (through repair actions). As the present research seeks to analyse and compare the performance of different repair strategies under a full range of potential disruption scenarios, the immediate response is considered outside the scope of this study. The recovery model focuses on the common element shared by all network recovery processes: the link repair sequence and its impact on the network performance. In reality, recovery processes could take many forms and durations depending on the nature of the disruption (car accident versus snow versus earthquake) and the resources allocated to response and repair. As detailed case-by-case modelling (Misra et al., 2020; Mitoulis et al., 2021) would be required to address this, the general framework presented here cannot take these into account and focuses instead on comparing link repair sequences without considering the duration of the repair actions performed on the individual links.

The present chapter considers a full range of predictable and unpredictable disruption scenarios using the hazard-independent disruption model developed and improved in Chapters 3 and 5, respectively. This approach allows for an assessment of the performance of different repair strategies under a multitude of disruption scenarios.

The chapter considers all possible link-repair sequences that can be implemented under each disruption scenario. This data is summarised into four recovery models. Firstly, the optimal (minimising the disruption consequences over the recovery process) and average (representing a basic recovery process where the disrupted links are repaired in random order) recovery curves are considered. These recovery models are compared and used to evaluate the variations in network resilience due to the network recovery strategy. To better characterise the optimal recovery strategy, two additional recovery models are considered and compared with the optimal recovery: the flow-based (where the links with the highest traffic flow in the undisrupted network are repaired first), and criticality-based (where the links whose individual failure would result in the highest impacts on the system performance are repaired first) recovery strategies.

The present chapter is structured as follows. Section 6.2 presents the methods and case study. In Section 6.3 and 6.4, the results of the network resilience assessment are presented and discussed, respectively. Section 6.5 provides some concluding remarks.

6.2 Methods

6.2.1 Disruption model and disrupted network performance quantification

Disruption model

The present chapter considers a full range of predictable and unpredictable disruption scenarios using the hazard-independent disruption model developed and improved in Chapters 3 and 5, respectively. All possible link-failure combinations concurrently disrupting up to four links in the Sioux Falls network were modelled and classified into damage type (localised, random and targeted) and damage extension (single-, two-, three- and four-link failures) groups.

Network performance quantification

The network performance indicator (NP) adopted in this study considers the relative change in travel time along the network Origin-Destination pairs. The relative changes measured on all OD pairs are then aggregated by a weighting average giving more importance to the OD pairs associated with higher demand.

$$NP = \sum_{w} k_w \Big(1 + \frac{TT_d^w - TT_0^w}{TT_0^w}\Big)^{-1} \tag{6.1}$$

where w and k_w are an OD pair and the associated weighting factor, respectively; k_w is the ratio between the demand for w and the total demand in the network; TT_0^w and TT_d^w are the undisrupted and disrupted travel times along w, respectively. NP is scaled in [0,1] and decreases as TT_d^w increases.

This network performance indicator can be complemented by a measure of the unsatisfied demand (USD) that represents the proportion of road users unable to reach their chosen destination in the disrupted network. These users wish to travel between disconnected OD pairs, hence their travel time becomes infinite i.e. $TT_d^w \to \infty$ and $1 + \frac{TT_d^w - TT_0^w}{TT_0^w} \to 0$

$$\begin{aligned} &USD = \textstyle\sum_w k_w \delta_w \\ &\text{where } \delta_w = \begin{cases} 0, & \text{if } TTC_w < 10^{-3} \\ 1, & \text{otherwise} \end{cases} \end{aligned} \tag{6.2}$$

This set of indicators was developed in Chapter 3, where it is shown that to effectively discriminate between the impacts of scenarios that lead to the disconnection of OD pairs, it is necessary to consider the impacts on the OD pairs (or road users) separately rather than the often adopted network-wide travel-time losses.

6.2.2 Recovery process modelling and resilience quantification

Resilience quantification

In this chapter, road network resilience is measured by the integral of the road network performance indicator (NP, Eq. 6.1) over the recovery process (Figure 6.1). This measure is an adaptation of the seminal framework of Bruneau et al. (2003), where system

resilience is measured by the integral over time of the expected degradation in system quality expressed in percentage (Figure 2.2).

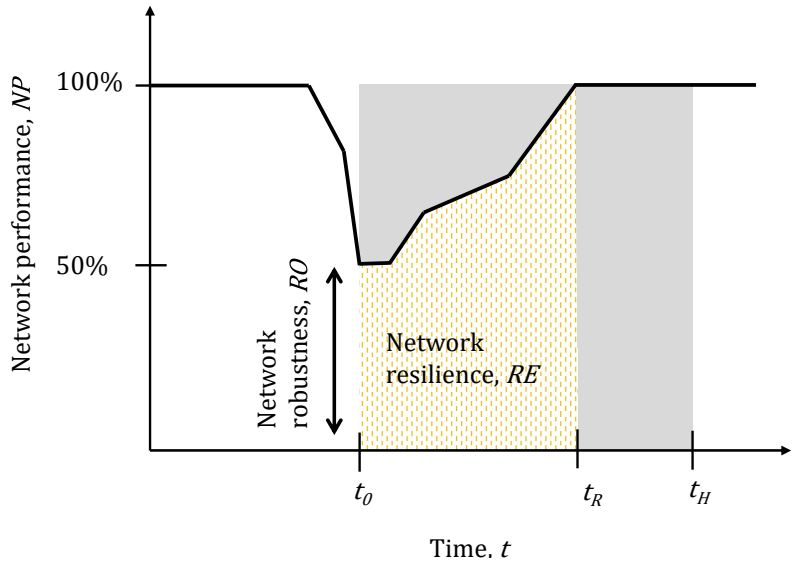

Figure 6.1: Illustration of the network robustness and resilience concepts and metrics

Figure 6.1 shows the evolution of the road network performance indicator following a multiple-link disruption. The disruption causes a sudden drop in the network performance, which reaches its lowest value at $t = t_0$. Subsequently, the network undergoes a recovery process until $t = t_R$ when the network is fully repaired (the repair could include improvements that lead to a network performance surpassing the original performance if desired). The resilience assessment focuses on the recovery process, which occurs between t_0 and t_H (grey rectangle in Figure 6.1); where t_H is the time horizon chosen to compute RE, defined here as the maximum time that the recovery process could require.

The network robustness corresponds to the lowest network performance value reached before the start of the recovery process (Figure 6.1). It is noted that in Chapter 3 to 5 no distinction is made between the network robustness and performance indicators. This distinction is necessary for the present analysis as the evolution of the network performance through the recovery process is considered. The network robustness indicator (RO) corresponds to the instantaneous loss of performance observed in the network without any recovery activity:

$$RO = NP(t = t_0) \tag{6.3}$$

The network resilience indicator (RE) measures the area below the recovery curve (yellow area in Figure 6.1), which is divided by τ_H to scale RE in [0,1]. This indicator is bounded by a worse-case scenario where the event causes a major decrease in network performance that is not restored until t_H, and a best-case scenario where the event causes a minor decrease in network performance that is rapidly recovered. The network resilience indicator (RE) is defined as follows:

$$RE = \frac{\int_0^{\tau_H} NP(\tau)d\tau}{\tau_H} \tag{6.4}$$

where $\tau = t - t_0$ is the time elapsed since the incident (or the start of the recovery process) at τ_0, and τ_H is the time horizon chosen to compute RE. The integral is divided by τ_H to normalize RE. A fully resilient system would either (i) be very robust i.e. $NP = 100\%$ before any repairs or (ii) be very rapid to recover i.e. NP quickly increases towards 100% as affected links are repaired. On the contrary, a non-resilience network will exhibit a low-performance level slowly increasing with the number of links repaired.

In many works—including in Bruneau et al. (2003) where it was first introduced—system resilience was measured until full recovery (τ_R). However, this expression can provide the same value of resilience for different recovery curves, $NP(\tau)$, (Sharma et al., 2018; Zobel, 2011). In this work, a fixed time horizon is used to overcome this limitation.

Recovery process model

As explained above, the present work focuses on link repair sequences and their impacts on network performance. Hence, recovery progress is measured by the number of links repaired (or cleared) following the disruption rather than the duration of the repair. Under this assumption, the time horizon corresponds to the maximum number of links that can be repaired between t_0 and t_H (N_H), which is also the number of disrupted links, resulting in:

$$RE = \frac{\sum_0^{N_H} NP(x)}{N_H} \tag{6.5}$$

where x corresponds to the number of links repaired following the disruption.

To conclude, as RE depends on N_H, the resilience of the network to a hazard is characterised by the tuple (RO, RE, N_H).

Recovery strategies

For each disruption scenario considered (Section 6.2.1), all possible link repair sequences were modelled, and the associated network performance (NP, Eq. 6.1) recovery curve and resilience indicator (RE, Eq. 6.5) computed. These results were used to consider two recovery strategies:

- the resilience-optimal recovery curve, obtained by selecting the repair sequence leading to the highest resilience indicator value.
- the average recovery curve, obtained by averaging the NP values of all curves at each stage of the repair process. This curve represents a basic recovery process where the disrupted links are repaired in random order.

To understand the mechanism behind the link order in the optimal recovery process, two additional processes were considered:

- the link-flow-based recovery curve, where the links with the highest traffic flow in the undisrupted network are repaired first
- the link-criticality based recovery curve, where the links with the highest criticality value are repaired first. The link criticality measures the impact of the link unavailability on the network performance.

The criticality-based recovery strategy is inspired by criticality studies (reviewed in Chapter 2), which seek to identify the links whose failure would result in the highest impacts on the network performance.

6.2.3 Case study and numerical simulations

The present chapter analyses the robustness of the Sioux Falls network, which is presented and studied in Chapter 3. The assumptions, transport model and disruption simulations used in Chapter 3 are also adopted here. This transport model implies that the network performance is compared across different equilibrium states, where road users have perfect information of the network state and accordingly minimises their TT. The assumption allows for a fair comparison of the impacts of the link disruptions and repairs on the network performance as the traffic should tend towards these equilibriums following each disruption and repair. However, it is noted that, in reality, the network will go through transition phases as users get updated about the network state and adapt as discussed in Nogal and Honfi (2019).

To speed up the resilience analysis, the recovery curves were computed based on the disruption-simulation data as the latter also correspond to the recovery states. For example, the link-repair sequence $[a, b, c]$ leads to the following states: concurrent failure of a, b and c; concurrent failure of b and c; and failure of c; that were all simulated as part of the disruption simulations. Therefore, the numerical simulations were divided into two main parts: the disruption simulations, and the recovery simulations that re-used the disruption data. The disruption and recovery simulations took 6h and 5h38 min, respectively, using parallel processing on an *Intel i5-8265U* 1.60Hz and 8GB memory laptop.

6.3 Results

6.3.1 Variations in network resilience due to the recovery strategy

This subsection seeks to evaluate the variations in network resilience due to the recovery strategy to better understand its importance for disruptive event management. To this end, the relationships between the robustness (RO, Eq. 6.3), unsatisfied demand (USD, Eq. 6.2) and resilience (RE, Eq. 6.5) indicators are evaluated across multiple disruption scenarios (Section 6.2.1). The efficiency of the optimal repair strategy (the difference between the resilience indicator values derived from the optimal and average recovery curves) is subsequently evaluated.

Network robustness versus network resilience

Figure 6.2 shows the relationship between the network robustness and resilience indicators across the damage extension groups in the Sioux Falls network. The resilience indicator values are derived from the average (Figure 6.2.a) and optimal (Figure 6.2.b) recovery curves. The results show that the two indicators were linearly correlated for both recovery curves (R^2 between 0.85 and 0.99) although the strength of the relationship increased with the average recovery curve (Figure 6.2). This linear relationship implies that when comparing perturbation scenarios that affect the same number of links, the network ro-

bustness (or instantaneous performance loss) can explain most of the variations in network resilience. Therefore, the recovery strategy has a minor impact on the network resilience. This impact increases with the damage extension (R^2 decreased as the number of disrupted links increases) and became significant under four-link failures ($R^2 < 0.95$ for both recovery curves).

The unsatisfied demand level is also included in Figure 6.2, where it seems that USD could also play a role in the prediction model. However, this role was not significant as the double regression performed on the data improved R^2 by around 0.5% only.

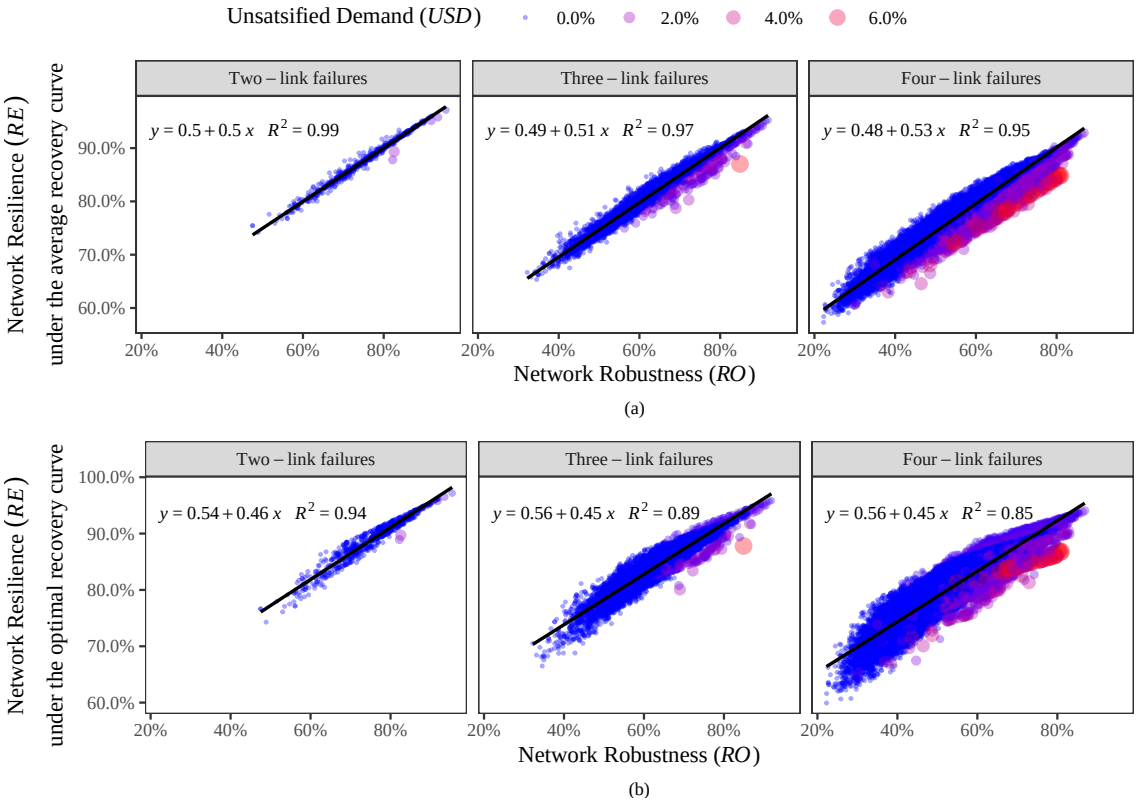

Figure 6.2: Relationship between the network robustness and resilience indicators across all possible two- to four-link failures in the Sioux Falls network—resilience computed under a) the average and b) optimal recovery models

Figure 6.3 shows the relationship between the network robustness and resilience indicators for the three damage types. The linear relationship found between the two metrics across the damage extension groups (Figure 6.2) remained relevant for the damage types (Figure 6.3). The strength of the linear model remained high for random and localised disruptions ($R^2 > 0.85$ for both the average and optimal recovery curves) but became moderate under targeted disruptions ($R^2 = 0.79$ and $R^2 = 0.48$ for the average and optimal recovery curves respectively).

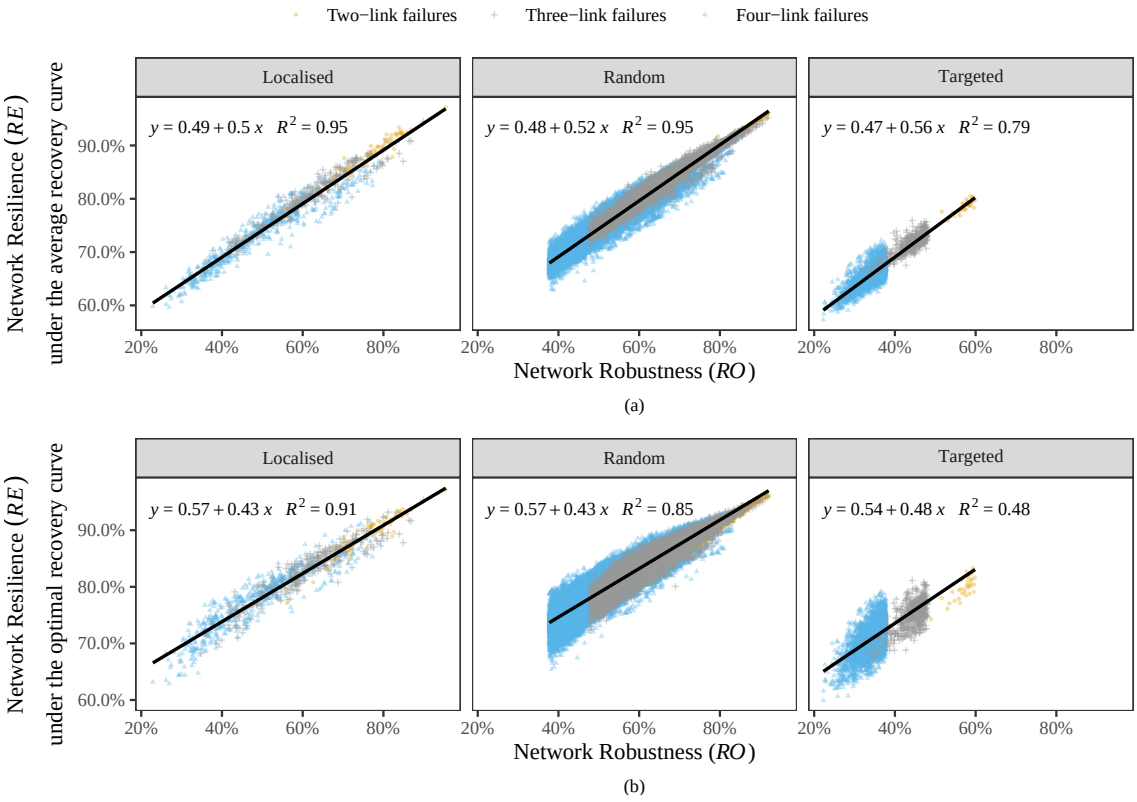

Figure 6.3: Relationship between the network robustness and resilience indicators across all possible localised-, random- and targeted-link failures concurrently disrupting two- to four- links in the Sioux Falls network—resilience computed under a) the average and b) optimal recovery models

Efficiency of the optimal repair strategy across the disruption scenarios

Figure 6.4 shows the evolution of the efficiency of the optimal recovery (the difference between the resilience indicator values derived from the optimal and average recovery curves) across the damage extension groups. This Figure shows that the efficiency of the resilience-optimal repair strategy generally increased with the damage extension (as the mean values of the efficiency in the 2LFs, 3LFs and 4LFs were 1.3%, 2.8% and 4.3%, respectively). In addition, the efficiency of the optimal repair strategy was generally higher under targeted attacks than under localised and random link-failures as shown by the positions of the medians in Figure 6.4. However, the scenarios with the highest efficiency were random failures for all damage extension groups as shown in Figure 6.4.

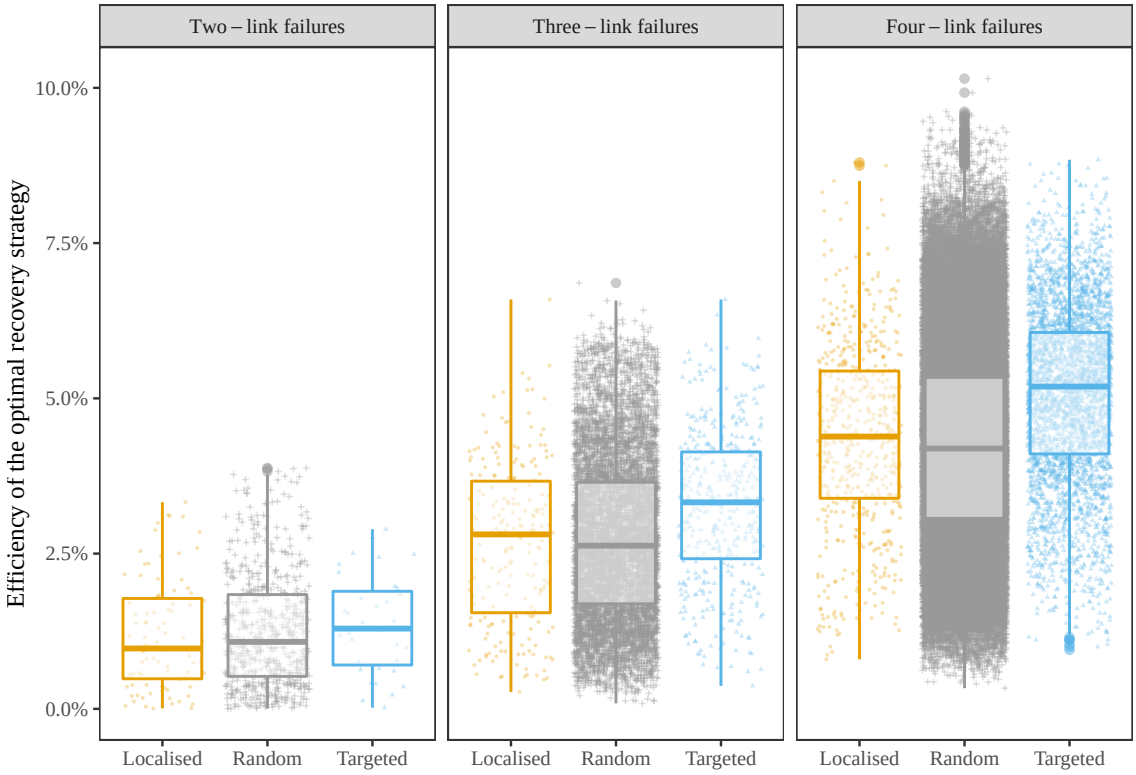

Figure 6.4: Efficiency of the optimal recovery strategy i.e. difference between the resilience indicator (RE) value derived from the optimal and average recovery—across the damage extension and type groups

6.3.2 Identification of the optimal repair strategy

This subsection seeks to characterise the optimal link-order repair strategy and understand the decision-making process that leads to this strategy. To this end, all possible repair strategies are firstly compared under a specific four-link failure scenario for illustrative purposes. This comparison allows the identification of the resilience optimal repair strategy, which is then compared to the criticality- and flow-based repair strategies in this specific scenario. The optimal, flow-based and criticality-based recovery strategies are subsequently compared across all possible disruption scenarios.

Comparison of all repair strategies following a four-link failure

This subsubsection focuses on a specific four-link failure scenario where (1,2), (1,3), (10,11) and (10,17) are concurrently disrupted in the Sioux Falls network (Figure 3.2). This scenario leads to a significant decrease in network performance (NP=66.6%) and a very small proportion of road users unable to reach their chosen destination (USD = 0.5%). The latter is due to the concurrent disruption of (1,2) and (1,3) that isolates node 1 from the rest of the network and disconnects all OD pairs involving this node (as suggested by the network structure shown in Figure 3.2). Figure 6.5.a and b show the evolution of the network performance and unsatisfied demand indicators along all possible repair strategies following this disruption scenario, respectively. The recovery curves are represented as step

functions because it is assumed that the network performance increased only once the links are fully repaired and traffic allowed to use them. The resilience indicator values associated with these different repair strategies are shown in Figure 6.5 using the colour and width of the curves. Thin blue curves correspond to the lowest resilience indicator values while large coral-coloured curves correspond to the highest resilience values.

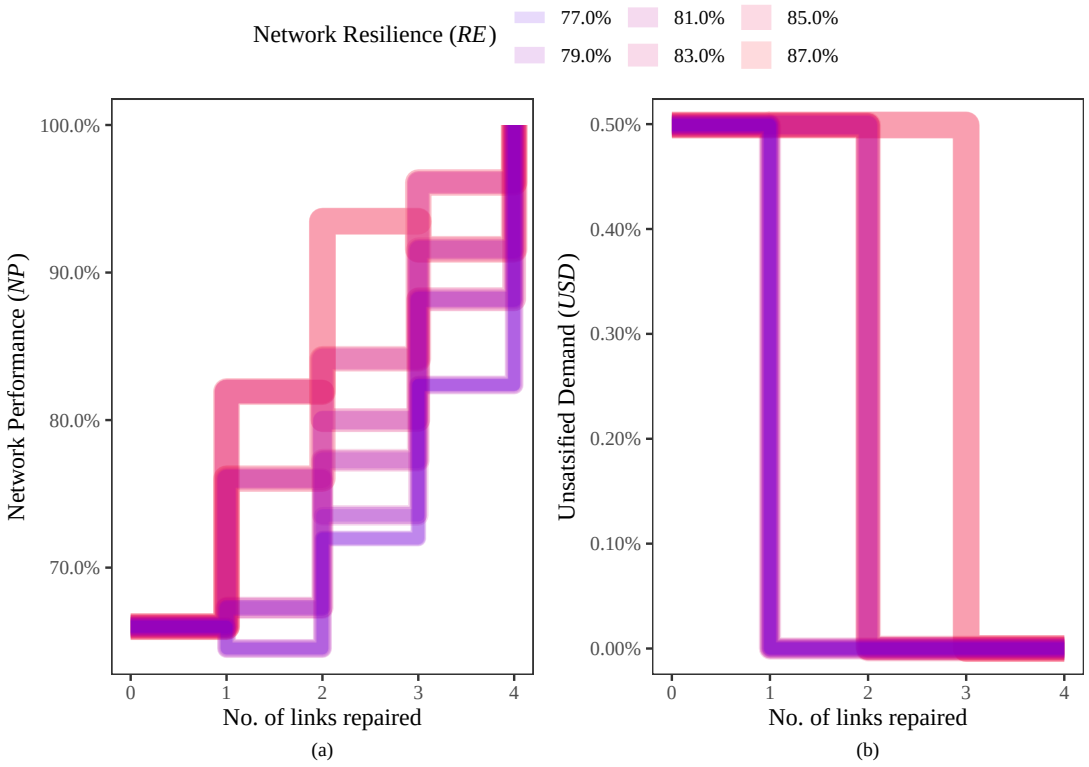

Figure 6.5: Evolution of the Sioux Falls a) network-performance and b) unsatisfied-demand indicators along all possible recovery processes following the concurrent failure of (1,2), (1,3), (10,11) and (10,17)

It can be observed in Figure 6.5.a, that the different repair strategies led to a variety of network performance recovery curves. The optimal repair strategy (large and coral-coloured curve) presents the sharpest increases in NP in the early stage recovery (when the first and second link are repaired), while the repair trajectories associated to the lowest RE values (thin blue curves) present slight network performance increases in the early stage recovery.

Furthermore, some recovery trajectories include a stage when NP slightly drops before increasing to a higher level. For example, the lowest blue curve in Figure 6.5.a presents a drop in NP following the repair of the first link. The link-repair order that leads to this NP curve is: (1,2), (10,11), (10,17) and (1,3). Along this curve, the network performance evolves from $NP = 66.0\%$ ($USD = 0.5\%$) to $NP = 64.5\%$ ($USD = 0\%$), before and after repairing (1,2), respectively. Hence, before (1,2) is repaired 0.5% of users cannot reach their chosen destination. After the repair, these users re-enter the network while there is no increase in capacity, which contributes to a congestion increase that affects the travel time of most travellers such that the overall network performance decreases (from 66.0%

to 64.5%). This explanation is confirmed by the evolution of the mean link flow/capacity ratio computed over all links except (1,2) that evolve from 1.65 (sd = 0.73) to 1.70 (sd = 0.78) before and after the repair of (1,2), respectively. This high mean flow/capacity ratio shows that the concurrent unavailability of (1,2), (1,3), (10,11), and (10,17) leads to a highly congested network which is further put under pressure when (1,2) re-opens. Therefore, in this example, it is more efficient to prioritise the re-opening of the inner links (10,11) and (10,17) to reduce the network congestion level before re-opening the outer links (1,2) and (1,3), which allow the users unable to leave/reach node 1 to re-enter the network. This conclusion can also be drawn from Figure 6.5.b, where it is interesting to note that the resilience-optimal strategy is not optimal in terms of the unsatisfied demand as the USD curve associated to the highest RE values drops after repairing three links.

Comparison between the optimal, criticality-based and flow-based repair strategies

To better characterise the decision-making process that leads to the optimal link repair strategy following the concurrent failure of (1,2), (1,3), (10,11) and (10,17), the latter was compared to two strategies that prioritise the links with the highest traffic flow and criticality values, respectively. The repair sequences and resilience indicator values resulting from these different strategies are shown in Table 6.1, where the resilience value derived from the average recovery curve is included for comparison. Table 6.1 shows that the flow- and criticality-based recovery strategies led to resilience indicator values superior to that of the average recovery curve. The criticality-based strategy led to the optimal repair sequence ($RE = 87.5\%$), while the flow-based strategy led to a slightly less efficient repair order ($RE = 85.6\%$), where (1,3) is repaired before (10,17).

Table 6.1: Comparison of different recovery strategies following the concurrent failure of link (1,2), (1,3), (10,11) and (10,17)

	Optimal recovery	Link-flow based recovery	Link-criticality based recovery	Average recovery curve (1)
Repair sequence	(10,11) (10,17) (1,3) (1,2)	(10,11) (1,3) (10,17) (1,2)	(10,11) (10,17) (1,3) (1,2)	-
Network resilience (RE)	0.875	0.856	0.875	0.816

(1) computed over all possible recovery curves

Comparison of the optimal, criticality-based and flow-based recovery strategies across multiple disruption scenarios

To validate the results obtained in the example above, the resilience indicator values resulting from the criticality- and flow-based repair strategies were compared to that of the optimal and average recovery curves in all two- to four-link-failure scenarios. Figure 6.6.a and b compare the link flow-based recovery strategy with the average and optimal recovery, respectively. Figure 6.6.a shows that the flow-based strategy is not necessarily

more efficient than the average recovery as the dots equally spread above and below the reference line. Figure 6.6.b shows that the flow-based strategy is rarely optimal as most dots appear below and far from the reference line. Figure 6.6.c and d compare the link-criticality based recovery strategy with the average and optimal recovery, respectively. Contrary to the flow-based recovery strategy, the criticality-based strategy (Figure 6.6.c) was more efficient than the average recovery curve in almost all cases as the dots appear above and far from the reference line. Accordingly, the criticality-based strategy was generally optimal or close to optimal as the dots appear close to the reference line in Figure 6.6.d.

In Figure 6.6, the damage extension groups are distinguished by different colours and shapes. A visual analysis of these colours and shapes shows that the difference between the network resilience values derived from the different strategies increased with the number of failed links (as 4LF and 3LF scenarios spread further away from the reference line than 3LF and 2LF scenarios, respectively). This can be explained by the fact that less failed links means fewer possible recovery strategies and less wrong choices.

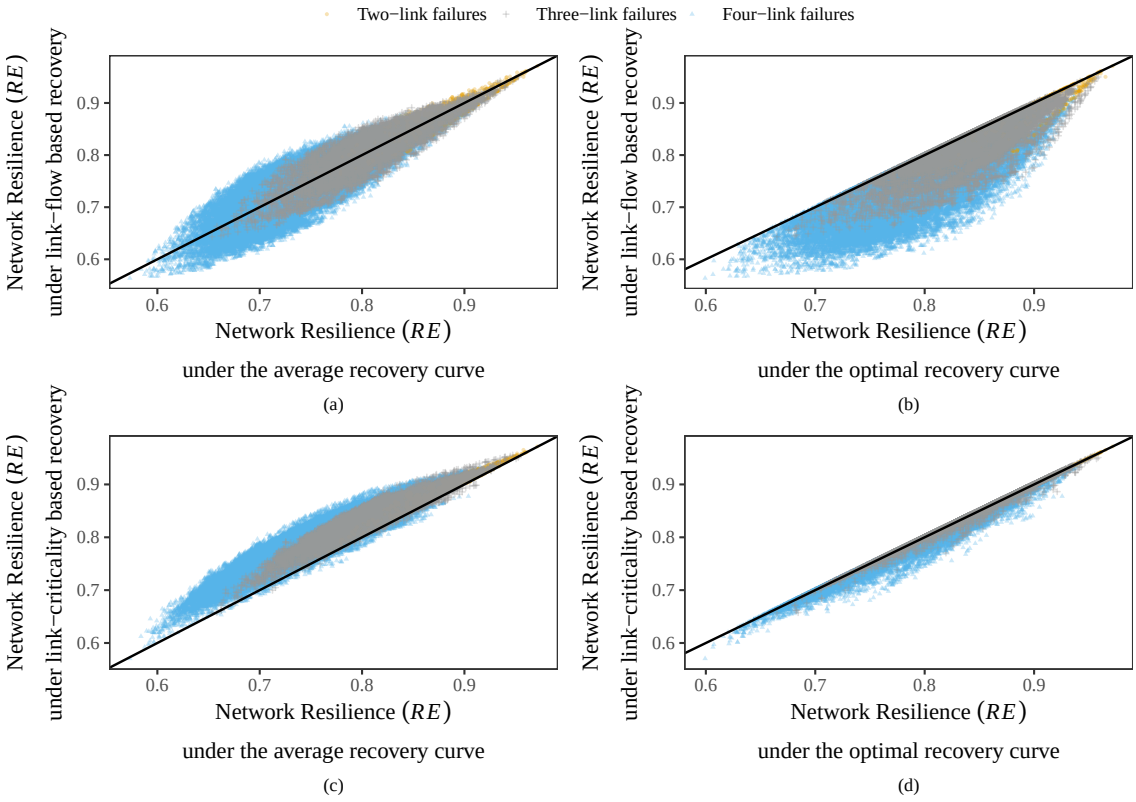

Figure 6.6: Comparison of the resilience indicator values resulting from different recovery strategies for all possible two- to four-link failures in the Sioux Falls network—a) link-flow based recovery vs average recovery, b) link-flow based recovery vs optimal recovery, c) link-criticality based recovery vs average recovery, d) link-criticality based recovery vs optimal recovery

As the criticality based recovery is closer to the optimal recovery than the flow-based and average recovery curves (Figure 6.6), the difference between the criticality and optimal

recovery was further investigated. Table 6.2 shows the evolution of the difference between the resilience indicator values resulting from the optimal and criticality-based recovery strategies across the damage extension groups. This table shows that the mean of the difference between the RE values of the two strategies remained small and slowly increased (from 0% in two- and three-link failures to 0.25% in four-link failures). The maximum value of this difference also increased with the damage extension reaching small but significant values of 4.91% and 6.96% in 3LFs and 4LFs, respectively.

Table 6.2: Summary statistics of the difference between the resilience indicator (RE) values resulting from the optimal and link-criticality based recovery strategies across the damage extension groups

	Two-link failures	Three-link failures	Four-link failures
Mean	0.00%	0.00%	0.25%
Standard deviation	0.00%	0.34%	0.61%
Max	0.00%	4.91%	6.96%

6.4 Discussion

6.4.1 Importance and role of recovery strategies in network resilience

The comparison of the network robustness and resilience indicators (Figures 6.2 and 6.3) showed that although the resilience indicator accounts for the network performance recovery in addition to the instantaneous performance losses (measured by the robustness indicator), the two indicators displayed a very strong linear relationship. This relationship shows that the network robustness bears most of the information about the impact of disruptions. In other words, recovery processes play a minor role in the comparison of the impacts of two damage scenarios such that the scenarios that lead to the highest instantaneous performance losses tend to also lead to the highest impacts over the recovery process.

Still, the strength of this relationship evolved depending on the recovery strategy considered. For example, in the four-link failures, R^2 went from 0.95 under the average recovery curve to 0.85 under the optimal recovery curve. This suggests that the optimal repair strategy can help counterbalance the instantaneous impact of damage scenarios such that two damage scenarios that lead to similar robustness values (i.e. instantaneous impacts) would lead to different resilience values (i.e. impacts over the recovery process).

Furthermore, the decrease of the strength of the linear model (Figure 6.2) as the damage extension increases shows that the importance of the role of recovery processes in network resilience gradually increases with the damage extension. Hence, the identification and implementation of the optimal recovery strategy appeared crucial for scenarios disrupting more than four links in the Sioux Falls network. This represents 10% of the links in the Sioux Falls network.

The comparison of the strength of the linear model across the damage types (Figure 6.3) showed that under random and localised damage the network robustness could

explain $\approx 95\%$ of the resilience variations with the average recovery curve ($\approx 85\%$ with the optimal recovery). This decreased to 79% with the average recovery curve (48% with the optimal recovery) under targeted attacks. This suggested that the identification and implementation of the optimal recovery strategy are crucial for targeted attacks.

Ultimately, the present results show that the network robustness is a good proxy for the network resilience for random and localised scenarios affecting a small number of links. For critical disruption scenarios affecting a large number of links it is important to consider and model recovery processes. The consideration of the latter may, for example, modify the lists identifying the most critical disruption scenarios, used by transport practitioners and public authorises to optimise the allocation of the limited resources available for road infrastructure construction and repair to the most critical scenarios and links.

6.4.2 Efficiency of the optimal recovery strategy

The evaluation of the efficiency of the optimal recovery strategy—i.e. the difference between the resilience indicator (RE) values derived from the optimal and average recovery—across the different disruption scenarios showed that the optimal repair strategy can lead to significantly higher resilience values (the maximum value of the efficiency was 10.1% for the four-link failures in Figure 6.4). The analysis of the sensitivity of this efficiency to the damage extension showed that it generally increases with the number of links affected (Figure 6.4). The mean efficiency values of the optimal recovery went from 1.3% in 2LFs to 2.8% in 3LFs to 4.3% in 4LFs and it can be expected that these values will continue to increase as the damage extends to more links. The number of possible repair strategies increases with the number of affected links (when R links are affected there are $R!$ possible link-repair sequences) such that the difference between the performance of the optimal and average recovery strategies also increases. Therefore, in accordance with the discussion above, the identification and implementation of the optimal repair strategy become more crucial when several links are affected.

The analysis of the sensitivity of the same efficiency to the damage type led to conflicting results. The efficiency of the optimal recovery strategy appeared generally higher in targeted attacks (as shown by the medians of the boxplots in Figure 6.4) while the maximum efficiency values did not necessarily appear among targeted attacks (Figure 6.4). It is hence difficult to characterise the specific scenarios for which the implementation of the optimal recovery strategies would be most effective.

6.4.3 Optimisation of the recovery strategy at the operational level

The present research also allowed to better characterise the optimal recovery strategy. The analysis of the disruption example (Figure 6.5) where (1,2), (1,3), (10,11) and (10,17) were concurrently disrupted showed that the optimal repair strategy (maximising the recovery of the network performance indicator) could give priority to the repair of the network inner links that reduce the travel time of most users over the repair of the network-outer links that allow a minority of road users to leave/reach the zones disconnected from the rest of the network. This choice can be explained by the fact that the disruption of the inner links (10,11) and (10,17) lead to severe congestion that would increase further when the minority of stranded users re-enter the network. This would not happen in an uncongested

network since the repair of the links allowing stranded road users to leave/reach the zones disconnected from the rest of the network would not affect the travel time of the other users. This shows that it is important to consider and model capacity constraints and congestion, and that the previous studies (Hu et al., 2016; Zhang et al., 2017) that did not consider capacity constraints and potential congestion may incorrectly prioritise the recovery of the network connectivity to the recovery of the users' travel time.

The comparison of the resilience indicator values resulting from the optimal recovery strategy with that of the link-flow and link-criticality based recovery strategies showed that the link criticality-order—based on the impacts of the single-link failures on the network performance—provides relevant information to establish an optimal link repair sequence (Figure 6.6.c and d), while the link flow provides irrelevant information (Figure 6.6.a and b). This shows that the identification of an optimal or close to optimal repair strategy requires the computation of disruption scenarios evaluating the impacts of the links unavailability on the network performance as the metrics based on the network usage in the undisrupted state such as the link flow are unable to account for the reserve capacity available in the network to absorb the disruptions.

These results also suggest that the link-criticality rankings can be used to find close to optimal repair strategies with a decreased computational burden. The comparison of all possible repair-orders requires $\sum_{i=1}^{R} \binom{R}{i}$ (15 if $R = 4$) disruption simulations while the identification of the link-criticality based recovery requires R (4 if $R = 4$) disruption simulations, R being the number of disrupted links. Furthermore, considering that the links involved in the most-critical multiple-link failures are not simply the combination of the most-critical links with single-link failure (Wang et al., 2016), it may be possible to increase further the ability of the criticality based recovery to tend to the optimal-repair strategy by adopting a link criticality indicator based on multiple-link failure simulations such as the one proposed in Chapter 4. The accuracy and extra computational cost of this method will increase with the size of the MLF scenarios considered (i.e. 2LF, 3LF, 4LF, etc.). Future research could seek to determine more precisely when it is necessary to consider 2LF, 3LF, 4LF, etc. and accordingly develop less computationally expensive methods for identifying the optimal recovery strategy.

6.5 Summary and concluding remarks

The present chapter assessed the effects of link-repair strategies on network resilience and analysed the characteristics of the optimal recovery strategy. Several link-repair strategies were compared across a multitude of perturbation scenarios. This approach allowed the analysis of a large set of scenarios resulting in a clearer understanding of the generality of the results and conclusions. The study led to four key conclusions:

- The network robustness (that measures the initial performance loss of the disrupted network) is a good proxy for the network resilience for random and localised scenarios affecting a small number of links. For critical disruption scenarios affecting a large number of links it is important to consider and model the recovery processes.
- The identification and implementation of the optimal repair strategy become more crucial when several links are affected since this leads to a multitude of decision

variables, constraints, and possible alternative strategies.

- It is possible to identify a close to optimal repair strategy with the results of a criticality analysis based on the impact caused by the individual or concurrent failure of the network links.
- The repair strategy should be adapted to the traffic conditions. In uncongested networks (found in rural areas or in off-peak hours in urban areas), the priority should be to reconnect as many people as possible to the network in the early stage recovery. In a highly congested network (found in peak hours in urban areas), it could be beneficial to prioritise the re-opening of the network inner links to reduce the overall congestion before re-opening of the outer links that will reconnect stranded travellers to the network.

Chapter 7

Conclusions

7.1 General discussion

The present thesis aimed at developing a theoretical framework to evaluate the resilience of road networks under a multitude of potentiality unpredictable disruptions and assess the role of different network design (e.g. network topology) and operation (e.g. travel demand and link repair strategies) characteristics in road network resilience. To this end, novel road network resilience assessment tools were developed and applied to a range of case studies.

7.1.1 Proposed resilience assessment framework for road networks

The proposed resilience framework encompasses the following elements:

- a hazard-independent disruption model that can be used to assess the potential impacts of a wide range of perturbation scenarios including random-, localised-, and targeted-link disruptions (Chapters 3 and 5).
- network performance, robustness and resilience indicators that provide an accurate and meaningful mean to quantify road network resilience (Chapters 3 to 6).
- a link-criticality-assessment method based on multiple-link failures that can be used as a tool to identify the road segments that should be given priority for pre-event reinforcement (which may involve building alternative connections) and post-event restoration (Chapters 4 to 6)
- procedures allowing to identify and assess the impacts of the most critical scenarios of multiple-link failures with decreased computational efforts (Chapter 5).
- a close to optimal link repair strategy (i.e. the link-flow-based recovery) that provides a link-repair strategy maximising resilience with decreased computational efforts (Chapter 6)
- a random road graph model and a methodology that can be used to accurately evaluate the influence of network size, topology and demand characteristics on transport network performance (Chapter 4)

- a general understanding of the influence of several network planning and management characteristics (including size, topology, demand distribution and intensity, and link repair strategy) on resilience (Chapters 3 to 6).

The general understanding of the role of the network planning and management characteristics in road network resilience is summarised in Table 7.1, which shows the influence of the different characteristics considered in this thesis on road network robustness and resilience. This table summarises the findings of Chapters 4 and 5. Considering the strong correlation observed between robustness and resilience in Chapter 6, it is assumed that the relationships found between the network characteristics and robustness are also applicable to network resilience. Ultimately, the resulting framework provides a starting point for creating a plan to assess and manage the resilience of a road network.

Table 7.1: Influence of network characteristics on road network resilience ("+" = positive relationship, "−"negative relationship, "none" = no relationship, and "uncertain" = uncertain correlation and relationship)

	Network robustness and resilience	Correlation between SLF and MLF based link criticality rankings[(1)]	Difference between random- and targeted-link failures
Network size (no. of nodes)	+	none	uncertain
Network connectivity	+	none	+
Network degree heterogeneity	uncertain	none	uncertain
Network link cost heterogeneity	uncertain	none	uncertain
Ratio of OD points/nodes	none	+	none
Network demand intensity	−	+	uncertain

[(1)]SLF = Single-link failure, MLF = Multiple-link failure.

7.1.2 Research insights

Besides the proposed resilience assessment framework mentioned above, the present research led to insights on road-network-resilience evaluation, implementation and strengthening. The insights related to resilience evaluation are the following:

- To effectively compare the impacts of disruption scenarios that lead to OD pairs disconnections, it is necessary to consider the impacts on the OD pairs (or road users) separately rather than the total travel-time losses in the network (which are often used in the literature). This can be achieved by measuring the relative change of the travel time along the OD pairs. The proposed network performance indicator uses a demand-weighted average to aggregate these relative change values into one indicator (Chapter 3).

- The demand distribution (i.e. how the demand for travel or population is distributed among the network intersections) and intensity (i.e. whether the network is congested in the undisrupted state) significantly influence the resilience assessment results especially the link criticality rankings. Hence, practitioners need to carefully consider the traffic conditions for which the resilience assessment is made and also the possible evolution of these traffic conditions (Chapter 5).

- The classical method assessing link criticality based exclusively on single-link failures (Taylor et al., 2006) is likely to misrepresent the link criticality that can be derived from multiple-link failures in road networks where the population (demand) is not homogeneously distributed among all the intersections. This could lead to inefficient prevention and restoration measures in the advent of events disrupting several road segments or several events affecting different parts of the network at the same time (Chapters 4 and 5)

- Network robustness (that measures the initial performance loss of the disrupted network) is a good proxy for network resilience in the case of random and localised scenarios affecting a small number of links. For critical disruption scenarios affecting a large number of links it is important to consider and model recovery processes (Chapter 6).

The insights related to resilience implementation and strengthening are the following:

- The addition of redundant routes in road networks (through additional roads and intermediate intersections) is an efficient way to enhance the network robustness under multiple-link failures up to a certain size and connectivity threshold, after which the return on investments would be limited (Chapter 4).

- Highly-connected networks are more robust but also offers more opportunities for malicious attacks to be more harmful than random failures. The identification and protection of the most critical road segments are hence more crucial in highly connected road networks than in sparse networks where most links are equally important to the network performance (Chapter 4).

- Although the most critical link combinations are not simply the combinations of the most critical links with singe-link failures the most critical multiple link failures tend to involve at least one of the most critical links with SLF. Hence, the protection or rapid repair of the top-5 most critical links with SLF can also help towards the protection of the network performance against the most critical MLF scenarios (Chapter 5).

- Link metrics derived from the network usage in the undisrupted state such as the link flow and flow/capacity ratio are of limited relevance for identifying the most critical links in a network and for optimising link-repair strategies. Instead, practitioners should consider metrics derived from disruption simulations such as the proposed link criticality indicator (Chapters 5 and 6, and Appendix C).

- Repair strategies should be adapted to the traffic conditions. In uncongested networks (found in rural areas or off-peak hours in urban areas), the priority should

be to reconnect as many people as possible to the network at the early stage of recovery. In highly congested networks (found in peak hours in urban areas), it could be beneficial to prioritise the re-opening of the network inner links to reduce the overall congestion before re-opening of the outer links that will reconnect stranded travellers to the network (Chapter 6).

These findings and implications should be of interest to researchers, industry professionals and policy-makers aiming to perform robustness and resilience analyses of road networks.

7.2 Limitations and recommendation for future work

The first limitation of this thesis is that the findings are theoretical and have not been validated against real data, for example, of a disrupted road network. Furthermore, two main types of limitations exist in the present research, related to resilience and transport modelling, which are both discussed below. Another potential limitation is the scalability of the approach adopted, which is also discussed below.

7.2.1 Scalability

The full-scan approach adopted in this study is limited by computational capacity as its computational cost increases exponentially with the number of links in the road network. Hence, its application is currently realistic for small to medium (sub)network models composed of up to a few hundred links only. The removal of residential and service roads (that are not designed for through movements) as well as intersections connecting one to two links from network models which have a minor impact on the estimated travel speeds as shown in Ganin et al. (2017), may help to reach this threshold in certain cases. Alternatively, future applications of this approach at larger scales could benefit from expected growth in computational capacity and further optimisation of traffic simulation algorithms.

Future works could further investigate the scalability of this approach and the applicability of the present findings to large networks. This may lead to the development of methods for assessing road network robustness under multiple disruption scenarios that rely on heuristics (such as the iterative procedure proposed in Chapter 5 for identifying the most critical scenarios) that decrease the computational burden of the assessment.

7.2.2 Limitations related to disruption and resilience modelling

As explained in Section 1.3.2, this thesis adopted an hazard-independent disruption model that equally considers all possible events to ensure that unknown and unpredictable hazards are accounted for in the resilience analysis. These hazards are events (e.g. cascading events or operational errors) that occur in complex systems that are in a perpetual dynamic state as they involve engineering, human and natural systems interacting together while they are subject to external and internal forces (Park et al., 2013). Hence, unknown and unpredictable hazards diminish as the state of knowledge increases but also appear

as complex systems evolve. Resilience approaches disregarding predictability are therefore required to account for unknown hazards. However, in reality, some events are more predictable (e.g. maintenance works) than others (e.g. terrorist attacks) and some parts of a road network are more frequently affected than others. Such considerations remain important to help decision-makers optimise resources allocation to the more probable hazards and more exposed parts of networks. Therefore, both approaches should be used and sometimes combined to reduce disruption impacts on road networks' resilience.

To allow the comparison between multiple potential disruption scenarios, the recovery model adopted in Chapter 6 focuses on link-repair sequences and their impacts on the network performance. In practice, an assessment considering only a few disruption scenarios should use a detailed case-by-case modelling approach to take into account the duration of the response and repair actions. This approach would allow to model and optimise other important characteristics of recovery strategies such as budget constraints and opportunistic interventions.

To limit the computational effort required to simulate all possible link failure combinations, the disruption simulations considered complete link unavailability only rather than partial link capacity (or speed) reductions. For the same reason, the recovery model assumed that repair works directly led to full link capacity recovery. Future research could work towards the inclusion of partial capacity reductions in the proposed disruption and recovery models to understand its impact on resilience, link criticality and recovery as proposed in Sullivan et al. (2010) and Cats et al. (2017). This would, however, require a reduction of the computational complexity of the simulations.

7.2.3 Limitations related to transport modelling

More realistic transport models

Chapter 4 analysed hundreds of networks to investigate the relationship between network robustness and topology. For the sake of computational efficiency, this chapter relied on a transport model that did not consider link capacity constraints and potential congestion, which implies that the results obtained in this chapter mainly apply to uncongested road networks. Although, it seems reasonable to consider that link capacity constraints would have a minor effect on the relationship between network topology and robustness (i.e. if network topology a is more robust than network topology b when they are both uncongested, a should remain more robust than b when they are congested) this should be validated.

Chapters 3, 5 and 6 analysed the robustness of the Sioux Falls network using a transport model that accounts for capacity constraints and congestion. This transport model was, however, static as it did not consider the variation of the travel demand over time. To address this limitation of the model, the robustness analysis was repeated under different demand distribution and intensity conditions in Chapter 5.

This limitation could have been addressed by using a dynamic transport model, which directly takes into account the variation of the travel demand over time. Dynamic transport models are more informative than their static counterparts as they model the formation and dispersion of vehicle queues caused by temporary saturation of link sections as well as queues propagation towards upstream links (called spillback). However, dynamic trans-

port models require detailed travel-demand data that are often unavailable. Furthermore, considering that dynamic transport models are more computationally demanding than their static counterparts, the application of the hazard-independent approach adopted in this thesis (that requires multiple disruption simulations) to dynamic traffic models would be limited by computational capacity.

More comprehensive transport models

To effectively compare the network performance under different disruption scenarios, travel demand was considered fixed in this thesis. In reality, road perturbation can also impact the travel demand as trips may be cancelled, delayed or modified due to usual routes and destinations being affected. The consideration of different demand distribution and intensity conditions in Chapter 5 provided some insights into the potential effects of travel demand alteration caused by disruptions on resilience. Following a major disruption, work and leisure trips are likely to be cancelled or delayed while emergency trips (e.g. evacuation and transport from/to hospitals) are likely to increase. Hence, travel demand will likely concentrate in a few zones while demand intensity decreases. The low- and medium- demand intensity concentrated in six nodes may represent such conditions in the Sioux Falls network. In these conditions, the network robustness increased and the link criticality rankings completely changed. A more detailed analysis would be required to fully capture these effects and their effect on network operations. Future works could adopt more comprehensive transport models capable of assessing the impacts of road disruptions on trip generation and distribution. This would, however, require detailed data on the travel demand and land use but also calibrated-behavioural models, which are often unavailable.

Finally, the present thesis focused on road networks. Future works could adapt the proposed resilience assessment methodology to multimodal transport systems to evaluate whether temporary intermodal solutions can be used to optimise congestion and connectivity in disrupted transport networks. Similarly, the approach adopted in Chapter 4—which consists in analysing a large set of randomly generated road networks—is scalable and probably applicable to other transport networks (using suitable random network models). Future works could hence extend this approach to other road network performance metrics or other transport modes.

Appendix A

Connectedness and attribute space of the GREREC networks

A.1 Connectedness of the GREREC model

As the GREREC model can generate disconnected networks, the probability of the networks being connected depending on the parameters n, m, p and q was estimated using Monte Carlo simulation (500 simulations per set of values). The results are shown in Figure A.1.

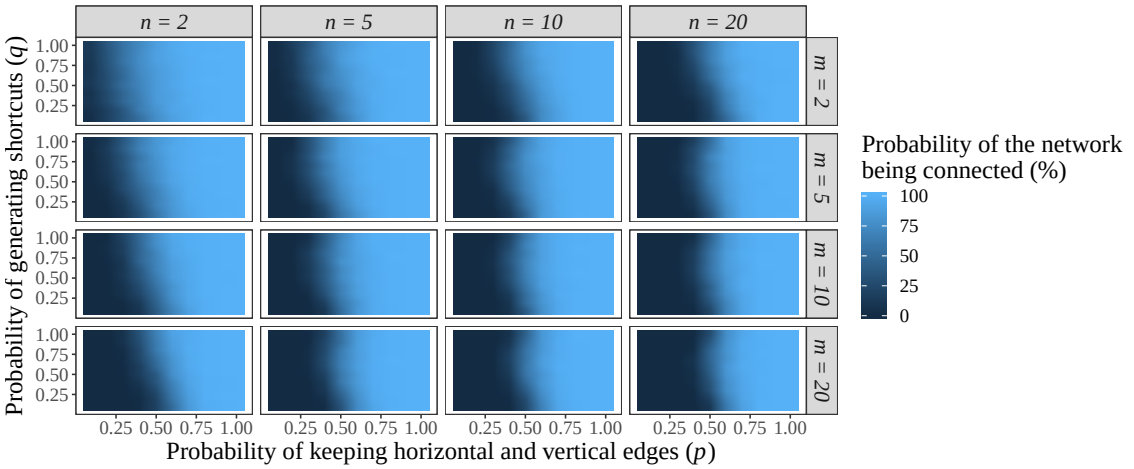

Figure A.1: Connectedness of the GREREC model depending on the dimensions m and n of the graph (i.e. number of nodes per row and columns in the rectangle respectively) and the parameters p and q

As shown in Figure A.1, the values of p and q for which the graphs were connected with a certain probability increased with their size (controlled by m and n). Furthermore, p plays a more important role than q, as the probability of the graph being connected exceeds 48% for $p \geq 0.6$ regardless of q. This is because the shortcuts alone are not sufficient to connect the network nodes since they only depart from certain nodes (see rule 3) and 4) in the procedure in section 4.2.1), whereas horizontal and vertical edges depart from every node.

A.2 Attribute space of the set of GREREC networks analysed

A Quasi-Monte Carlo method was used to obtain a sample of networks that homogeneously covered the parameter space of the GREREC model, which however did not necessarily imply that the space of the network attributes would be also homogeneously covered. This appendix evaluates the distribution of the attribute values in the set of networks analysed to verify if the possible attribute values were well represented in this sample. Figure A.2 shows the histograms of the network attributes considered in this study. It can be observed that the distributions were generally well-spread in their domains. The largest networks were less represented because they correspond to high values of m and n (the dimensions of the rectangular grid). The lowest values of α, β and γ were under-represented because they correspond to unconnected graphs. As an indication the minimum number of links required to connect a planar graph of N nodes is $N-1$ (Cardillo et al., 2006). Hence, the minimum values of β are, for example, $\beta = 0.90$ and $\beta = 0.99$ for $N = 10$ and $N = 200$ respectively.

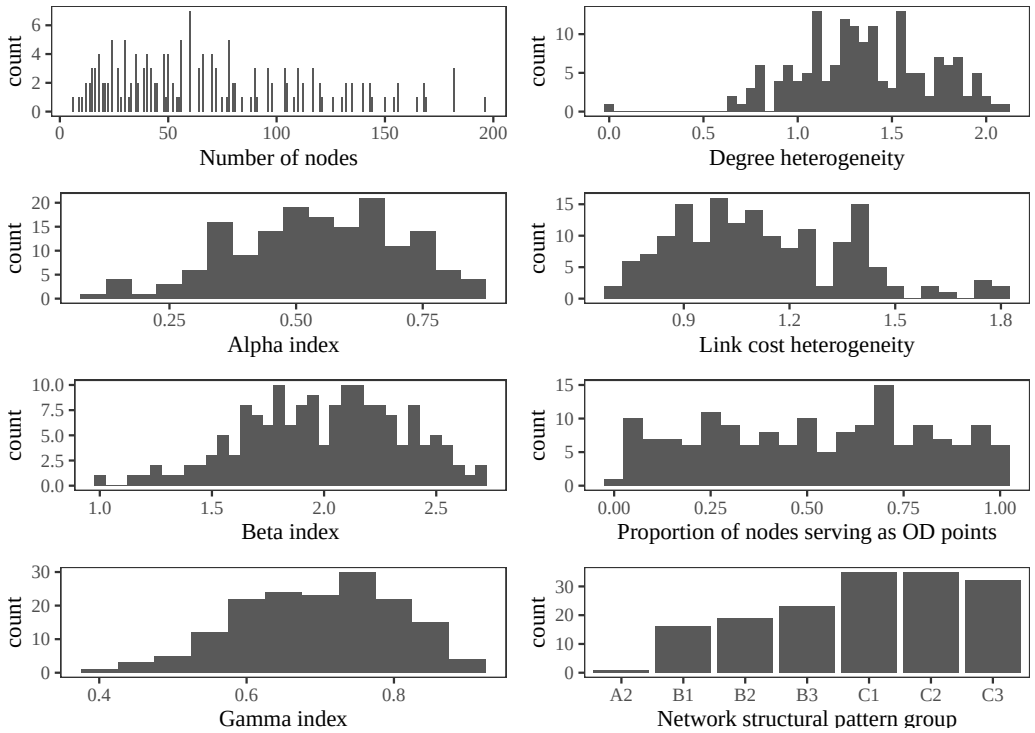

Figure A.2: Histograms of the network attributes in the set of GREREC networks analysed

.

The relationships between the network attributes are shown in Figure A.3, where it can be seen that these attributes were generally uncorrelated.

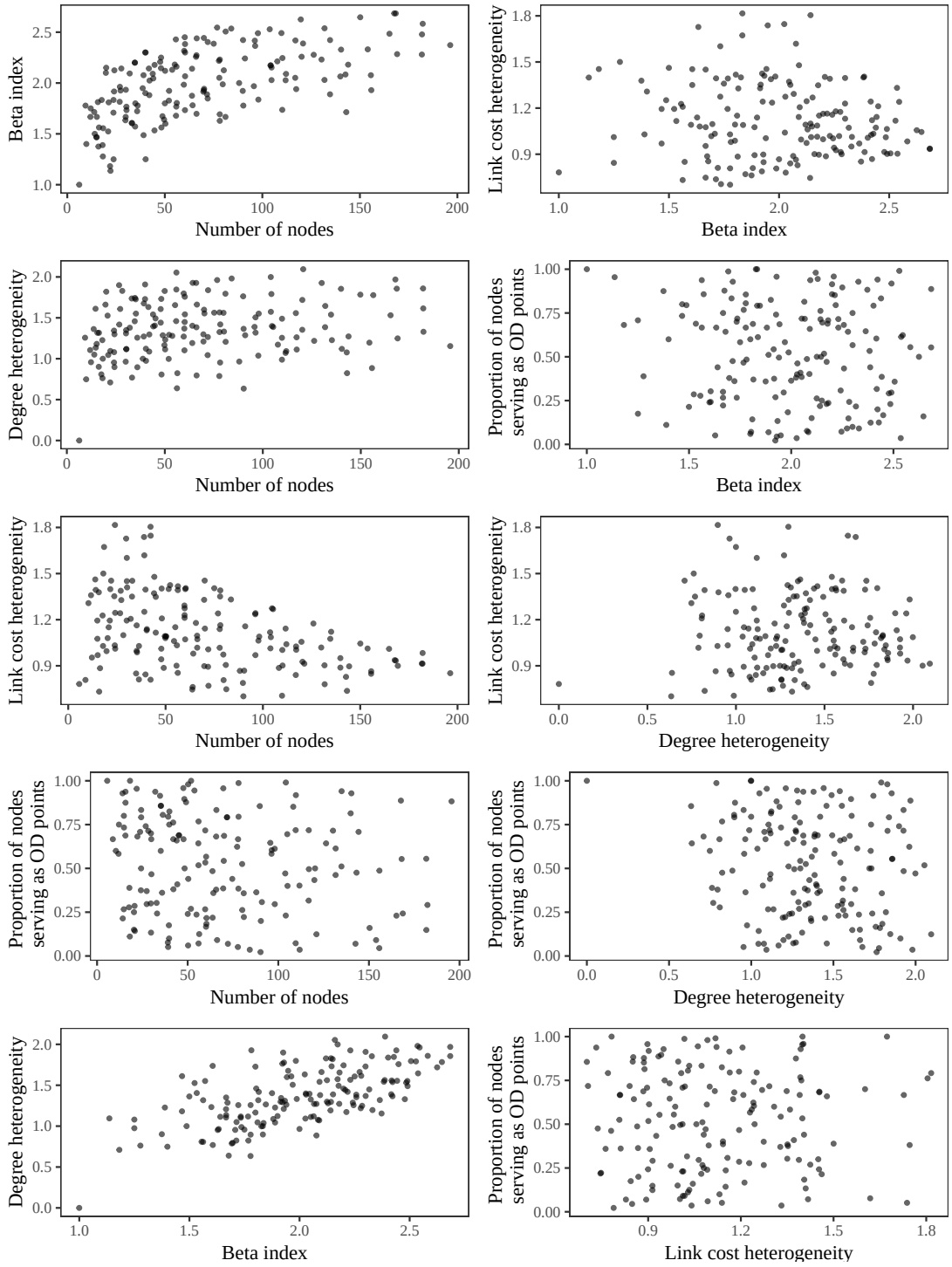

Figure A.3: Relationship between the network attributes in the set of GREREC networks analysed

.

Appendix B

Real maps considered in Chapter 4

In Chapter 4, a robustness analysis of 30 network models derived from real maps (from *OpenStreetMap*, www.openstreetmap.org) is performed to validate the results obtained with the GREREC network models. For brevity, Figure 4.4 only presented five examples of the 30 networks. This appendix presents all of these maps. The networks are shown in Figures B.1 to B.6. Table B.1 provides the coordinates of the bounding boxes used to build the graphs.

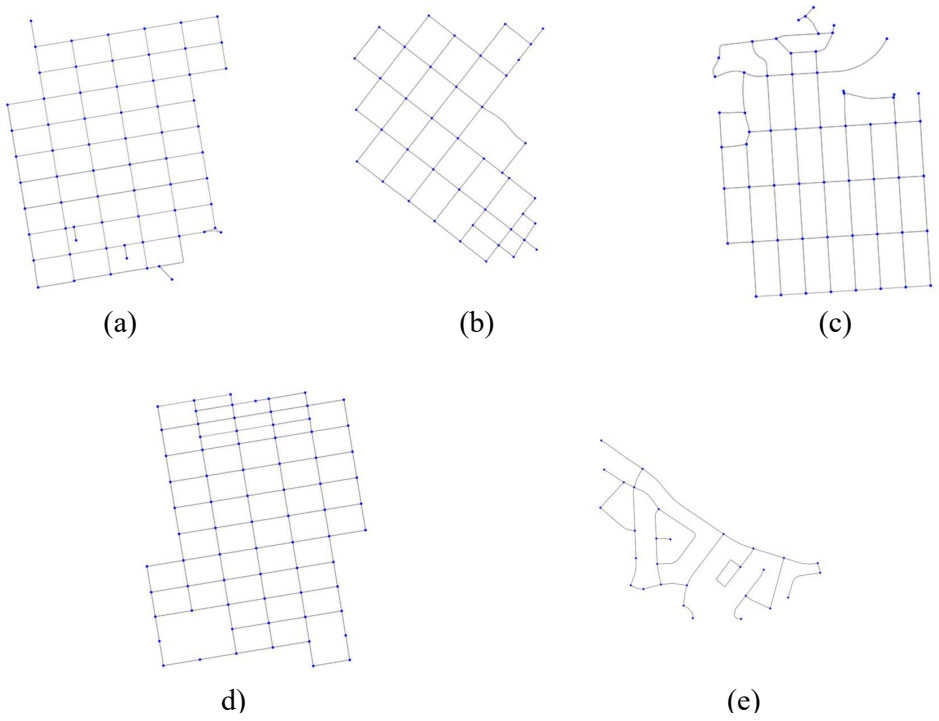

Figure B.1: Network models derived from different neighbourhoods in Greater San Francisco (USA): (a) North-East San Francisco, (b) Old Palo Alto, (c) Sea Cliff and Outer Richmond, (d) Pacific Heights, and (e) South San Francisco.

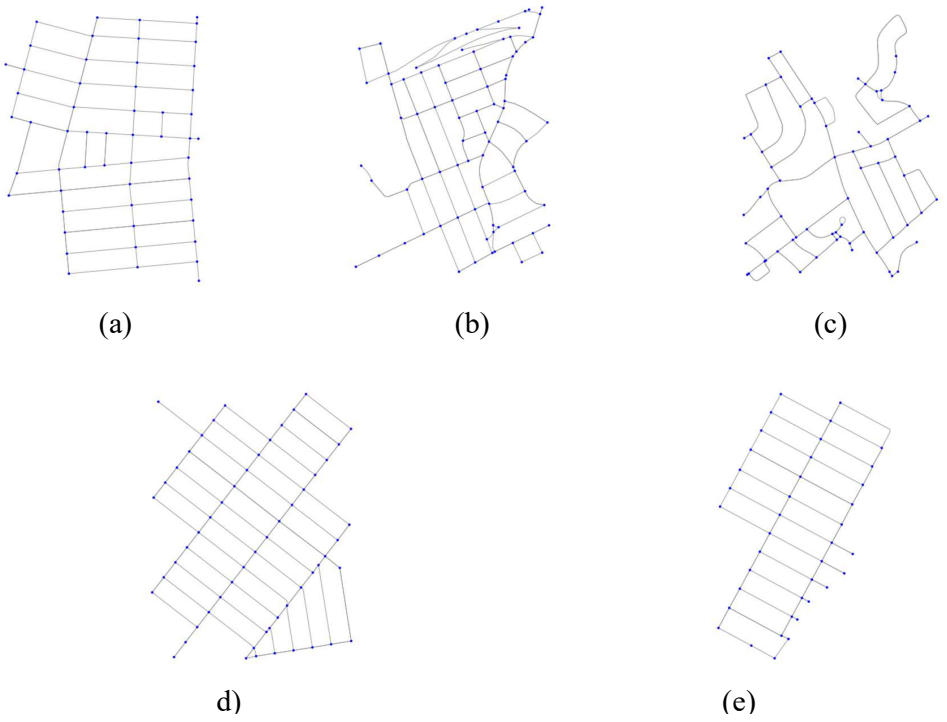

Figure B.2: Network models derived from different neighbourhoods in New York (USA): (a) Crown heights in Brooklyn, (b) Jamaica Hills and Jamaica Estates in Queens, (c) Saddle Rock and Great Neck, (d) Mapleton and Bensonhurst in Brooklyn, and (e) Yorkville in Manhattan.

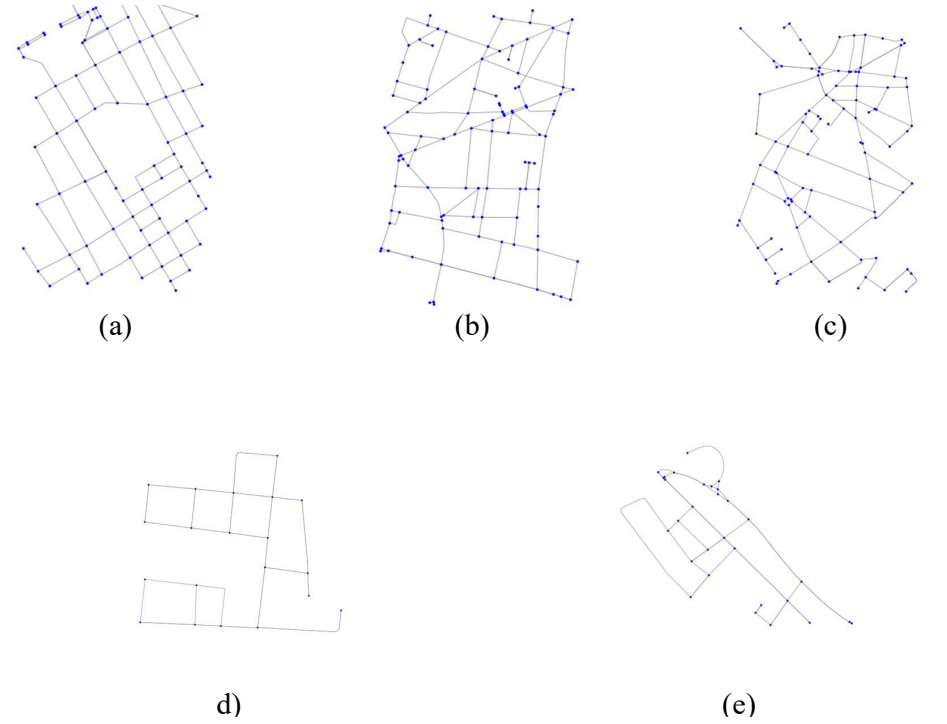

Figure B.3: Network models derived from different neighbourhoods in Greater Paris (France): (a) Levallois-Perret, (b) 9th district, (c) 16th district, (d) Saint-Denis, and (e) Charenton-le-Pont.

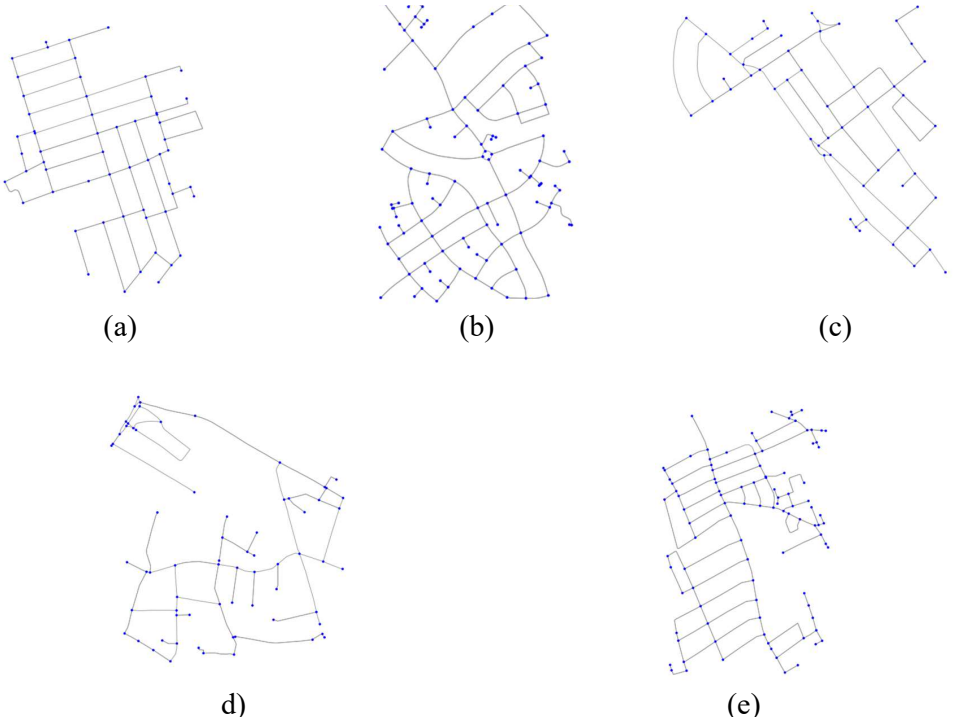

Figure B.4: Network models derived from different neighbourhoods in London (UK): (a) South Tottenham, (b) The Wrythe, (c) Kensington, (d) Southwark, and (e) Fulham.

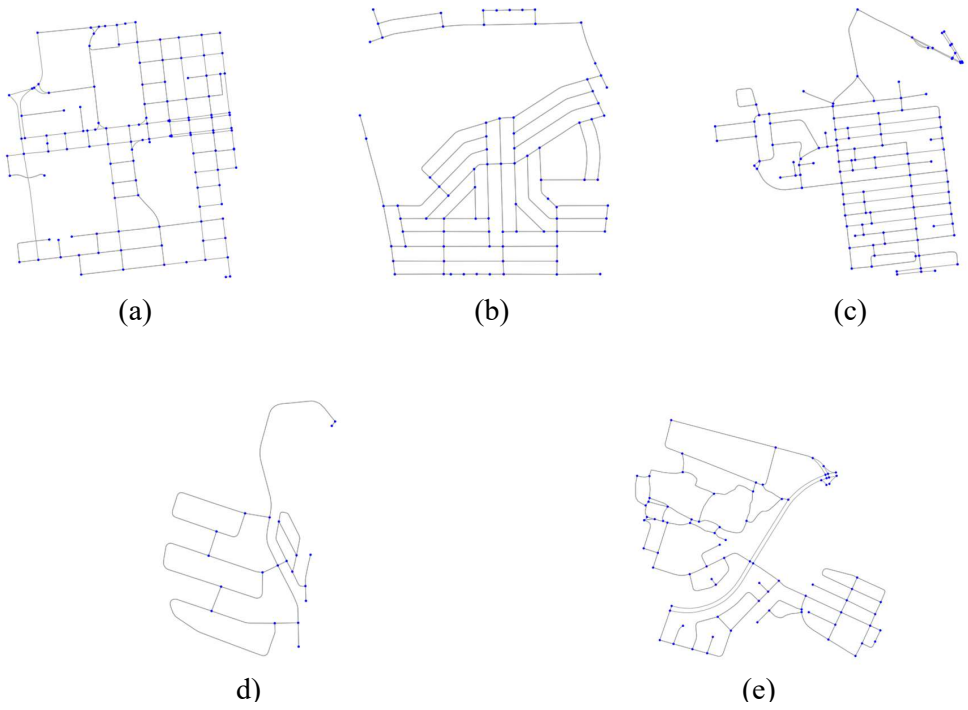

Figure B.5: Network models derived from different neighbourhoods in Greater Johannesburg (South Africa): (a) Braamfontein and Hillbrow , (b) Zola in Soweto, (c) Jan Hofmeyer and Vrededorp, (d) Johannesburg South, and (e) Longdale and Riverlea.

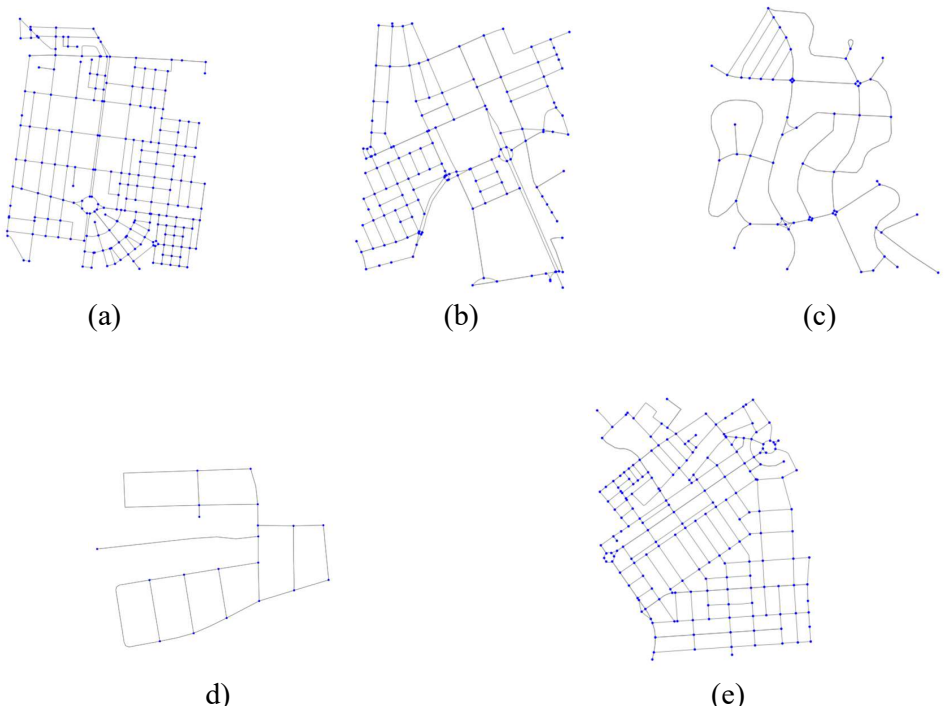

Figure B.6: Network models derived from different neighbourhoods in Seville (Spain): (a) Nervión, (b) Heliópolis and Bami, (c) Urb. el Pandero, (d) Urb. las Tres Barras, and (e) Los Remedios.

Table B.1: Coordinates of the bounding boxes used to build the 30 graphs extracted from *OpenStreetMap* (www.openstreetmap.org).

Id	Area (Country)	North[(1)]	South[(1)]	East[(3)]	West[(4)]
1	Greater San Francisco (USA)	37.79	37.78	-122.41	-122.42
2	Greater San Francisco (USA)	37.44	37.43	-122.14	-122.15
3	Greater San Francisco (USA)	37.79	37.78	-122.48	-122.49
4	Greater San Francisco (USA)	37.80	37.79	-122.43	-122.44
5	Greater San Francisco (USA)	37.675	37.665	-122.425	-122.435
6	New York (USA)	40.67	40.66	-73.95	-73.96
7	New York (USA)	40.72	40.71	-73.79	-73.80
8	New York (USA)	40.80	40.79	-73.74	-73.75
9	New York (USA)	40.62	40.61	-73.98	-73.99
10	New York (USA)	40.779	40.769	-73.941	-73.951
11	Greater Paris (France)	48.90	48.89	2.29	2.28
12	Greater Paris (France)	48.88	48.87	2.35	2.34
13	Greater Paris (France)	48.86	48.85	2.278	2.268
14	Greater Paris (France)	48.91	48.90	2.37	2.36
15	Greater Paris (France)	48.835	48.825	2.41	2.40
16	London (UK)	51.583	51.573	-0.062	-0.072
17	London (UK)	51.39	51.38	-0.17	-0.18
18	London (UK)	51.49	51.48	-0.186	-0.1965
19	London (UK)	51.51	51.50	-0.08	-0.09
20	London (UK)	51.487	51.477	-0.213	-0.223
21	Greater Johannesburg (South Africa)	-26.19	-26.20	28.05	28.04
22	Greater Johannesburg (South Africa)	-26.24	-26.25	27.85	27.84
23	Greater Johannesburg (South Africa)	-26.188	-26.198	28.02	28.01
24	Greater Johannesburg (South Africa)	-26.26	-26.27	27.99	27.98
25	Greater Johannesburg (South Africa)	-26.20	-26.21	27.97	27.96
26	Seville (Spain)	37.389	37.379	-05.96	-05.972
27	Seville (Spain)	37.361	37.351	-05.977	-05.987
28	Seville (Spain)	37.3485	37.3385	-06.03	-06.04
29	Seville (Spain)	37.335	37.325	-06.071	-06.081
30	Seville (Spain)	37.382	37.372	-05.996	-06.006

[(1)] northern latitude of bounding box,[(2)] southern latitude of bounding box, [(3)] eastern longitude of bounding box, [(4)]western longitude of bounding box.

Appendix C

Additional results of the Sioux Falls network case study

The Sioux Falls case study was used in Chapters 3, 5 and 6 to test the proposed robustness, resilience and link criticality indicators, and also assess the effects of demand variations on the robustness, resilience and link criticality results. In Chapter 5, Spearman's coefficient was used to quantify the difference between the link criticality rankings derived from multiple-link failures and less computationally expensive criticality metrics including the link flow, flow/capacity ratio and single-link failures. For the sake of brevity, Chapter 5 only presented and discussed the correlation between single- and multiple-link-failure-based criticality rankings. This appendix presents and discusses the correlation between the rankings based on the multiple-ink failures, the link flows and the link flow/capacity ratio. Table C.1 shows the evolution of the rankings correlation across the different demand distribution and level conditions considered in Chapter 5. The correlation between single- and multiple-link-failure based criticality rankings (SLF vs ALL) is included for comparison.

Table C.1 shows that the rankings based on the flow/capacity ratio and the MLF simulations were uncorrelated ($R_s \approx 0$) in the network with medium demand distributed to all nodes and strongly correlated ($R_s \approx 0.70$) in the network with low demand distributed to six nodes. In contrast, the rankings based on the link flow and SLFs appeared always strongly ($R_s \geq 0.60$) and very strongly ($R_s \geq 0.80$) correlated with the rankings based on MLFs, respectively. The correlation between the rankings based on the link flow and MLFs was higher in the network with concentrated demand compared to the network with distributed demand. Furthermore, the correlation seemed to decrease with the congestion level when the demand was concentrated but increase with the congestion level when demand was distributed to all nodes.

The higher heterogeneity of the link flow/capacity ratio and criticality values observed in the networks with concentrated demand (Table 5.3) suggested that in such networks a few links tend to attract most of the traffic and form the network weaknesses. The present results confirm that these links (i.e. the links with highest flow/capacity ratio) are not necessarily the most critical as shown by the rank correlation between these metrics ($0.322 \leq R_s \leq 0.706$).

Ultimately, this shows that the link criticality can partly be explained by the link traffic

Table C.1: Effect of the demand distribution and intensity on the network initial state and link-criticality rankings correlation

	Demand concentrated in six nodes			Original Sioux Falls network	Demand distributed to all nodes		
Network initial state							
Demand level	Low	Medium	High	High	Low	Medium	High
Link flow/capacity ratio	0.40(0.40)	1.08(0.57)	2.19(0.99)	1.47(0.57)	0.41(0.30)	0.93(0.43)	1.79(0.62)
Link criticality							
SLF vs ALL[(1)]	0.971	0.991	0.998	0.993	0.994	0.996	0.998
FLOW vs ALL[(1)]	0.938	0.874	0.870	0.897	0.783	0.854	0.861
FLOW/CAP vs ALL[(1)]	0.706	0.331	0.322	0.147	0.164	-0.010	0.040

mean (standard deviation); [(1)] Correlation between the link criticality rankings derived from the single-link failures (SLF), link flow (FLOW), flow/capacity ratio (FLOW/CAP), and the multiple-link failures (ALL, ALL = SLF + 2LF +3LF)

flow while the link flow/capacity ratio appears irrelevant. Still, the link rankings based on the link flow were always less correlated with the rankings based on the multiple-link failures than the SLF-based rankings (Table C.1). Hence, failure simulations are generally required to properly assess the link criticality as the metrics based on the network usage in the undisrupted state are unable to account for the reserve capacity available in the network to absorb disruptions.

References

Alderson, D. L., Brown, G. G., Carlyle, W. M., & Wood, R. K. (2017). Assessing and Improving the Operational Resilience of a Large Highway Infrastructure System to Worst-Case Losses. *Transportation Science*, *52*(4), 1012–1034. https://doi.org/10.1287/trsc.2017.0749

Arter, K., & Buchanan, C. (2010). Economic Impact of Road Works, In *European transport conference, 10-13 october 2010*, Glasgow, UK, Association for European Transport.

ARUP. (2014). *City Resilience Framework* (tech. rep.). Arup. London, UK. https://www.preparecenter.org/sites/default/files/arup%7B%5C_%7Drockefeller%7B%5C_%7Dresilient%7B%5C_%7Dcities%7B%5C_%7Dreport.pdf

Austroads. (2017). *Road Transport Management Framework and Principles - Research Report AP-R552-17* (tech. rep.). Austroads. Sidney, Australia, Austroads Ltd.

Bagloee, S. A., Sarvi, M., Wolshon, B., & Dixit, V. (2017). Identifying critical disruption scenarios and a global robustness index tailored to real life road networks. *Transportation Research Part E: Logistics and Transportation Review*, *98*, 60–81. https://doi.org/10.1016/j.tre.2016.12.003

Bai, F., Sadagopan, N., & Helmy, A. (2003). IMPORTANT: a Framework to Systematically Analyze the Impact of Mobility on Performance of RouTing Protocols for Adhoc NeTworks, In *Iee@e infocom*. https://doi.org/http://dx.doi.org/10.1109/INFCOM.2003.1208920

Barabási, A.-L., & Pósfai, M. (2016). *Network Science*. Cambridge, Cambridge University Press. http://barabasi.com/networksciencebook/

BBC. (2014). Two killed in M26 five-vehicle crash in Kent.

Bhavathrathan, B. K., & Patil, G. R. (2015a). Capacity uncertainty on urban road networks: A critical state and its applicability in resilience quantification. *Computers, Environment and Urban Systems*, *54*, 108–118. https://doi.org/10.1016/j.compenvurbsys.2015.07.005

Bhavathrathan, B. K., & Patil, G. R. (2015b). Quantifying resilience using a unique critical cost on road networks subject to recurring capacity disruptions. *Transportmetrica A: Transport Science*, *11*(9), 836–855. https://doi.org/10.1080/23249935.2015.1087230

Bhavathrathan, B. K., & Patil, G. R. (2018). Algorithm to Compute Urban Road Network Resilience. *Transportation Research Record*, *2672*(48), 104–115. https://doi.org/10.1177/0361198118793329

Boeing, G. (2017). OSMnx: New methods for acquiring, constructing, analyzing, and visualizing complex street networks. *Computers, Environment and Urban Systems*, *65*, 126–139. https://doi.org/10.1016/j.compenvurbsys.2017.05.004

Boeing, G. (2018). Planarity and street network representation in urban form analysis. *Environment and Planning B: Urban Analytics and City Science*. https://doi.org/10.1177/2399808318802941

Boyce, D., Ralevic-Dekic, B., & Bar-Gera, H. (2004). Convergence of traffic assignments: How much is enough? *Journal of Transportation Engineering*, *130*(1), 49–55. https://doi.org/10.1061/(ASCE)0733-947X(2004)130:1(49)

Bratley, P., & Fox, B. L. (1988). ALGORITHM 659: implementing Sobol's quasirandom sequence generator. *ACM Transactions on Mathematical Software*, *14*(1), 88–100. https://doi.org/10.1145/42288.214372

Brown, B., & Baass, K. (1997). Seasonal Variation in Frequencies and Rates of Highway Accidents as Function of Severity. *Transportation Research Record: Journal of the Transportation Research Board*, *1581*, 59–65.

Bruneau, M., Chang, S. E., Eguchi, R. T., Lee, G. C., O'Rourke, T. D., Reinhorn, A. M., Shinozuka, M., Tierney, K., Wallace, W. A., & Von Winterfeldt, D. (2003). A Framework to Quantitatively Assess and Enhance the Seismic Resilience of Communities. *Earthquake Spectra*, *19*(4), 733–752. https://doi.org/10.1193/1.1623497

Buhl, J., Gautrais, J., Reeves, N., Solé, R. V., Valverde, S., Kuntz, P., & Theraulaz, G. (2006). Topological patterns in street networks of self-organized urban settlements. *European Physical Journal B*, *49*(4), 513–522. https://doi.org/10.1140/epjb/e2006-00085-1

Buhl, J., Gautrais, J., Solé, R. V., Kuntz, P., Valverde, S., Deneubourg, J. L., & Theraulaz, G. (2004). Efficiency and robustness in ant networks of galleries. *European Physical Journal B*, *42*(1), 123–129. https://doi.org/10.1140/epjb/e2004-00364-9

Bureau of Public Roads. (1964). *Traffic Assignment Manual: Bureau of Public Roads* (tech. rep.). U.S. Department of Commerce. Washington, D.C.

Cardillo, A., Scellato, S., Latora, V., & Porta, S. (2006). Structural properties of planar graphs of urban street patterns. *Physical Review E - Statistical, Nonlinear, and Soft Matter Physics*, *73*(6)arXiv 0510162, 1–8. https://doi.org/10.1103/PhysRevE.73.066107

Casali, Y., & Heinimann, H. R. (2019). A topological characterization of flooding impacts on the Zurich road network. *PLoS ONE*, *14*(7). https://doi.org/https://doi.org/10.1371/journal.pone.0220338

Casali, Y., & Heinimann, H. R. (2020). Robustness response of the Zurich road network under different disruption processes. *Computers, Environment and Urban Systems*, *81*(101460). https://doi.org/10.1016/j.compenvurbsys.2020.101460

Cats, O., Yap, M., & van Oort, N. (2016). Exposing the role of exposure: Public transport network risk analysis. *Transportation Research Part A: Policy and Practice*, *88*, 1–14. https://doi.org/10.1016/j.tra.2016.03.015

Cats, O., Koppenol, G. J., & Warnier, M. (2017). Robustness assessment of link capacity reduction for complex networks: Application for public transport systems. *Reliability Engineering and System Safety*, *167*(July), 544–553. https://doi.org/10.1016/j.ress.2017.07.009

CEDR. (2009). *Traffic Incident Management* (tech. rep.). Conference of European Directors of Roads (CEDR). La Défense, France. http://www.cedr.eu/download/

Publications/2009/e%7B%5C_%7DTraffic%7B%5C_%7DIncident%7B%5C_%7DManagement.pdf

Chatterton, J., Viviattene, C., Morris, J., Penning-Rowsell, E. C., & Tapsell, S. M. (2010). *The costs of the summer 2007 floods in England* (tech. rep.). Environment Agency. Bristol, UK. https://doi.org/978-1-84911-146-1

Colin, M., Palhol, F., & Leuxe, A. (2016). Adaptation of Transport Infrastructures and Networks to Climate Change. *Transportation Research Procedia*, *14*(0), 86–95. https://doi.org/10.1016/j.trpro.2016.05.044

Cox, A., Prager, F., & Rose, A. (2011). Transportation security and the role of resilience: A foundation for operational metrics. *Transport Policy*, *18*(2), 307–317. https://doi.org/10.1016/j.tranpol.2010.09.004

Crucitti, P., Latora, V., & Porta, S. (2006). Centrality in networks of urban streets. *Chaos*, *16*(1). https://doi.org/10.1063/1.2150162

Cutter, S. L., Barnes, L., Berry, M., Burton, C., Evans, E., Tate, E., & Webb, J. (2008). A place-based model for understanding community resilience to natural disasters. *Global Environmental Change*, *18*(4), 598–606. https://doi.org/10.1016/j.gloenvcha.2008.07.013

Dalal, I. L., Stefan, D., & Harwayne-Gidansky, J. (2008). Low discrepancy sequences for monte carlo simulations on reconfigurable platforms. *Proceedings of the International Conference on Application-Specific Systems, Architectures and Processors*, 108–113. https://doi.org/10.1109/ASAP.2008.4580163

De Meo, P., Ferrara, E., Fiumara, G., & Ricciardello, A. (2012). A novel measure of edge centrality in social networks. *Knowledge-Based Systems*, *30*, 136–150. https://doi.org/10.1016/j.knosys.2012.01.007

DEFRA. (2011). *National Flood and Coastal Erosion Risk Management Strategy for England* (tech. rep.). Department for Environment, Food and Rural Affairs (DEFRA). London, UK. https://assets.publishing.service.gov.uk/government/uploads/system/uploads/attachment%7B%5C_%7Ddata/file/228898/9780108510366.pdf

Demirel, H., Kompil, M., & Nemry, F. (2015). A framework to analyze the vulnerability of European road networks due to Sea-Level Rise (SLR) and sea storm surges. *Transportation Research Part A: Policy and Practice*, *81*, 62–76. https://doi.org/10.1016/j.tra.2015.05.002

D'Lima, M., & Medda, F. (2015). A new measure of resilience: An application to the London Underground. *Transportation Research Part A: Policy and Practice*, *81*, 35–46. https://doi.org/10.1016/j.tra.2015.05.017

Eisenstat, D. (2011). Random road networks: the quadtree model (P. Flajolet & D. Panario, Eds.). In P. Flajolet & D. Panario (Eds.), *Proceedings of the eighth workshop on analytic algorithmics and combinatorics (analco)*, San Francisco, CA, USA. https://doi.org/https://doi.org/10.1137/1.9781611973013.9

El-Rashidy, R. A. (2014). *The Resilience of Road Transport Networks: Redundancy , Vulnerability and Mobility characteristics* (Doctoral dissertation September). The University of Leeds.

Enei, R., Doll, C., Klug, S., Partzsch, I., Sedlacek, N., Nesterova, N., Kiel, J., Rudzikaite, L., Papanikolau, A., & Mitsakis, V. (2011). *Vulnerability of transport systems - Main report: WEATHER Deliverable 2* (tech. rep.).

Faturechi, R., & Miller-Hooks, E. (2014). Travel time resilience of roadway networks under disaster. *Transportation Research Part B: Methodological*, *70*arXiv 1103.5451, 47–64. https://doi.org/10.1016/j.trb.2014.08.007

FEMA. (2012). *Traffic Incident Management Systems* (tech. rep. FA-330/ March 2012). Federal Emergency Management Agency (FEMA).

Freeman, L. C. (1979). Centrality in social networks. *Social Networks*, *1*(3)arXiv 0112110, 215–239. https://doi.org/10.1016/0378-8733(78)90021-7

Ganin, A. A., Kitsak, M., Marchese, D., Keisler, J. M., Seager, T., & Linkov, I. (2017). Resilience and efficiency in transportation networks. *Science Advances*, *3*(12), e1701079. https://doi.org/10.1126/sciadv.1701079

Gauthier, P., Furno, A., & El Faouzi, N. E. (2018). Road network resilience: how to identify critical links subject to day-to-day disruptions. *Transportation Research Record*, *2672*(1), 54–65. https://doi.org/10.1177/0361198118792115

Gerke, S., Schlatter, D., Steger, A., & Taraz, A. (2007). The Random Planar Graph Process. *Random Structures and Algorithms*, 236–261. https://doi.org/10.1002/rsa

Godschalk, D. R. (2003). Urban Hazard Mitigation: Creating Resilient Cities. *Natural Hazards Review*, *4*(3), 136–143. https://doi.org/10.1061/(ASCE)1527-6988(2003)4:3(136)

Hallegatte, S., Rentschler, J., & Rozenberg, J. (2019). *Lifelines: The Resilient Infrastructure Opportunity* (tech. rep.). World Bank. Washington, DC. https://doi.org/10.1596/978-1-4648-1430-3

Henry, D., & Ramirez-Marquez, J. E. (2012). Generic metrics and quantitative approaches for system resilience as a function of time. *Reliability Engineering and System Safety*, *99*, 114–122. https://doi.org/10.1016/j.ress.2011.09.002

Highways England. (2015). *Planning for the future: guide to working with Highways England on planning matters* (tech. rep.). Highways England.

Holling, C. S. (1973). Resilience and stability of ecological systems. *Annual Review of Ecology and Systematics*, *4*arXiv arXiv:1011.1669v3, 1–23. https://doi.org/10.1146/annurev.es.04.110173.000245

Holme, P., Kim, B. J., Yoon, C. N., & Han, S. K. (2002). Attack vulnerability of complex networks. *Physical Review E - Statistical Physics, Plasmas, Fluids, and Related Interdisciplinary Topics*, *65*(5), 14. https://doi.org/10.1103/PhysRevE.65.056109

Hosseini, S., Barker, K., & Ramirez-Marquez, J. E. (2016). A review of definitions and measures of system resilience. *Reliability Engineering and System Safety*, *145*, 47–61. https://doi.org/10.1016/j.ress.2015.08.006

Hu, F., Yeung, C. H., Yang, S., Wang, W., & Zeng, A. (2016). Recovery of infrastructure networks after localised attacks. *Scientific Reports*, *6*(24522). https://doi.org/10.1038/srep24522

IEEE Computer Society. (1991). *IEEE Standard Computer Dictionary: A compilation of IEEE Standard computer Glossaries (610-1900)*. Piscataway, USA, IEEE. http://elib.peaceland.edu.ng:8383/greenstone3/sites/localsite/collect/peacelan/index/assoc/HASHbaad/2439e09f.dir/doc.pdf

Ip, W. H., & Wang, D. (2011). Resilience and friability of transportation networks: Evaluation, analysis and optimization. *IEEE Systems Journal*, *5*(2), 189–198. https://doi.org/10.1109/JSYST.2010.2096670

IPCC. (2012). *Managing the Risks of Extreme Events and Disasters to Advance Climate Change Adaptation. A Special Report of Working Groups I and II of the Intergovernmental Panel on Climate Change* (tech. rep.). Intergovernmental Panel on Climate Change. New York, USA. https://doi.org/10.1017/CBO9781139177245

Kalapala, V., Sanwalani, V., Clauset, A., & Moore, C. (2006). Scale invariance in road networks. *Physical Review E - Statistical, Nonlinear, and Soft Matter Physics*, *73*(2)arXiv 0510198, 1–6. https://doi.org/10.1103/PhysRevE.73.026130

Kansky, K. J. (1963). *Structure of transportation networks : relationships between network geometry and regional characteristics*. Chicago, USA, University of Chicago, Dept. of Geography.

Karlaftis, M. G., Latoski, S. P., Richards, N. J., & Sinha, K. C. (1999). ITS Impacts on Safety and Traffic Management: An Investigation of Secondary Crash Causes. *Intelligent Transportation Systems Journal*, *5*(1), 39–52. https://doi.org/10.1080/10248079908903756

Kiel, J., Petiet, P., Nieuwenhuis, A., Peters, T., & Van Ruiten, K. (2016). A Decision Support System for the Resilience of Critical Transport Infrastructure to Extreme Weather Events. *Transportation Research Procedia*, *14*, 68–77. https://doi.org/10.1016/j.trpro.2016.05.042

Koliou, M., van de Lindt, J. W., McAllister, T. P., Ellingwood, B. R., Dillard, M., & Cutler, H. (2018). State of the research in community resilience: progress and challenges. *Sustainable and Resilient Infrastructure*, *9689*, 1–21. https://doi.org/10.1080/23789689.2017.1418547

Kurth, M., Kozlowski, W., Ganin, A., Mersky, A., Leung, B., Dykes, J., Kitsak, M., & Linkov, I. (2020). Lack of resilience in transportation networks: Economic implications. *Transportation Research Part D: Transport and Environment*, *86*, 102419. https://doi.org/10.1016/j.trd.2020.102419

LeBlanc, L. J., Morlok, E. K., & Pierskalla, W. P. (1975). An efficient approach to solving the road network equilibrium traffic assignment problem. *Transportation Research*, *9*(5), 309–318. https://doi.org/10.1016/0041-1647(75)90030-1

Lin, J., & Ban, Y. (2013). Complex Network Topology of Transportation Systems. *Transport Reviews*, *33*(6), 658–685. https://doi.org/10.1080/01441647.2013.848955

Manca, A. R., Benczur, P., & Giovannini, E. (2017). Building a Scientific Narrative Towards a More Resilient EU Society Part 1: a Conceptual Framework. https://doi.org/10.2760/635528

Marshall, S. (2005). *Streets and Patterns*. London, UK, Spon press.

Martinson, R. (2017). Resilience in a Transportation System: A Whole System Approach. *Transportation Research Circular: Transportation Systems Resilience - Preparation, Recovery and Adaptation*, (E-C226), 1–9. http://onlinepubs.trb.org/onlinepubs/circulars/ec226.pdf

Masucci, A. P., Smith, D., Crooks, A., & Batty, M. (2009). Random planar graphs and the London street network. *European Physical Journal B*, *71*(2)arXiv 0706.0024, 259–271. https://doi.org/10.1140/epjb/e2009-00290-4

Mattsson, L. G., & Jenelius, E. (2015). Vulnerability and resilience of transport systems - A discussion of recent research. *Transportation Research Part A: Policy and Practice*, *81*, 16–34. https://doi.org/10.1016/j.tra.2015.06.002

Maze, T. H., Agarwal, M., & Burchett, G. (2005). *Whether weather matters to traffic demand, traffic safety, and traffic flow.* (tech. rep. Final General Report, August 2005). Iowa State University. Ames, USA.

Misra, S., Padgett, J. E., Barbosa, A. R., & Webb, B. M. (2020). An expert opinion survey on post-hazard restoration of roadways and bridges: Data and key insights. *Earthquake Spectra*, *36*(2), 983–1004. https://doi.org/10.1177/8755293019891722

Mitoulis, S. A., Argyroudis, S. A., Loli, M., & Imam, B. (2021). Restoration models for quantifying flood resilience of bridges. *Engineering Structures*, *238*(February), (accepted). https://doi.org/10.1016/j.engstruct.2021.112180

Mitradjieva, M., & Lindberg, P. O. (2013). The Stiff Is Moving - Conjugate Direction Frank-Wolfe Methods with Applications to Traffic Assignment. *Transportation Science*, *47*(2), 280–293.

Murray-Tuite, P. (2006). A comparison of network transportation resilience under simulated system optimum and user equilibrium conditions (L. F. Perrone, F. P. Wieland, J. Liu, B. Lawson, D. M. Nicol, & R. M. Fujimoto, Eds.). In L. F. Perrone, F. P. Wieland, J. Liu, B. Lawson, D. M. Nicol, & R. M. Fujimoto (Eds.), *Proceedings of the 2006 winter simulation conference*, Monterey, California (USA), IEEE. https://doi.org/10.1109/WSC.2006.323240

Murray-Tuite, P., & Wolshon, B. (2013). Evacuation transportation modeling: An overview of research, development, and practice. *Transportation Research Part C: Emerging Technologies*, *27*, 25–45. https://doi.org/10.1016/j.trc.2012.11.005

Nogal, M., & Honfi, D. (2019). Assessment of road traffic resilience assuming stochastic user behaviour. *Reliability Engineering and System Safety*, *185*(July 2018), 72–83. https://doi.org/10.1016/j.ress.2018.12.013

Nogal, M., O'Connor, A., Caulfield, B., & Martinez-Pastor, B. (2016). Resilience of traffic networks: From perturbation to recovery via a dynamic restricted equilibrium model. *Reliability Engineering and System Safety*, *156*, 84–96. https://doi.org/10.1016/j.ress.2016.07.020

Omer, M., Mostashari, A., & Nilchiani, R. (2013). Assessing resilience in a regional road-based transportation network. *International Journal of Industrial and Systems Engineering*, *13*(4), 389–408. https://doi.org/10.1504/IJISE.2013.052605

Ortúzar, J. d. D., & Willusem, L. G. (2011). *Modelling Transport* (4th Editio). Oxford, Wiley. https://doi.org/10.1002/9781119993308

Park, J., Seager, T. P., Rao, P. S., Convertino, M., & Linkov, I. (2013). Integrating risk and resilience approaches to catastrophe management in engineering systems. *Risk Analysis*, *33*(3), 356–367. https://doi.org/10.1111/j.1539-6924.2012.01885.x

Pelling, M., Özerdem, A., & Barakat, S. (2002). The macro-economic impact of disasters. *Progress in Development Studies*, *2*(4), 283–305. https://doi.org/10.1191/1464993402ps042ra

Peng, W., Dong, G., Yang, K., & Su, J. (2014). A random road network model and its effects on topological characteristics of mobile delay-tolerant networks. *IEEE Transactions on Mobile Computing*, *13*(12), 2706–2718. https://doi.org/10.1109/TMC.2013.66

Pimm, S. L. (1984). The complexity and stability of ecosystems. *Nature*, *307*(5949)arXiv arXiv:1011.1669v3, 321–326. https://doi.org/10.1038/307321a0

Pisano, P., & Goodwin, L. (2004). Research Needs for Weather-Responsive Traffic Management. *Transportation Research Record: Journal of the Transportation Research Board*, *1867*(1), 127–131. https://doi.org/10.3141/1867-15

Prescott, D. (2017). *H23TRE Traffic Engineering [Lecture material]*. Nottingham, University of Nottingham.

Puth, M. T., Neuhäuser, M., & Ruxton, G. D. (2015). Effective use of Spearman's and Kendall's correlation coefficients for association between two measured traits. *Animal Behaviour*, *102*, 77–84. https://doi.org/10.1016/j.anbehav.2015.01.010

Reed, D. A., Kapur, K. C., & Christie, R. D. (2009). Methodology for assessing the resilience of networked infrastructure. *IEEE Systems Journal*, *3*(2), 174–180. https://doi.org/10.1109/JSYST.2009.2017396

Reggiani, A. (2013). Network resilience for transport security: Some methodological considerations. *Transport Policy*, *28*, 63–68. https://doi.org/10.1016/j.tranpol.2012.09.007

Réka, A., Hawoong, J., & Barabási, A.-L. (2000). Error and attack tolerance of complex networks. *Nature*, *406*, 378–382.

Rifaat, S. M., Tay, R., & De Barros, A. (2011). Effect of street pattern on the severity of crashes involving vulnerable road users. *Accident Analysis and Prevention*, *43*(1), 276–283. https://doi.org/10.1016/j.aap.2010.08.024

Sharma, N., Tabandeh, A., & Gardoni, P. (2018). Resilience analysis: a mathematical formulation to model resilience of engineering systems. *Sustainable and Resilient Infrastructure*, *3*(2), 49–67. https://doi.org/10.1080/23789689.2017.1345257

Simonovic, S. P. (2018). *Chapter 14 – From Risk Management to Quantitative Disaster Resilience: A New Paradigm for Catastrophe Modeling* (G. Michel, Ed.). Elsevier Inc. https://doi.org/10.1016/B978-0-12-804071-3.00014-8

Southworth, M., & Ben-Joseph, E. (2003). *Streets and the Shaping of Towns and Cities*. Washington, DC (USA), Island press (first edition McGraw-Hill).

Spaans, M., & Waterhout, B. (2017). Building up resilience in cities worldwide – Rotterdam as participant in the 100 Resilient Cities Programme. *Cities*, *61*, 109–116. https://doi.org/10.1016/j.cities.2016.05.011

Strano, E., Viana, M., Costa, L. d. F., Cardillo, A., Porta, S., & Latora, V. (2013). Urban street networks, a comparative analysis of ten European cities. *Environment and Planning B: Planning and Design*, *40*(6)arXiv 1211.0259v1, 1071–1086. https://doi.org/10.1068/b38216

Sullivan, J. L., Novak, D. C., Aultman-Hall, L., & Scott, D. M. (2010). Identifying critical road segments and measuring system-wide robustness in transportation networks with isolating links: A link-based capacity-reduction approach. *Transportation Research Part A: Policy and Practice*, *44*(5), 323–336. https://doi.org/10.1016/j.tra.2010.02.003

Taylor, M. A., Sekhar, S. V., & D'Este, G. M. (2006). Application of accessibility based methods for vulnerability analysis of strategic road networks. *Networks and Spatial Economics*, *6*, 267–291. https://doi.org/10.1007/s11067-006-9284-9

Transportation Networks for Research Core Team. (2019). Transportation Networks for Research. Retrieved December 8, 2019, from https://github.com/bstabler/TransportationNetworks

Tuzun Aksu, D., & Ozdamar, L. (2014). A mathematical model for post-disaster road restoration: Enabling accessibility and evacuation. *Transportation Research Part E: Logistics and Transportation Review*, *61*(January), 56–67. https://doi.org/10.1016/j.tre.2013.10.009

UK Department for Transport. (2012). *Guidance on Road Classification and the Primary Route Network* (tech. rep. January). UK Department for Transport. London, UK. https://www.gov.uk/government/uploads/system/uploads/attachment%7B%5C_%7Ddata/file/315783/road-classification-guidance.pdf

UK Department for Transport. (2014). *Transport Resilience Review - A review of the resilience of the transport network to extreme weather events* (tech. rep. July). UK Department for Transport. London, UK. https://www.gov.uk/government/uploads/system/uploads/attachment%7B%5C_%7Ddata/file/335115/transport-resilience-review-web.pdf

Wang, D. Z. W., Liu, H., Szeto, W. Y., & Chow, A. H. F. (2016). Identification of critical combination of vulnerable links in transportation networks – a global optimisation approach. *Transportmetrica A: Transport Science*, *12*(4), 346–365. https://doi.org/10.1080/23249935.2015.1137373

Wang, S., Zheng, L., & Yu, D. (2017a). The improved degree of urban road traffic network: A case study of Xiamen, China. *Physica A: Statistical Mechanics and its Applications*, *469*, 256–264. https://doi.org/10.1016/j.physa.2016.11.090

Wang, X., You, S., & Wang, L. (2017b). Classifying road network patterns using multinomial logit model. *Journal of Transport Geography*, *58*, 104–112. https://doi.org/10.1016/j.jtrangeo.2016.11.013

Wisetjindawat, W., Kermanshah, A., Derrible, S., & Fujita, M. (2017). Stochastic Modeling of Road System Performance during Multihazard Events: Flash Floods and Earthquakes. *Journal of Infrastructure Systems*, *23*(4), 04017031. https://doi.org/10.1061/(asce)is.1943-555x.0000391

Woods, D. D. (2015). Four concepts for resilience and the implications for the future of resilience engineering. *Reliability Engineering and System Safety*, *141*, 5–9. https://doi.org/10.1016/j.ress.2015.03.018

Xie, F., & Levinson, D. (2007). Measuring the structure of road networks. *Geographical Analysis*, *39*(3), 336–356. https://doi.org/10.1111/j.1538-4632.2007.00707.x

Xie, F., & Levinson, D. (2011). Evaluating the effects of the I-35W bridge collapse on road-users in the twin cities metropolitan region. *Transportation Planning and Technology*, *34*(7), 691–703. https://doi.org/10.1080/03081060.2011.602850

Zanin, M., Sun, X., & Wandelt, S. (2018). Studying the Topology of Transportation Systems through Complex Networks: Handle with Care. *Journal of Advanced Transportation*, *2018*. https://doi.org/10.1155/2018/3156137

Zhang, W., & Wang, N. (2016). Resilience-based risk mitigation for road networks. *Structural Safety*, *62*, 57–65. https://doi.org/10.1016/j.strusafe.2016.06.003

Zhang, W., Wang, N., & Nicholson, C. (2017). Resilience-based post-disaster recovery strategies for road-bridge networks. *Structure and Infrastructure Engineering*, *13*(11), 1404–1413. https://doi.org/10.1080/15732479.2016.1271813

Zhang, X., Miller-Hooks, E., & Denny, K. (2015). Assessing the role of network topology in transportation network resilience. *Journal of Transport Geography*, *46*, 35–45. https://doi.org/10.1016/j.jtrangeo.2015.05.006

Zhou, Y., Sheu, J.-b., & Wang, J. (2017). Robustness Assessment of Urban Road Network with Consideration of Multiple Hazard Events. *Risk Analysis*, *37*(8), 1477–1494. https://doi.org/10.1111/risa.12802

Zobel, C. W. (2011). Representing perceived tradeoffs in defining disaster resilience. *Decision Support Systems*, *50*(2), 394–403. https://doi.org/10.1016/j.dss.2010.10.001

List of Figures

List of Tables

Nomenclature

τ	Time elapsed since the start of the recovery
a	A link in a road network
$BET(a)$	Betweenness centrality of link a
$BETWI$	Interactive betweenness attack
c_a	Capacity of link a
Cr_a	Criticality indicator of link a
CRO_z	"Cumulative" robustness of a network to an attack mode z
d_w	Travel demand on the OD pair w
$G(V, E)$	Graphs composed of a set of vertices (V) and edges (E)
h_{degree}	Degree heterogeneity (i.e. standard deviation)
h_{lc}	Heterogeneity (i.e. standard deviation) of the link cost distribution in a network
k_w	Weighting factor associated with the OD pair w
L	Number of links in a network
L_s	Number of links damaged by the hazard s
m	Number of nodes per row in the GREREC model
N	Number of nodes in a network
n	Number of nodes per column in the GREREC model
N_H	Maximum number of links that can be repaired between t_0 and t_H
NP	Road network performance indicator
p	Probability of keeping horizontal and vertical edges in the GREREC model
q	Probability of generating shortcuts in the GREREC model
r	Probability of considering additional nodes as OD points in the GREREC model

R_S	Spearman's rank order correlation coefficient
r_{OD}	Ratio between the number of OD points and the number of nodes in a road network
$RAND$	Representative random attack
RE	Road network resilience indicator
RO	Road network robustness indicator
s	Hazard
t	Time
t_0	Start time of the recovery process
t_H	Time horizon chosen to compute RE
TA_{EI}	Targeted-attack-extended-impact indicator
$ToTTC$	Total travel time change indicator
TT	Travel Time
TT_0^w	Undisrupted TT along w
tt_a	Travel time of link a
tt_a^f	Free-flow travel time of link a
TT_d^w	Disrupted TT along w
TTC_w	TT relative change index - along w
USD	Proportion of unsatisfied demand
$v_{i,j}$	The vertex on the i-th column and j-th row in the GREREC model
w	OD pair
$WIPW$	Weighted average number of reliable Independent Path Ways
x_a	Flow on link a
z	An attack mode
2LF	Two-link failure
2LF vs ALL	Correlation between the link criticality rankings based on 2LFs and ALL
3LF	Three-link failure
3LF vs ALL	Correlation between the link criticality rankings based on 3LFs and ALL

4LF	Four-link failure
5LF	Five-link failure
ALL	SLFs + 2LFs + 3LFs
BPR	Bureau of Public Roads
CEDR	Conference of European Directors of Roads
DEFRA	Department for Environment, Food & Rural Affairs
FEMA	Federal Emergency Management Agency
FLOW vs ALL	Correlation between the link criticality rankings based on the link flow and ALL
FLOW/CAP vs ALL	Correlation between the link criticality rankings based on the flow/capacity ratio and ALL
FW	Franke-Wolfe (algorithm)
GRE	Grid network with Random Edges
GREREC	Grid network with Random Edges and Regional Edge Costs
GRPG	Growing Random Planar Graph
IPW	Independent Path Ways
LCAM	Life-Cycle Asset Management
MLF	Multiple-link failure
OD	Origin-Destination
PRN	Primary Route Network
QMC	Quasi Monte-Carlo
RTM	Road Transport Management
SLF	Single-link failure
SLF vs ALL	Correlation between the link criticality rankings based on SLFs and ALL
SRN	Strategic Road Network